University of Stavanger

Faculty of Science and Technology

MASTER'S THESIS

Study program/Specialization: Petroleum Engineering/Reservoir Engineering	Spring semester, 2016 Open / ~~Restricted~~ access
Writer: Sachin Gupta	…… (Writer's signature)
Faculty supervisor: Prof. Aly Anis Hamouda	
Thesis title: Effect of ions on Oil recovery by Low salinity water flooding on chalk reservoir	
Credits (ECTS): 30	
Key words: Low Salinity Water Flooding Single salt brine Chalk Pressure drop pH Ion tracking Oil Recovery Fines Migration Calcite Dissolution Multicomponent Ion Exchange	Pages: 120 + enclosure: 10 Stavanger,15/06/2016 Date/year

ACKNOWLEDMENT

First of all, I would like to present my gratitude to University of Stavanger for giving me the opportunity to be the part of the UiS family. Then I want to thank Professor Aly Anis Hamouda for allowing me to work under his guidance and for his continuous help throughout this period. I was fortunate enough to be the part of his team and learned a lot under his supervision.

I want to thanks Krzysiek Nowicki for his assistance and hands on training in the laboratory work and Arif Pranoto for his help in CMG simulation.

Last but not the least, I thank my family for their support and being with me during my sorrow and happiness.

Sachin Gupta

ABSTRACT

Low salinity water flooding has shown its potential for incremental oil recovery. It has been widely researched Oil Recovery method. However, the mechanism of the method has not fully understood. This is mainly due to complexity of rock/brine/oil interaction.

In this paper all the experiments were performed on Stevens-Klint Chalk, Denmark, which were initially saturated with model oil {N-Decane + Stearic Acid (SA), 0.005 mole/l} and Crude Oil X, from North Sea field. Different LSW were investigated here with emphasis on understanding the role of some ions that were recognized form our previous work as well as literature on their effect on wettability alteration.

The flooding fluids were synthetic sea water (SSW) and the diluted SSW by 10 (LSW1:10) and 50 (LSW1:50) times, single and two salts brines, such as Na_2SO_4, $MgCl_2$, and $NaCl+MgCl_2$. at 70˚C. SSW was used as the primary flooding fluid, while other flooding fluids were injected as secondary flooding fluids to estimate the potential incremental oil recovery. This is mainly due to the fact that most of the fields are flooded with seawater. Injection rates effect (4PV/day and 16PV/day) were also investigated, following the changes of the pressure drop, effluent ion concentrations and pH.

An increase in pH was observed during flooding with LSW and single salt brine flooding. Increase in pH is attributed to mineral dissolution which is demonstrated by ion tracking results. Few aspects were observed: 1) As dilution factor increases, slower response in oil recovery observed. 2) In presence of SO_4^{2-}, Ca/Mg enhances the sweep efficiency. 3) It is interesting to observe deficiency in [Mg^{+2}] in effluents than injected. This may confirm the exchange between Ca/Mg, that was observed in the field. From literature and our previous work, this exchange process alters the chalk surface to more water wet. 4) Magnesium reactivity increases with temperature beyond 70°C. Increase in oil recovery at 90°C observed when flooding with Mg brine. The impact of Na^+ on oil recovery was addressed.

TABLE OF CONTENTS

LIST OF FIGURES

LIST OF TABLES

ABBREVIATIONS

$[]_r$ssw: Concentration of ion relative to SSW
μ: Dynamic viscosity
A: Cross sectional area
AN: Acid number
BN: Base number
BPV: Back Pressure Valve
d: Diameter
dP: Pressure drop across the core
DW: Distilled Water
EOR: Enhanced Oil Recovery
HPLC: High-performance liquid chromatography
I: ionic strength
IC: Ion Chromatography
IFT: Interfacial Tension
IOR: Improved oil recovery
k: Absolute permeability
K^o_{rw}: the end point of the water relative permeability.
K_{ro} : Relative permeability for oil,
K_{rw}: Relative permeability for water,
L: Length
LS: Low salinity
LSW: Low Salinity Water
LSWF: Low salinity water flooding
m: Mass
M_{dry}: Weight of the dry core
MIE: Multi-component Ion Exchange
M_{wt}: Weight of the wet core
OOIP: Original oil in place
P: Pressure
P_c: Capillary pressure
P_d: Displacement pressure
P_{nw}: Pressure in the non-wetting phase
PV: Pore volume
P_w: Pressure in the wetting phase
Q: Flow rate
r: Radius
SA: Stearic acid
S_o: Oil saturation
S_{or}: Residual oil saturation
SSW: Synthetic Sea Water
S_w: Water saturation
S_{wi}: Initial water saturation
T: Temperature
TDS: Total dissolved solids
V: Volume
V_B: Bulk Volume

Δ: Difference
θ: Contact angle
ρ: Density
ρ_{ssw}: Density of SSW
σ: Interfacial tension
φ: Porosity

Subscripts
o: oil
orw: oil residual water
ro: relative oil
rw: relative water
w: water
wc: water critical
wi: water initial

1. INTRODUCTION

During the early life of reservoir, the hydrocarbons are produced by the natural energy of the reservoir. As the pressure of the reservoir depletes, there is a need of maintaining the reservoir pressure by means of some external help. Water has been proven to be an economical and effective source of secondary recovery.

Over the last decade, Low salinity water (LSW) flooding has been considered as a viable Enhanced Oil Recovery (EOR) method. Several Lab experiments has been performed, which shows a significant increase in oil recovery in chalk from LSW after the injection of High salinity water/brine.

Low Salinity Water Flooding was first attempted by Tang, G.Q. and Morrow, N.R. (1997) at the University of Wyoming. Since then Both laboratory experiments and various field tests had shown that injecting modified water can help in increment of oil recovery. A number of mechanism of Low Salinity water flooding has been proposed, i.e. Fine migration (dispersion of rock minerals), pH increase, Double layer expansion effect and wettability alteration, including adsorption of SO_4^{-2} with co-adsorption of Ca^{+2} and replacement of Ca^{+2} by Mg^{+2} on chalk surface because of increase in ion reactivity at higher temperature (Austad et.al, 2005). But a concise mechanism which conforms to the LSW effect is still debatable. Based on whatever has been published so far in literatures, the mechanisms are mainly related to the presence of clay minerals, oil composition, and presence of formation water. Concentration of divalent ions (Ca^{+2}, Mg^{+2}, SO_4^{2-}) and salinity level of high saline water in range of 1000 ppm – 3000 ppm also play an important role in LSW effects (Ali A. Yousef, Salah Al Saleh, Mohammed Al-Jawfi, 2012).

This work is focused mainly on observing the effects of ions on increase in secondary recovery. From the experiments it has shown that injecting water/brine with modified composition alter the wettability and enhance the oil recovery. These effects are linked to exchange of effective ions (Ca^{+2}, Mg^{+2}, SO_4^{-2}) from/to surface and brine. This thesis is concerned towards secondary injection of brine only with single ion (Mg^{+2}/ SO_4^{-2}) and brines prepared by diluting SSW in proportion of 10 and 50 times with DW.

The objective of this work is to observe effects of cation type and concentration in the injected brine on the increment in secondary oil recovery. This work was also contributed towards

confirming the best possible dilution ratio of SSW, to observe optimum oil recovery. Obtained experimental results were compared with the numerical results generated with the help of CMG-GEM simulator. In addition, all the experiments were performed at 25bar & 70°C/90°C. SSW is used as primary injection brine and brines with different monovalent and divalent cations were used as secondary injection brines. Effluents' pH, pressure drop and oil recovery were measured. Ion tracking results were obtained from Ion Chromatograph and analyzed to assess the ion exchange between rock and brine.

2. THEORY

A detailed research has been done to present the theory and mechanism to understand the low salinity water flooding. A comprehensive review of research papers, books and journal articles are presented in this section.

2.1. Carbonate Rock Classification

Carbonate rocks are formed by the sedimentation of calcareous plant and animal debris. They are also referred as biogenic, i.e. containing majorly organic material generated by living organisms. Carbonate rocks are categorized into clastic rocks and non-clastic rocks. the rock is classified as a clastic rock, If the sediments are fragmented. Whereas, a nonclastic rock consists mostly of intact sediments. A bioclastic rock is a type of rock which is composed of fragmented or detrital organic material, that has not been fully homogenized by chemical processes (Skinner and Porter, 1991). Limestone and dolomite can be classified as either clastic or non-clastic rocks (Puntervold, T., 2008).

More than 50% of the known petroleum reserves are trapped in carbonate reservoirs, which can be divided into limestones, chalk, and dolomite (Austad T., 2014)[8]. Carbonate rocks are defined as rock containing 50% of Carbonate minerals (Mazzullo et al., 1992). Based on the ion composition, mineralogy, grain type and size, lithology of carbonate rocks can be differentiated.

2.1.1. Mineralogy

Considering age and mineralogical stability, ancient limestone and dolomites are composed majorly of calcite and dolomite with limited amounts of Magnesite ($MgCO_3$), Siderite ($FeCO_3$), and Ankerite ($CaFe(CO_3)_2$) (Bjørlykke, 2001). Recrystallization during diagenesis of metastable aragonite ($CaCO_3$) and magnesium-rich calcite form modern calcite. Carbonate rocks are classified based on % of calcite: Pure limestone is regarded as the rock containing 90% or more of calcite; calcitic dolomite is that carbonate rock containing from 50 to 90 % dolomite and the end member dolomite contains more than 90% of mineral dolomite (adapted from Pourmohammadi, S., 2009)[34].

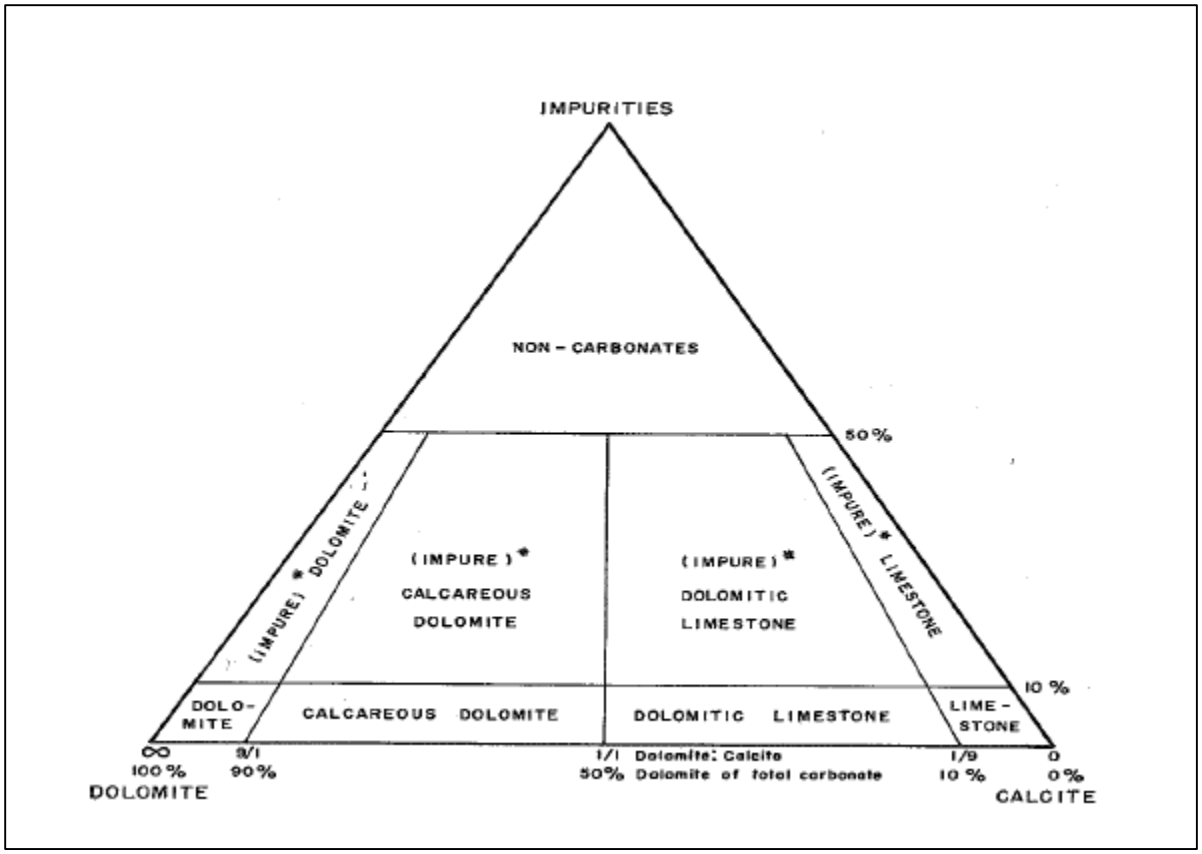

Figure 1: Compositional terminology for carbonate rocks. Percentage of impurities and the ratio of dolomite: Calcite is used to define compositional groups for carbonate rocks, that is, those rocks containing more than 50% carbonate minerals.[34]

2.1.2. Chalk

Chalk is classified as a limestone, formed from the deposition and sedimentation of calcareous skeletal debris from the unicellular planktonic algae coccolithophorid, plus a small amount of foraminiferal material (Milter, 1996). The coccolithophorid algae consist of many spherical coccospheres (2-20 μm diameter), which are built up by coccolithic ring structures (3-15 μm diameter), which in turn are composed of ring fragments or platelets consisting of calcite crystals (0.25-1 μm diameter). Figure 2 shows a coccolithic ring and ring fragments, intact and non-intact.

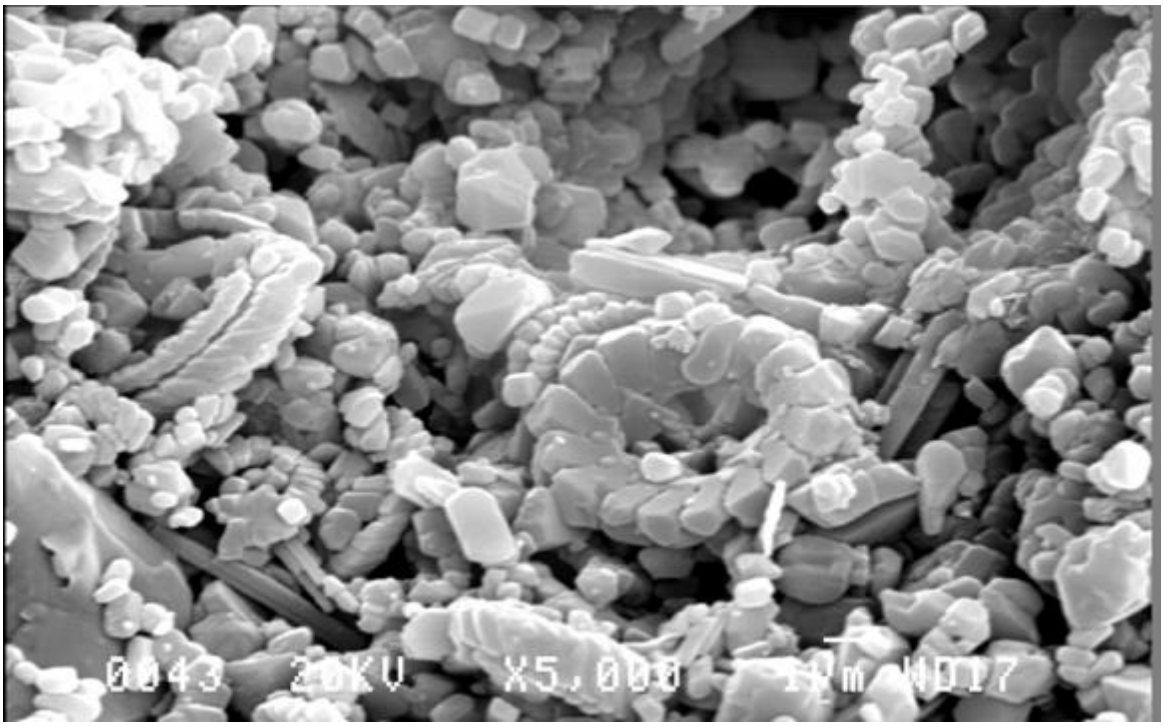

Figure 2: SEM picture of chalk showing the coccolithic rings, ring fragments and pore space.[35]

Chalk is finely grained and is usually of high porosity because of small pores, visible as black spots in Figure 2, but with low permeability because of microscopic size of the constituents.

2.1.3. Outcrop Material

For study purposes in the laboratory, outcrop chalk material is often used as a representation of the reservoir rock. Outcrop chalk is cheap and readily available, unlike the real reservoir rock samples. Despite of similar lithology, chalk behaves differently (Milter and Øxnevad, 1996). Therefore, it's a prerequisite to select the outcrop material for experiments. The geological descriptions of four types of outcrop chalks, Stevns Klint, Aalborg, Liége and Beer Stone are shown in Table 1.

	Stevns Klint	Aalborg	Liége	Beer Stone
Origin	Sigerslev, Denmark	Roerdal, Denmark	Halembaye, Belgium	Beer, England
Geologic age	Maastrichtian	Maastrichtian	Campanian	Turonian
Silica Content (wt%)	~1	2-7	<2	-
Porosity (%)	45-50	45	40	24-30
Permeability (mD)	2-5	3-5	1-2	1-2
Specific Surface area (m^2/g)	~2	~2	~2	1

Table 1: Geological descriptions of Stevns Klint, Aalborg, Liége[35] and Beer Stone (Milter and Øxnevad, 1996).

2.2. Oil Recovery Mechanisms

Oil Recovery operations traditionally have been subdivided into three stages: Primary, secondary, and tertiary. These stages are described the production from a reservoir in a Chronological sense, not necessarily, based on the situation of their applicability. Primary production, the initial production stage, resulted from the pressure energy naturally existing in a reservoir. Secondary recovery, is the second stage of operations, usually was executed after primary production declined. Traditional secondary recovery processes are water flooding, pressure maintenance, and gas injection, although the term secondary recovery is now almost synonymous with water flooding. Tertiary recovery, the third stage of production, was that obtained after water flooding. Tertiary processes used miscible gases, chemicals, and/or thermal energy to displace additional oil after the secondary recovery process became uneconomical (Green and Willhite, 1998). But it's not necessary that these stages are conducted in their chronological order.

2.2.1. Primary Recovery

When Oil recovered with the natural energy present in the reservoir as the main source of energy for the oil displacement to the surface. In other words, reservoir pressure is uses as the primary source of oil recovery. The natural mechanism contributes in the oil recovery are Solution-gas drive, gas-cap drive, natural water drive, fluid and rock expansion, and gravity drainage. The recovery factory obtained from primary recovery methods is 5-50% of original oil in place Green and Willhite, 1998).

2.2.2. Secondary Recovery

As the pressure in the reservoir decline, primary recovery of oil starts decreasing. So recovery obtained by augmentation of the natural energy, i.e. reservoir pressure by means of gas injection or water injection to displace oil towards the producing wells. Gas injected either into a gas cap for pressure maintenance and gas cap expansion or into an oil column wells to displace oil[18]. In this case to maintain the pressure other methods are water flooding, water alternating gas (WAG) injection. Today water flooding is considered as secondary recovery method. The recovery factor could boost up to 30-50% after water flooding.

2.2.3. Tertiary Recovery/EOR

After secondary recovery methods become uneconomical and still there is significant amount of oil left in the un-swept part of reservoir, that is where tertiary oil recovery methods come into picture. In some situations, the so-called tertiary recovery methods might act as secondary recovery operations. Because of such situations, tertiary recovery can also be defined into "Enhanced Oil Recovery".[18] Tertiary oil recovery can be achieved by numerous means (Green and Willhite, 1998), such as:

2.2.3.1. Mobility-Control Process

The main purpose of this process is to develop a favorable mobility ratio between injected solution and oil bank. Which eventually generate a uniform volumetric sweep of reservoir. An unfavorable mobility ratio creates viscous fingering which causes an early breakthrough (Green and Willhite, 1998).

2.2.3.2. Chemical Processes

Chemical processes involve the injection of surfactant and polymers that effectively displace oil because of their phase-behavior properties. The motive behind injecting chemical is to decrease the IFT between the displacing liquid and oil, which keep the discontinuous oil drop or films mobilize and improve the sweep efficiency (Green and Willhite, 1998).

2.2.3.3. Miscible Processes

The main objective is to displace oil by injecting a fluid, which is miscible with oil at the existing conditions. The CO_2 miscible process is one such process. In which volume of pure CO_2 is injected to mobilize and displace the oil (Green and Willhite, 1998).

2.2.3.4. Thermal Processes

Thermal processes are classified into hot-water floods, steam processes, and in-situ combustions. Sweep efficiency increases by means of several mechanisms such as viscosity reduction, steam flashing, oil swelling, and steam stripping (Green and Willhite, 1998).

2.2.3.5. Low salinity water flooding

By altering the ion composition of injecting brine helps in improving the sweep efficiency. LSWF majorly depends on the rock, oil and brine interaction. Some of the most relevant previously proposed mechanisms are[2]:

- Migration of fines (Tang and Morrow, 1999).
- Multi-ion exchange (MIE) (Lager et al., 2008).
- Extension of the electrical double layer (Ligthelm et al., 2009).

2.3. Displacement Forces involved in Recovery Mechanism

This section involves understanding of forces acting in trapping and mobilization of phases in the pores. These forces include Capillary forces, viscous forces, and gravity forces, which govern phase trapping and mobilization of fluids.

2.3.1. Capillary Forces

A pressure difference exists across the interface between two immiscible fluids. From equation (1)[18], we can relate that capillary pressure is related to fluid/fluid IFT, relative wettability (θ), and the size of the capillary (r) (Green and Willhite, 1998).

$$P_c = \frac{2\sigma_{ow} cos\theta}{r} \quad (1)$$

Where:

P_c: Capillary Pressure

σ_{ow} : Interfacial Tension

θ: Contact Angle

r: Capillary radius

2.3.2. Viscous Forces

Viscous forces are defined in terms of pressure difference, which forces the fluid to flow through the pores. To force the fluid through the pores viscous forces should be greater than the capillary forces. The pressure drop caused by viscous forces between the reservoir fluid and the pore walls is given by equation (2) (Green and willhite, 1998):

$$\Delta P = -\frac{8\mu LV}{r^2} \qquad (2)$$

Where:

ΔP: Pressure drop

μ: Viscosity

L: Length of the pore filled with the phase

V: Velocity

r: radius of pore

2.3.3. Gravity Forces

Gravity forces plays an important role in mobilization of fluids due the density differences between displaced and displacing fluid. In presence of fluids with different densities, fluid with lower density have density to flow upwards. Gravity force can be shown with following expression[6]:

$$\Delta P_g = \Delta\rho . g . h \quad (3)$$

Where:

ΔP_g: Pressure drop due to gravity forces

Δρ: Density difference between fluids

g: Gravitational forces

h: Height

2.4. Wettability

Wettability is the tendency of one fluid to spread on or adhere a surface in presence of another fluid. Wettability describes the distribution of fluids in pores of the rock. When two fluids are present simultaneously in the pore, one fluid has stronger tendency to adhere the rock surface than the other does. The stronger phase called as wetting phase. Rock wettability affects the nature of fluid saturation and relative permeability in the fluid/rock system (Green and Willhite, 1998).

2.4.1. Classification of Wettability

Wettability can be classified as strongly-oil wet, strongly-water wet, and intermediate wet, as shown in Figure 3.

In strongly-oil wet rock, trapped oil is held in smaller cracks and fractures and water trapped as isolated phase in the larger pores.

In strongly-water wet rock, water trapped in small cracks and oil trapped in larger pores.

If rock is wetted by both the fluids in proportions, but fluid which is slightly more attracted to rock than the other called as intermediate wet rock.

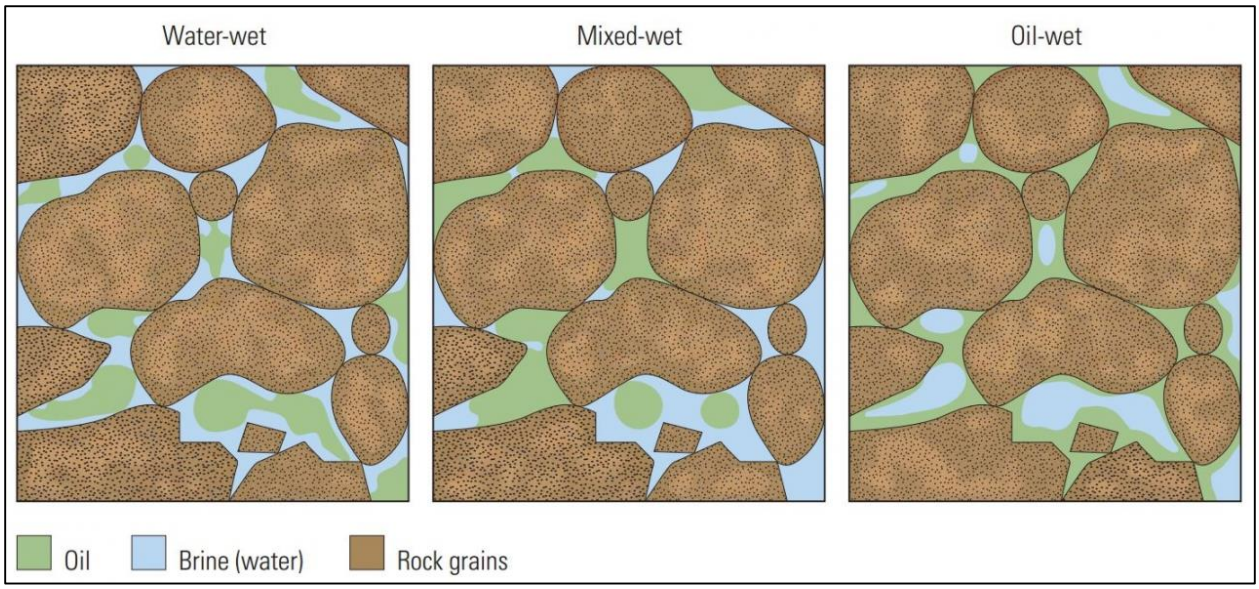

Figure 3: Fluid distribution in different wetting conditions.

2.4.2. Methods of Wettability Measurements

Various methods have been developed, both qualitative and quantitative, to estimate wettability of rock/fluid system (Anderson et al, 1986). Qualitative methods (Anderson et al) are: imbibition rates, microscope examination, floatation, glass slide method, relative permeability curves permeability/saturation relationships, capillary pressure curves, capillarimetric method, displacement capillary pressure, reservoir logs, nuclear magnetic resonance and dye adsorption, and quantitative methods are: contact angles, imbibition and forced displacement (Amott[5]), USBM and electrical resistivity wettability method.

2.4.3. Contact Angle

By measuring the angle of contact at the surface shows the tendency of spreading of a liquid on the surface (Ahmed Tarek, 2001). A contact angle, θ, is the angle between the fluid-solid interfaces measured with respect to water phase, for an oil-water system. If $\theta < 90°$ then the system is water-wet, $\theta > 90°$ then system is water-wet, and $\theta \sim 90°$, then system is considered mixed-wet (Nnaemeka Ezekwe, 2011).

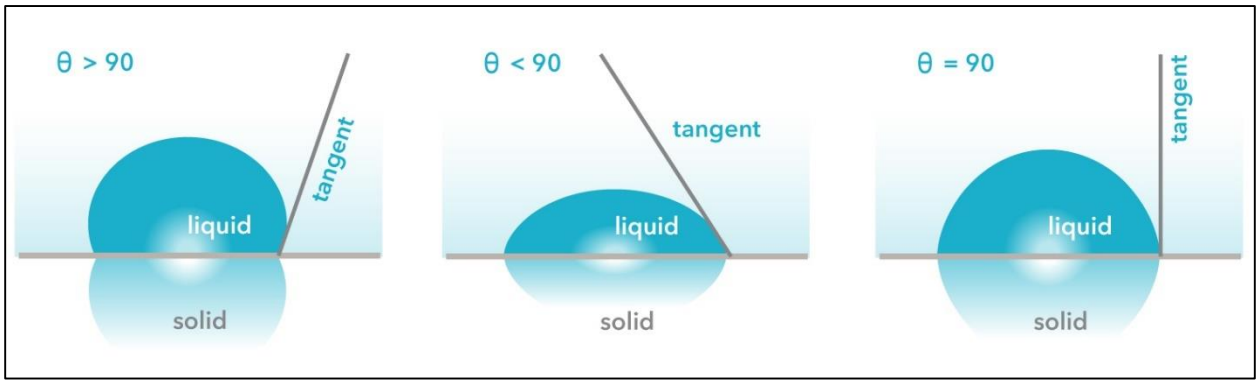

Figure 4: Contact angle representation. Oil wet, Water wet, and Mixed wet.

2.5. Rock Properties

The properties of reservoir rocks with respect to the fluids they contain and with respect to the fluids that will be injected into them are important when characterizing a reservoir in terms of its reserves and the mobility of the fluids.[43] Knowledge of these properties are important to understand the characteristics of a reservoir (Ahmed Tarek, 2001).

2.5.1. Porosity

Porosity of a rock is defined as the capacity of rock to hold the reservoir fluids (Ahmed Tarek, 2001). In addition, the porosity is the ratio between the pore volumes of the rock to the bulk volume of the rock. It can be expressed by equation (4):

$$Porosity\ (\varphi) = \frac{Pore\ Volume}{Bulk\ Volume} \quad (4)$$

One method of classifying reservoir rocks, therefore, is based on whether pore spaces (in which the oil and gas is found) originated when the formation was laid down or whether they were formed through subsequent earth stresses or ground water action.[43]

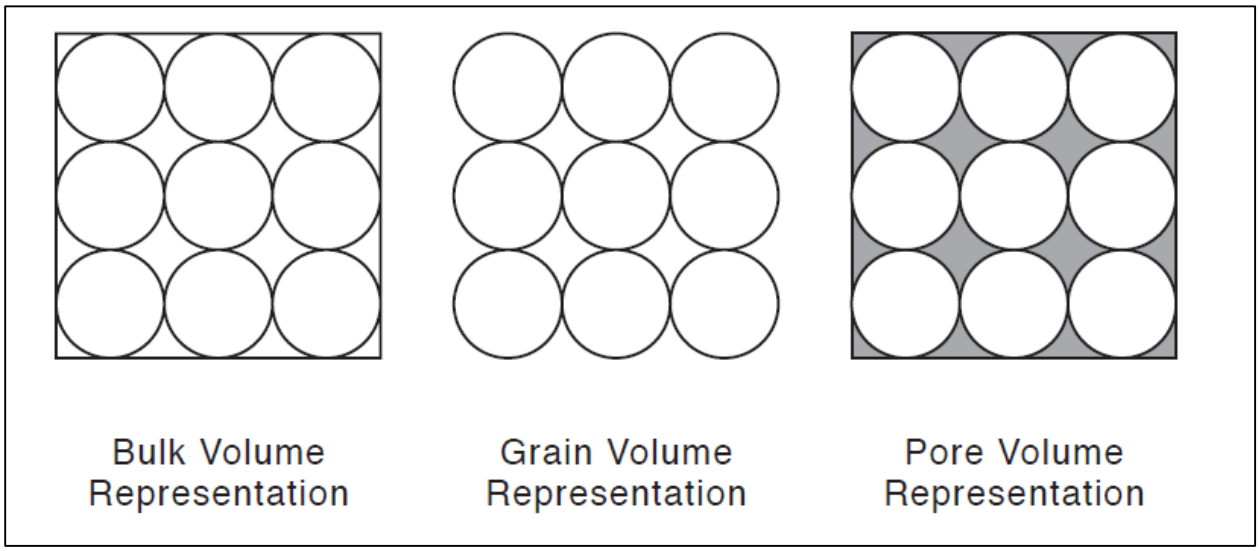

Figure 5: Representation of bulk, grain, and pore volume.[43]

Due to deposition, some void spaces that developed became isolated from the other void spaces by excessive cementation. Thus, many of the void spaces are interconnected while some of the pore spaces are completely isolated (Ahmed Tarek, 2001). Based on void spaces, there are two types of porosity:

- Absolute Porosity
- Effective Porosity

➢ **Absolute Porosity**

It is defined as ratio of total void spaces to the bulk volume.

- **Effective Porosity**

The effective porosity is the percentage of interconnected pore spaces with respect to the bulk volume.

Carbonates, especially chalk, has comparatively high range of porosity value, and varies from 5% to 40%. Stevens Klint chalk used in this study have comparatively high porosity ~40-45%.

2.5.2. Permeability

Permeability is the capacity and ability of rock to transmit the fluid through the interconnected pores. The permeability, k, is an important factor because it controls the movement and flow of the reservoir fluids (Ahmed Tarek, 2001).

The equation that describes the permeability is known as Darcy's law. If a horizontal, linear flow of an incompressible fluid is established through a core sample of length L and a cross-section of area A, and then the governing fluid flow equation is defined as

$$q = -\frac{kA}{\mu}\frac{dP}{dL} \quad (5)$$

Where:

q: fluid flow rate through porous media

A: cross-sectional area

k: permeability

μ: viscosity

dP/dL: pressure drop per unit length

If one or more than one fluid is present, then the permeability of rock with respect to individual fluid will be different. Based on this, permeability is classified as:

- **Absolute Permeability**

If the rock is fully saturated with a single fluid, then the permeability is called as absolute permeability.

- **Effective Permeability**

When the pore spaces are occupied by more than one fluid, then the permeability measured is the effective permeability. For instance, the effective permeability of a porous medium to oil is the

permeability to oil when other fluids, including oil, occupy the pore spaces (Nnaemeka Ezekwe, 2011).

- **Relative Permeability**

It is defined as the ratio of effective permeability to absolute permeability of the porous medium. It is represented graphically in plots called relative permeability curves. Relative permeability curves are represented by (Green and Willhite, 2001):

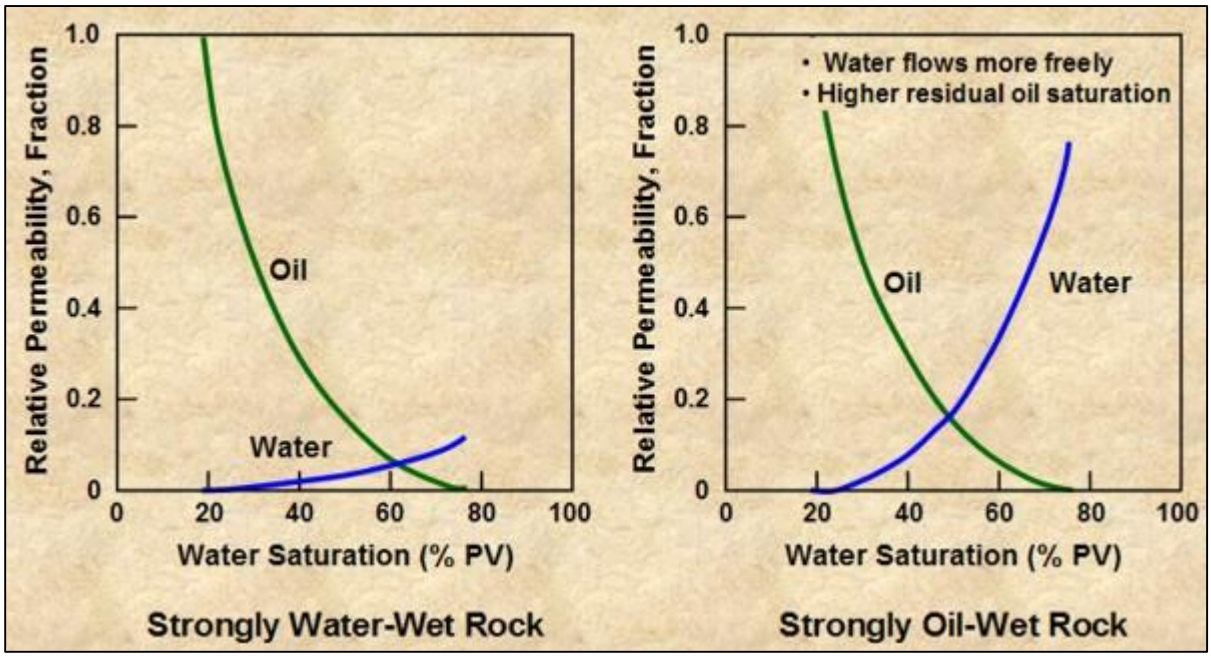

Figure 6: Oil-water relative permeability curves for oil wet and water wet rock (Green and Willhite, 2001).

2.6. Low Salinity Flooding in Chalk

Low salinity water flooding has been shown to improve both secondary and tertiary recovery in core floods (Yildiz and Morrow 1996; Lager et al. 2008). Low salinity water-flooding is an enhanced oil recovery technique that is especially attractive due to its relatively low cost, its simple operational design and its low environmental risk. It has been observed by these researchers that injection of brine with a different composition than formation water or seawater, may give an increase in recovery and acts as secondary or tertiary injection fluid.

Several mechanisms were proposed which helps in improving oil recovery by injection of low salinity water. The debate about the primary mechanism of IOR by low-salinity water creates some uncertainties about the success and the optimum conditions of the application of low-salinity water-flooding on the field scale (Ramez A. Nasralla and Hisham A. Nasr-El-Din, 2014). The main proposed low salinity mechanisms are:

2.6.1. Fines Migration

An attempt was made by Tang and Morrow (1999) to explain migration of fines in low salinity flooding. They observed that migration of fines and wettability alteration is interlinked. Previous work has also shown that water flooding works in case of water-wet conditions. In presence of high salinity brine, clay minerals remain undisturbed, which makes rock oil-wet and results in poorer sweep efficiency. On the other hand, they found removal of fines from the surface in case of low salinity brines. They concluded that fines mobilization resulted in exposure of underlying surfaces, which increased water-wetness of the system.[27] Removal of particles block the pore throats and diverts the flow to the un-swept area thus improves the sweep efficiency (Figure 7). The mechanism of fines migration was explained by the Deryaguin-Landau-Verwey-Overbeek (DLVO) theory of colloids (Deryaguin and Landau, 1941; Verwey and Overbeek, 1948). The permeability reduction occurs if the ionic strength of the injected brine is equal to or less than, the critical flocculation concentration (CFC), which is strongly dependent on the relative con centration of divalent cations such as Ca^{2+} and Mg^{2+} (Khilar et al., 1990). Divalent cations have been known to stabilize the clay by lowering the zeta potential resulting in the lowering of the repulsive force.

Tang and Morrow, 1999, has shown that fine migration is likely to occur during the low salinity flooding. However, enhancement in oil recovery has also observed without any fine migrations.

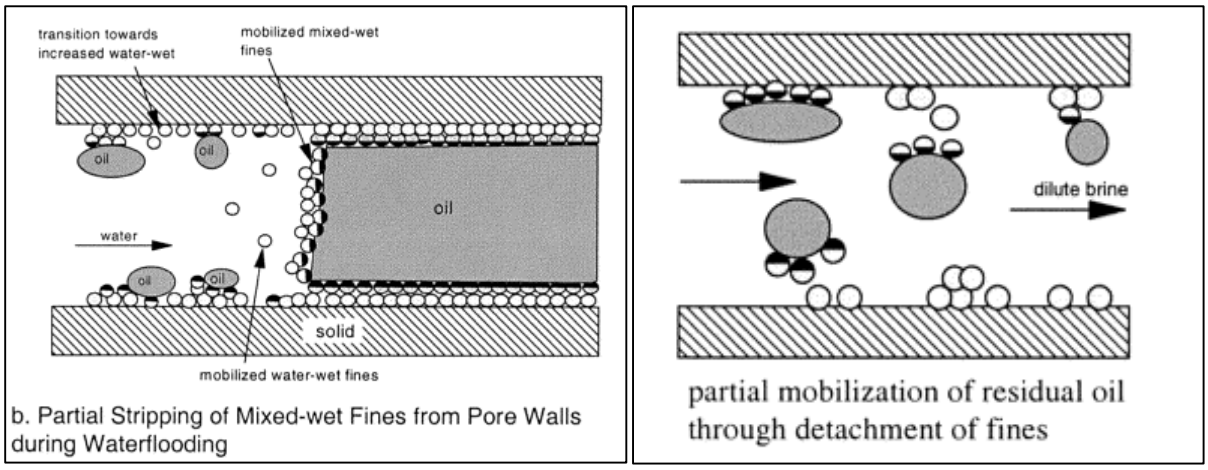

Figure 7: Fine migration mechanism (Tang and Morrow, 1999)

2.6.2. pH Increase

Some studies have shown a rise in pH during low salinity production laboratory experiments (Figure 8). There are mainly two reasons for increase in pH are: 1) dissolution of minerals, 2) exchange of cations.

Dissolution of carbonate results high amount of hydroxyl ions (OH^-) and cation exchange between the rock and the brine, which could explain the pH increase.

Dissolution reactions expressed by Lager et al, 2008:

$$CaCO_3 \leftrightarrow Ca^{+2} + CO_3^{-2} \quad (6)$$

$$CO_3^{-2} + H_2O \leftrightarrow HCO_3^- + OH^- \quad (7)$$

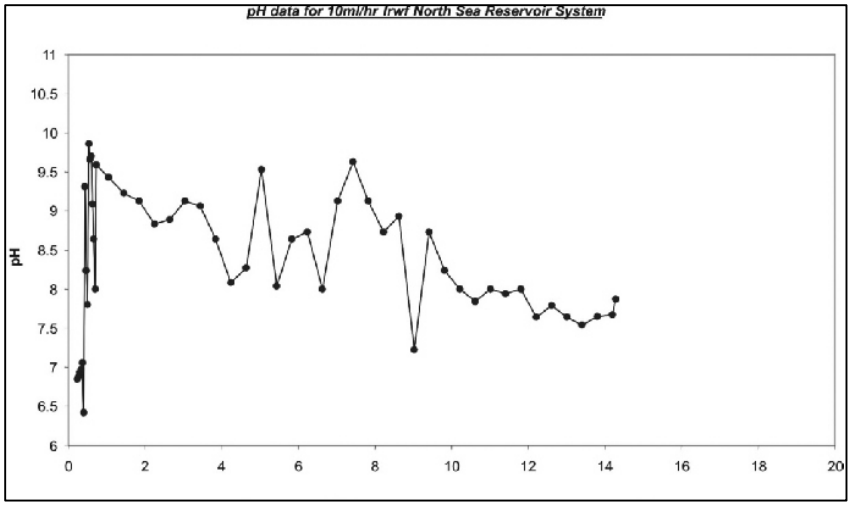

Figure 8: pH variation during a low salinity flood (Lager et al, 2008)

However, in cation exchange process, the mineral surface will exchange H^+ ion in the brine. This decreases H^+ concentrations in the brine, resulting increases in pH. Speed of reactions depend on the amount of calcite mineral present.

Lager et al, 2008, stated that if a pH of above 9 was observed inside the reservoir then it would consider equivalent to alkaline flooding. They added that the increase in pH level allows the reaction of some of the oil compounds that result in generation of in-situ surfactants. Hence, the oil recovery could also be increased from the production of surfactant and interfacial tension reduction, by increase in pH.

2.6.3. Multicomponent Ion Exchange

Sposito[38] stated that Vander Waals interactions, ligand exchange and cation bridging are some of the dominant adsorption mechanisms. According to DLVO theory, at high ionic strengths Vander Waals forces allow particles to be located close to each other. Ligand exchange occurs when carboxylate groups substitute hydroxyl group[38]. In cation bridging, a cation acts as a bridge between a negative charged surface and negatively charged functional groups (Arnarson and Keil, 2000).

Lager[25] observed that presence of divalent ions is essential in order to achieve multi-component ion exchange (MIE), hence, increase in recovery by injecting a low salinity brine. Second

observation was made that decrease in Mg^{+2} concentration in effluent indicates adsorption of magnesium ion.

Low concentration of divalent ions in low salinity brine causes MIE to take place between adsorbed crude oil components, cations in brine and clay surfaces[37]. The result is that organic polar compounds and organic-metallic complexes are removed from the surface, causing increase in water-wetness and an increase in oil recovery.

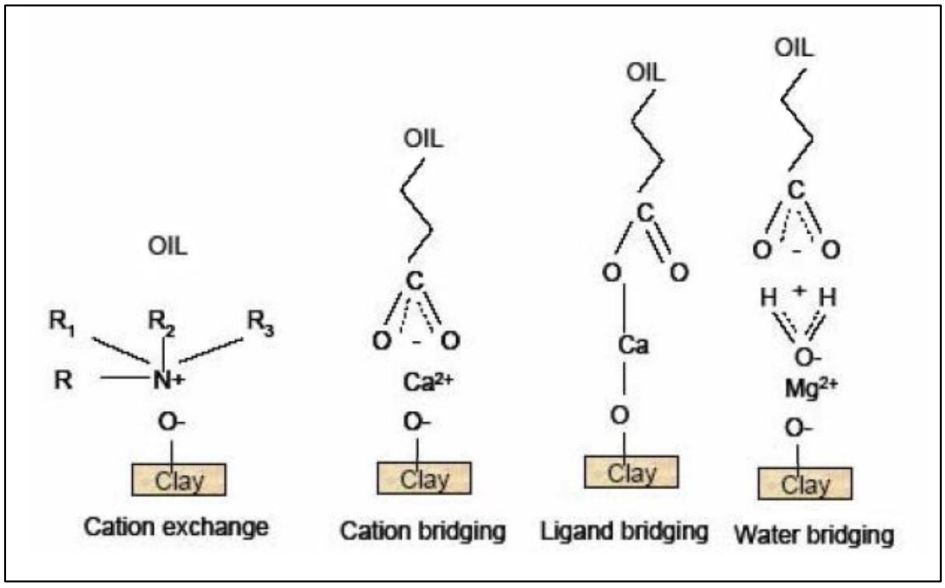

Figure 9: Adsorption mechanisms (Webb et al., 2008) (adapted from[37])

2.6.4. Double layer Effects

An electrical double layer is a thin surface layer of spatially separated opposite electrical charges, formed at the interface of two phases (Figure 10). According to Ligthelm, in case of low salinity brine injection, cations have the lower ability to take down the negative charges of the oil and clay. Which increase the repulsive forces between the oil/water and rock surface. Hence, helps in releasing of oil components and increase in oil recovery. In practical terms, in a high saline environment, polar components of oil form organo-metallic complexes by adsorbing on surface (Zhang et al, 2006). This changes wettability of rock to the less water-wetness.

When low salinity brine is injected, the ability of cations to screen off the negative charges between oil and rock is reduced; electrical double layer expands and repulsive forces increases. This scrape off the oil molecules from surface and increase in oil recovery.

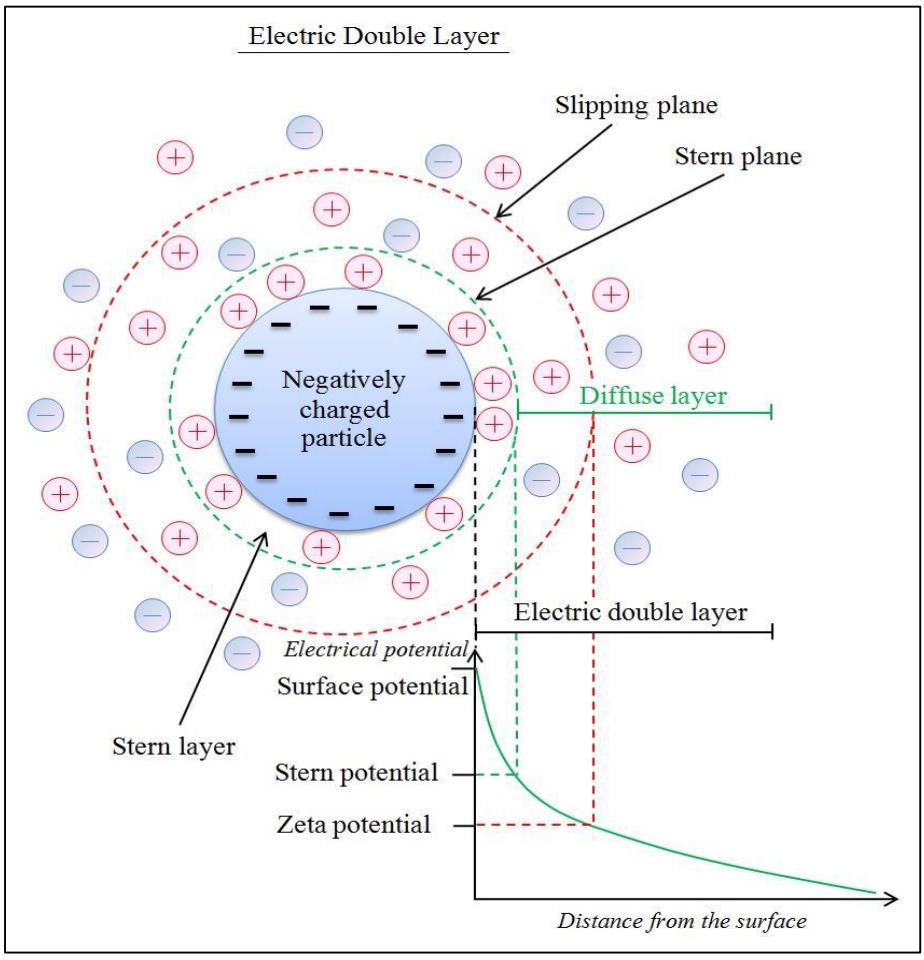

Figure 10: Double layer structure near the negatively charged surface (Ramez A. Nasralla and Hisham A. Nasr-El-Din, 2014).

3. Experimental Work

Flooding experiments were performed in order to evaluate the EOR methods. This way we will be able to suggest an effective brine composition which leads to a significant increase in oil recovery. In this section we will discuss mainly about the experimental procedure, apparatus, and materials used.

This section includes core details, fluid properties, operating conditions, brine composition, preparation & execution of experiments and analysis after.

3.1. Experimental materials

3.1.1. Porous Media

Stevens Klint, Denmark, chalk is used as the porous media for the experiments. Similar cores were created from the same rock. Stevns Klint chalk is comparable stratigraphically to the interval including the uppermost Tor formation and the lower Ekofisk formation in North Sea chalk reservoirs (Hamouda et al, 2014b). All the core details such as, porosity, initial water saturation (S_{wi}), Residual Oil Saturation (S_{or}) etc. are given in Table 10 & 11. Some common details of each core are given in Table 2.

Length(cm)	6.00
Diameter(cm)	3.78
Permeability(mD)	3.9

Table 2: Physical Core Data

3.1.2. Oil Details

For experiments both crude oil and model oil is used. Model-oil-a mixture of n-decane and stearic acid was used for the flooding experiments. The concentration of stearic acid in n-decane is 0.005 mole/L. n-Decane was supplied by Chiron AS at 99% purity. Aldrich supplied stearic acid at 98.5% purity. The physical properties of synthetic oil are:

Property	Value at 20 °C	Value at 50 °C	Value at 70 °C
Density (g/cc)	0.73	0.705	0.67
Dynamic Viscosity (cP)	0.92	0.61	0.41

Table 3: Model Oil Properties

A crude oil X, of a composition given in Table 5, is also used for experiments. The physical properties and composition of the crude is given in Table 4 & 5.

Property	Value at 25°C	Value at 50°C	Value at 70°C
Density (g/cc)	0.845	0.7009	0.7537
DynamicViscosity (cP)	0.76	0.5938	0.4976

Table 4: Crude Oil Properties

Also,

Components	**Mole Fraction**
i-C5	1.79E-05
n-C5	0.000117
C6	0.002371
C7	0.013287
C8	0.039608
C9	0.062886
C10	0.881712

Table 5: Crude Oil Composition

3.1.2.1. Acid Number (AN) and Base Number (BN) measurements

The automatic titrator was used to determine the acid and base numbers of the oil. The automatic titrator used in this experiment was Mettler Toledo DL55 as shown in Figure 11. Different types of solvent were used for the measurement of AN and BN, however the procedure was the same. Procedures of AN and BN measurement are presented in the Appendix A.2, in detail. AN and BN for Crude Oil X are 0.05 and 0.6 mgKOH/g, respectively.

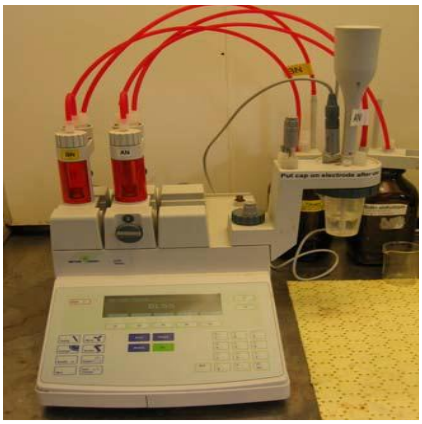

Figure 11: Automatic Titrator to measure AN & BN[38]

3.1.3. Brines

Synthetic Seawater (SSW) was used in initial saturation of core and also as a primary injection brine in flooding sequence. As a secondary brine, brines with different ionic composition were prepared and injected. Overall, 6 modified brines are prepared, with different salt concentrations and dilution ratio, into distilled water (DW). The composition of all the brines are given in Table 6.

Ions/Brine	SSW (mole/l)	LSW 1:10 (mole/l)	LSW 1:50 (mole/l)	Mg+NaCl 1 to 10 (mole/l)	SO_4^{2-} brine 1 to 10 (mole/l)	SO_4^{2-} brine 1 to 50 (mole/l)	Mg^{2+} brine 1to 10 (mole/l)
HCO_3^-	0.002	0.0002	0.00004				
Cl^-	0.525	0.0525	0.0105	0.0493			0.009
SO_4^{2-}	0.024	0.0024	0.00048		0.0024	0.00048	
Mg^{+2}	0.045	0.0045	0.0009	0.0045			0.0045
Ca^{+2}	0.013	0.0013	0.00026				
Na^+	0.45	0.045	0.009	0.0403	0.0046	0.00092	
K^+	0.01	0.001	0.0002				
TDS(ppm)	33388	3338.8	667.76	2785	336.2	67.24	423
TDS (g/l)	33.33	3.33	0.667	2.78	0.336	0.067	0.423
Ionic Strength	0.657	0.0657	0.01314	0.0538	0.007	0.0014	0.0135
pH	7.83	7.32	6.74	5.85	7.12	6.74	6.11

Table 6: Ion Composition in Brines

The ionic strength of the solution is defined as (Burgot J.L., 2012):

$$I_c = \frac{1}{2}\sum_i C_i \cdot Z_i \quad (6)$$

Here, the concentration C_i of i ion is multiplied by square of its charge Z_i, with the sum of all the ion terms. I_c is expressed in mole/L, thus explaining the subscript (Burgot J.-L., 2012). Also the physical properties, densities and viscosities, of brines are given in Table 7&8. So, densities of brines are given as:

	Density (g/cc)		
brine	**At 20°C**	**At 50°C**	**At 70°C**
SSW	1.024	1.012	1.002
LSW 1:10	1.001	0.991	0.980
LSW 1:50	0.998	0.989	0.978

Table 7: Density of Brines

and, the viscosities of brines are given as:

	Viscosity (mPa.s)		
brine	**At 20°C**	**At 50°C**	**At 70°C**
SSW	1.073	0.592	0.440
LSW 1:10	1.008	0.551	0.407
LSW 1:50	1.002	0.546	0.404

Table 8: Viscosity of Brines

3.1.3.1. Brine Preparation

All the LSW, Single and two salts brines were prepared by mixing the salts into the DW and diluting them as per the required ratio. LSWs are prepared by dilution of SSW as per the required

ratio. To prepare 1 liter of SSW, all the salts (in standard amount) are added into 1L of DW. Salts and the amount, which are required to prepare SSW are:

Salt	Amount (g/l)
NaCl	23.38
$NaHCO_3$	0.17
KCl	0.75
$MgCl_2*6H_2O$	9.05
$CaCl_2*6H_2O$	1.91
Na_2SO_4	3.41

Table 9: Salt content in SSW.

After addition of salts into DW, this non-filtered water was left for mixing, for few hours. After proper mixing, SSW was filtered using 0.22µm filtered paper. The schematic of the filtration setup is shown in Figure 12. The setup consists of a vacuum pump, a Büchner flask, a filtering funnel and an adapter for sealing. The filtering paper is placed between funnel and another flask.

Figure 12: Brine Preparation: Filtration setup[27]

3.2. Core Preparation and Flooding

Core flooding is the main part of the experiments. To prepare the system and core for main flooding, few necessary preparations are required. Before flooding the core, creating initial water saturation (S_{wi}) and aging of core is mandatory.

3.2.1. Initial Water Saturation

To simulate the reservoir condition at lab scale, creating initial water saturation and aging of core becomes necessary**.**

The chalk cores were first dried at 100 °C for several days to remove all water that might be contained in the pore spaces. Cores are weighted every day, until the weight of core becomes constant. Weighing is done using the Mettler Toledo PM4600 DeltaRange Balance.

Figure 13: Weighing balance

After measuring the dry weight of the core, dimensions (diameter, length) are measured. Then, they were then saturated with SSW using a vacuum setup (Figure 14).

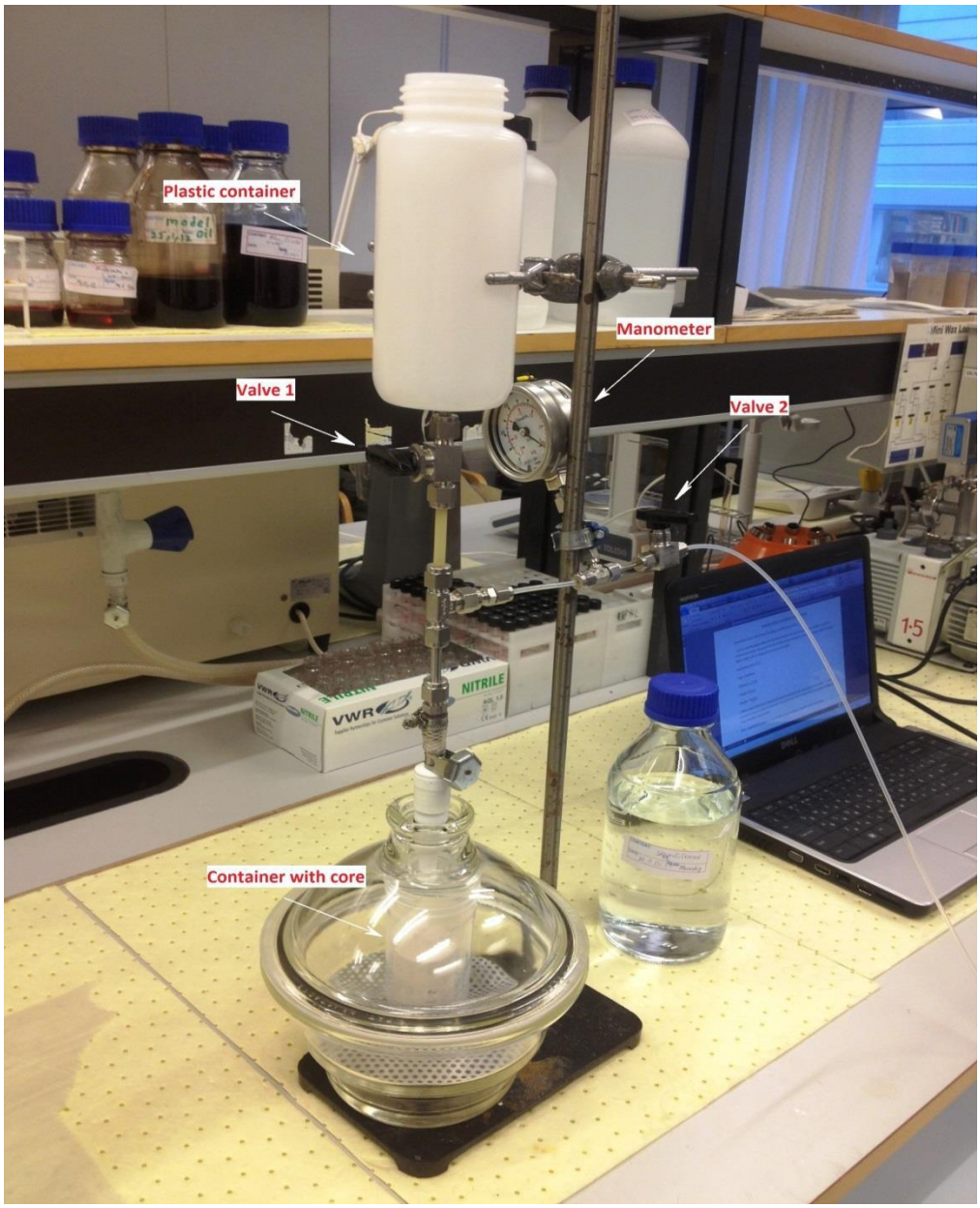

Figure 14: Vacuum setup for Core Saturation[27]

Vacuum setup creates vacuum in glass airtight bowl by using pump (manometer shows a pressure of -1bar) and thereby removing air from pore space. Then SSW from upper plastic container goes to the top of the core by slowly opening Valve 1. Core is fully saturated when manometer shows atmospheric pressure and all water came to the container with core.

After saturation, weight of the wet core is measured. Then pore volume of core is calculated using,

$$Pore\ Volume\ (PV) = \frac{M_{wt} - M_{dry}}{\rho_{ssw}} \quad (7)$$

Where;

M_{wt} = Weight of the wet core

M_{dry}= Weight of th dry core

ρ_{ssw}= Density of SSW, 1.013g/cc

and porosity is given by,

$$\varphi = \frac{PV}{V_B}, V_B = \frac{\pi \cdot d^2 \cdot L}{4} \quad (8), (9)$$

Where;

φ= Porosity

V_B= Bulk Volume

d= Diameter of core

L= Length of core

The cores were flooded with the synthetic oil to establish initial water saturation, for this core is placed into Hassler core holder (Figure 15).

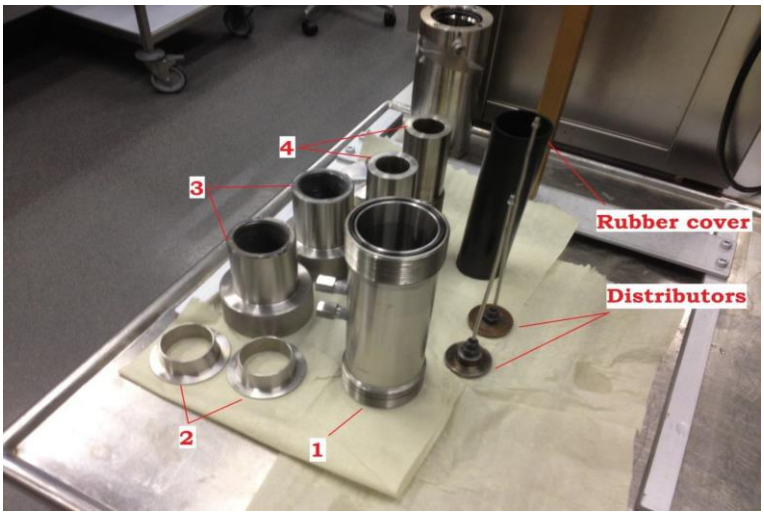

Figure 15: Hassler Core Holder[27]

Core was placed on the distributors and wrapped up by Teflon tape. To avoid any fluid escape from the core, a plastic cover was place on the core and heated up to establish a tight fit.

Figure 16: Core wrapping, Heating of plastic cover &putting rubber cover[27]

The core was then placed inside the oven. The setup (Figure 17) consists of manometers, pumps, and outlet separator. Core was placed inside the oven and connected to the inlet pump and the outlet valve. The initial water saturation process was taking place at 50 °C.

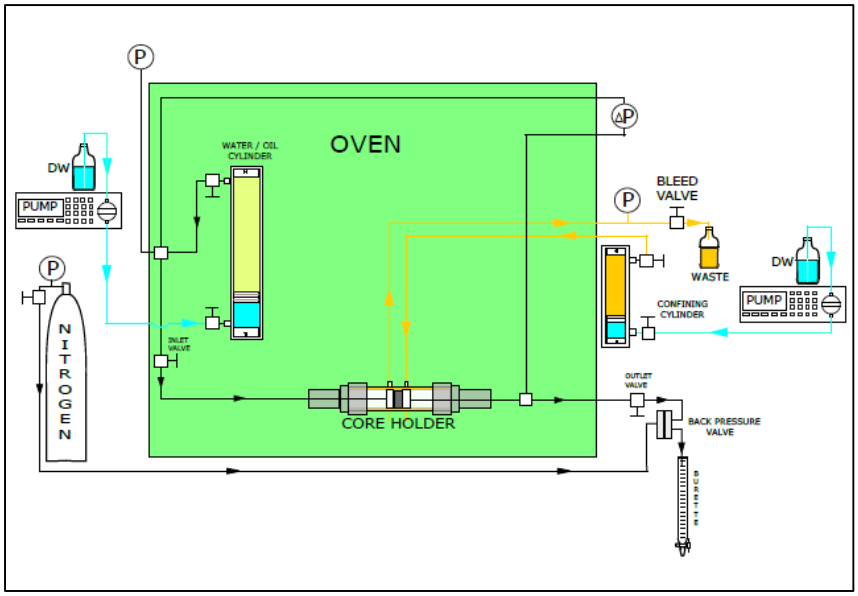

Figure 17: Schematic of flooding system

Cores were aged to simulate the cores to reservoir condition. After establishing initial water saturation, cores were aged with the same oil for 2 weeks at 50°C.

3.2.2. Core Flooding

After two weeks of aging, the cores were flooded by different brines. Flooding preparation procedure is similar to the saturation procedure.

Once the cores were aged, they were flooded with different brines at 70 °C. The confining pressure was set at 25-30 bar, to simulate reservoir conditions and give a good seal between the shrinkable sleeve and core and the outlet pressure at 9-10 bar. For all floodings, either brine or oil injection, the core was weighed before and after to check for any discrepancy between the measured volumes and calculated saturations. Each core was flooded for at least 4 PV (PV = pore volume) at the low flow rate of 4 PV/day, and then at 4 PV at the high flow rate of 16 PV/day. The schematic of system is shown in Figure 17. The pressure drop across the core was measured by the manometer, and the data were transferred to the computer and saved using the Labview program.

3.2.3. pH analysis and Ion Chromatography

The pH values of the effluent were measured using a Mettler Toledo pH meter at intervals according to the data plotted (Figure 18).

Figure 18: pH Meter[27]

The quantities of anions and cations in the effluent were measured using a Dionex ICS-3000 chromatograph. Data were processed manually after the analyses using the Chromeleon 7 program (Figure 19).

Figure 19: Dionex ICS-3000 chromatograph

4. RESULTS AND DISCUSSION

In this part of thesis, we will discuss the results obtain from the experiments performed and a detailed interpretation will be drawn out of it, to study the behavior of brines with modified composition. All the cores are SK-chalk with almost same dimensions. In all of the experiments performed, cores are flooded with SSW and brine with modified composition/LSW as primary and secondary injection brine, respectively.

4.1. Core Floods overview

Details of cores and core flooding are:

- Total 8 experiments were performed for the study.
- All cores are SK-chalk, Denmark.
- Dimensions are almost same for all cores.
- 6 experiments were performed with Model Oil (N-Decane + SA) & 2 experiments were performed with Crude Oil X. Composition of crude oil X is given in table.
- 2 flooding sequences:
    - Primary Flooding – SSW
    - Secondary Flooding – Brines with tuned composition
- Secondary flooding Brines:
    - SO_4^{2-} Brine (Diluted 1: 10 and 1:50)
    - Mg^{+2} Brine (Diluted 1:10)
    - LSW (Diluted 1:10 and 1:50)
    - Mg^{+2} + NaCl Brine (Diluted 1:10)
- All the experiments have been performed at 70°C except one, which is performed at 90°C.

Physical parameters and other details: Length, Diameter, Pore volume, Porosity, Initial water saturation (*Swi*), Permeability and Flooding Sequences are shown in the Table 10 & 11. The only differences among all the cores are: *Porosities, Pore volumes, Swi and Flooding Sequences*. Since Cores are saturated with Model Oil and Crude Oil, so core details are shown in the tables accordingly.

Core	Length (cm)	Diameter (cm)	*Swi* (%)	Pore Volume (ml)	Porosity (%)	Permeability (mD)	Flooding Sequence
SG-1	5.92	3.78	23	34.23	51.8	3.9	SSW/SO_4^{2-} Brine (1:10)
SG-2	6.01	3.78	21	34.23	51.8	3.9	SSW/Mg^{2+} Brine (1:10)
SG-3	5.97	3.78	29	30.75	49.17	3.9	SSW/LSW (1:50)
SG-4	5.95	3.78	22.3	31.94	50.12	3.9	SSW/SO_4^{2-} Brine (1:50)
SG-7	6.00	3.78	21.8	34.8	52.22	3.9	SSW/ Mg^{2+}+NaCl Brine (1:10)
SG-8	6.00	3.78	28.5	33	50.99	3.9	SSW/Mg^{2+} Brine (1:10) at 90°C

Table 10: Core details and Flooding Sequence (core saturated with Model Oil).

Core	Length (cm)	Diameter (cm)	*Swi* (%)	Pore Volume (ml)	Porosity (%)	Permeability (mD)	Flooding Sequence
SG-5	6.008	3.78	19.01	32.50	50.55	3.9	SSW/LSW (1:10)
SG-6	6.00	3.78	21.1	34.50	52.04	3.9	SSW/LSW (1:50)

Table 11: Core details and Flooding Sequence (core saturated with Crude Oil X).

4.2. Flooding in Core SG-1 with SSW/ SO_4^{2-} Brine (1:10)

After saturating the core with Model oil to create initial water saturation core was kept in aging cell for 2 weeks in the aging oven for 50°C. After aging, the core was flooded with SSW, followed by SO_4^{2-} Brine at a constant temperature of 70°C. The experiment runs in 2 phases: In first phase 4 PV of SSW was injected at a rate of 4PV/day (0.095 ml/min). The next 4 PV of SSW were injected at an increased injection rate of 16 PV/day (0.38 ml/min), in order to increase the injection pressure to overcome capillary pressure to displace the trapped oil.

In second phase, the cylinder of SSW was replaced by cylinder of SO_4^{2-} brine by stopping the pump and closing the inlet valve. The flooding sequence were also followed same as SSW. First 4 PVs of SO_4^{2-} brine were injected at a rate of 4 PV/day (0.095 ml/min) and next 4 PVs were injected at 16 PV/day. Among all the mechanism of LSWF increase in pH and Fine migration was observed during the previous experience in the laboratory (Hamouda et al, 2014a). Addition to these hypothesis, to observe the impact of certain ions on oil recovery single ion brines were injected as a secondary injection fluid.

All the analyzed results such as pH of effluent, Pressure drop (dP), and Oil recovery are shown in Figure 20. In Figure 20, dP and Oil Recovery (% OOIP) is plotted with respect to PV of SSW & SO_4^{2-} Brine injected. Oil recovery is shown in blue solid line on y-axis to the left. Whereas, dP (Bar) is shown in orange solid line on y-axis to the right. The flooding sequence and change in brine is shown with black solid vertical lines.

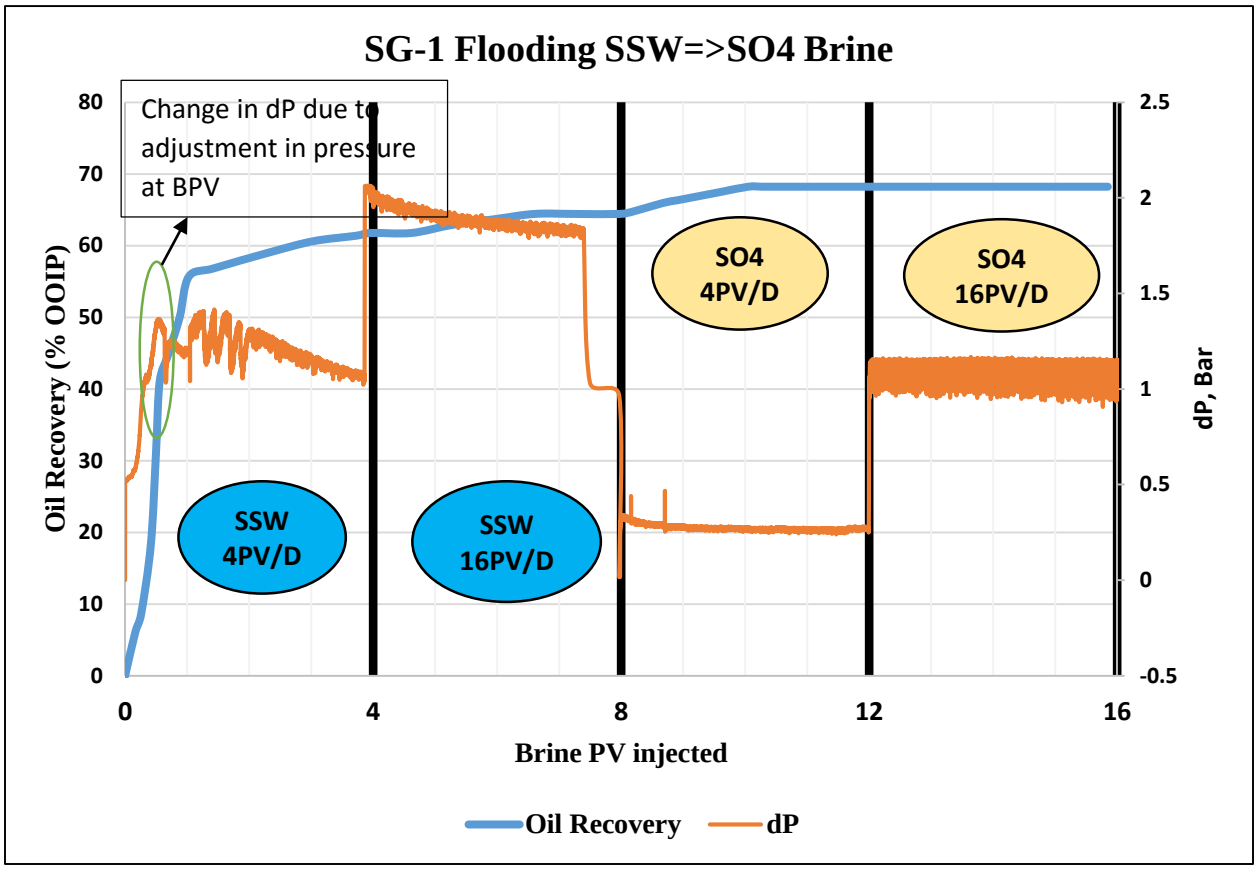

Figure 20: Oil Recovery and dP measured during flooding with SSW and SO4 brine in Core SG-1.

pH of effluents and influents are shown in Figure 21. pHs of influents (SSW and SO4 brine) are constant respective of the brine but pH of effluents varied as the flooding proceeds, as it can be observed in the Figure 21. The results are analyzed later in this section.

From the Figure 20 we can see that when first 4 PV of SSW is injected at 4PV/day, the total oil recovery obtained after injection of 4PV at this rate was 61.76% of OOIP. Water breakthrough takes place at ~1 PV, recovery after breakthrough is quite significant during the SSW injection. It might possible that injection of more SSW at 16 PV/day may lead to higher recovery. But as per the experience from the previous laboratory experiments, we chose 16PV/day as the

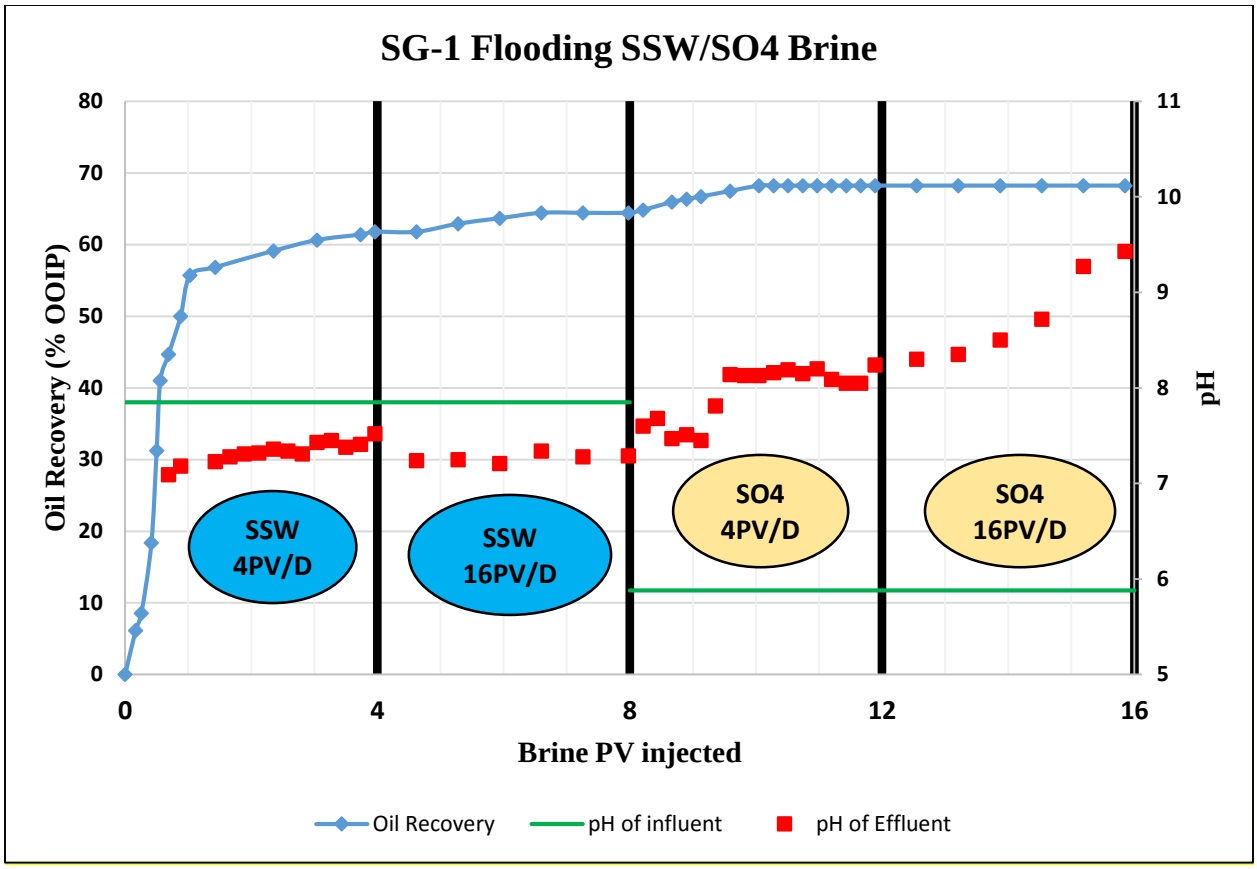

Figure 21: Oil Recovery, pH of effluent and influent measured during flooding with SSW and SO4 brine in Core SG-1.

maximum injection rate (Hamouda et al, 2014b, Mamonov A., 2014). Switching to SO_4^{2-} Brine an increase in Oil recovery of ~4% was observed. Most of the oil recovered during injection with rate of 4PV/day. Increase in rate gave no additional oil recovery. To explain the increase in recovery, we will try to analyze all the results one by one.

If we look at the Figure 21 pHs of effluents are lower than the pH of influent, during injection of SSW at 4PV/day. The pH of effluents varied between 7.09-7.29, which is approximately 0.5 lower than the pH of SSW. This decrease in pH during SSW injection was also observed by various researchers, (Hamouda et al, 2014, Alireza RezaeiDoust, 2011). This might be due to hydration of magnesium ion, which increases the H^+ concentration in the effluents (Hamouda et al, 2014b). Low pH in case of SSW flooding may also reflects adsorption is faster than desorption.

When increasing the injection rate to 16PV/day while flooding with SSW, pH values decreased slightly more. This could be because of variation in the rock/brine interaction. This is in agreement with the results obtained by Fjelde et al, Hamouda et al, 2014b..

One of most important mechanism to look at incase of water flooding is the exchange of ions from or to brine and surface. The ion analysis of effluents represents the interaction of brine and rock minerals. Figure 22 shows the ionic concentration relative to SSW measured in all the effluent samples using Ion-Chromatograph. The relative values on the plot displayed that the value 1 on the y-axis is ionic concentrations of SSW, and the value 10 on the y-axis is ionic concentration of SO_4^{2-} Brine. The effluent ion concentration in the first phase stabilized very early (after at ~1 PV), which showed that SSW only interact with rock surface initially. One more interesting trend has been observed that $[Ca^{2+}]$, $[Mg^{2+}]$ and $[SO_4^{2-}]$ trends are moving in the opposite directions

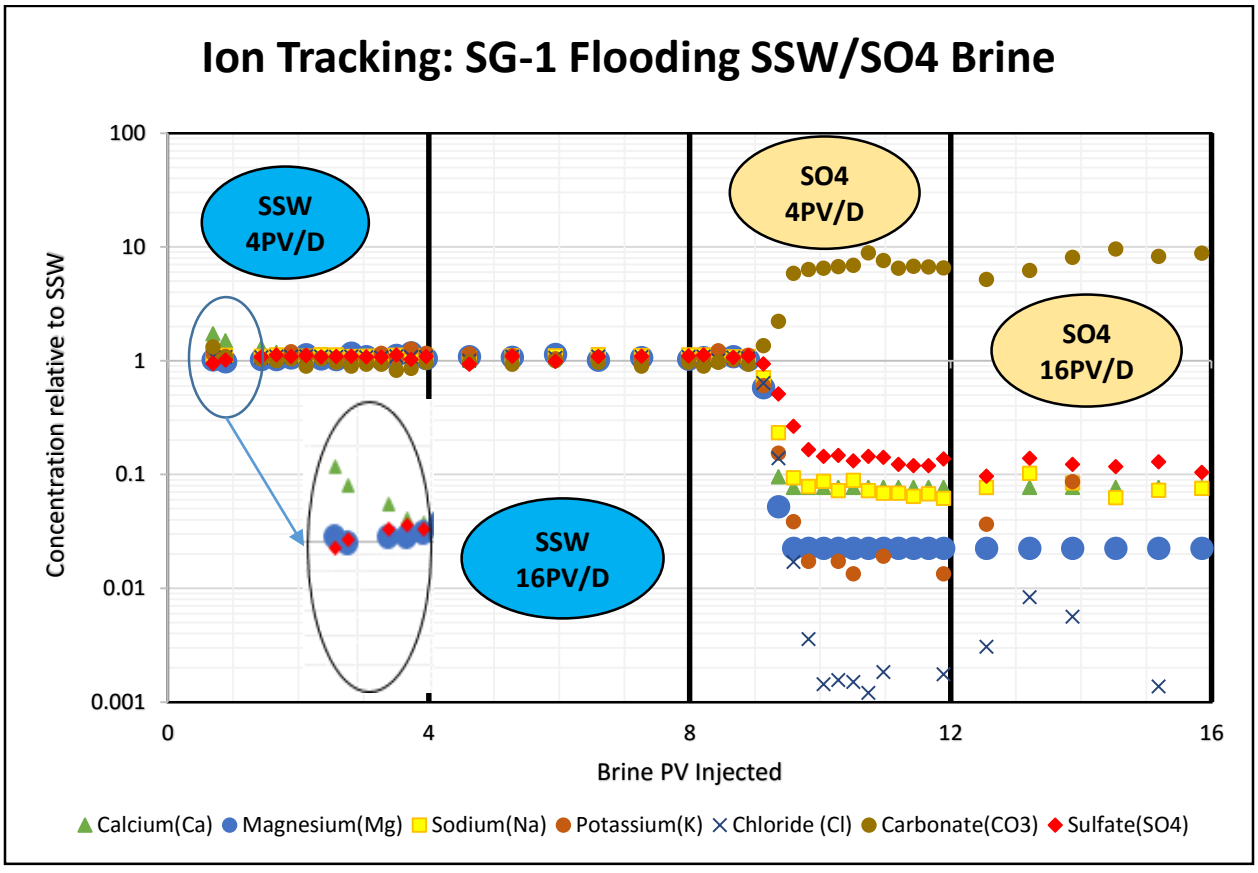

Figure 22: Ion concentrations of effluents relative to SSW taken while flooding with SSW-SO4 brine in core SG-1.

(enlarged part in Figure 3). The [Ca^{2+}] declined from 1.7 SSW and stabilized at 1 SSW. While [Mg^{2+}] and [SO_4^{2-}] increased from 1.01 SSW and 0.94 SSW, respectively and stabilized at 1 SSW. This is in agreement results observed by Petrovich and Hamouda, 1998.

During the flooding process, continuous monitoring of pressure difference was taken place, as shown in Figure 23. We can also relate the production of oil with change in pressure differences. Throughout the process the maximum dP reached to 2.03 Bar. To simulate the reservoir condition, a Back Pressure Valve (BPV) has been set at 10 Bar. Since we have to increase pressure at BPV gradually, a wide fluctuation in dP can be seen initially (circled in green color) in dP curve (Figure 20).

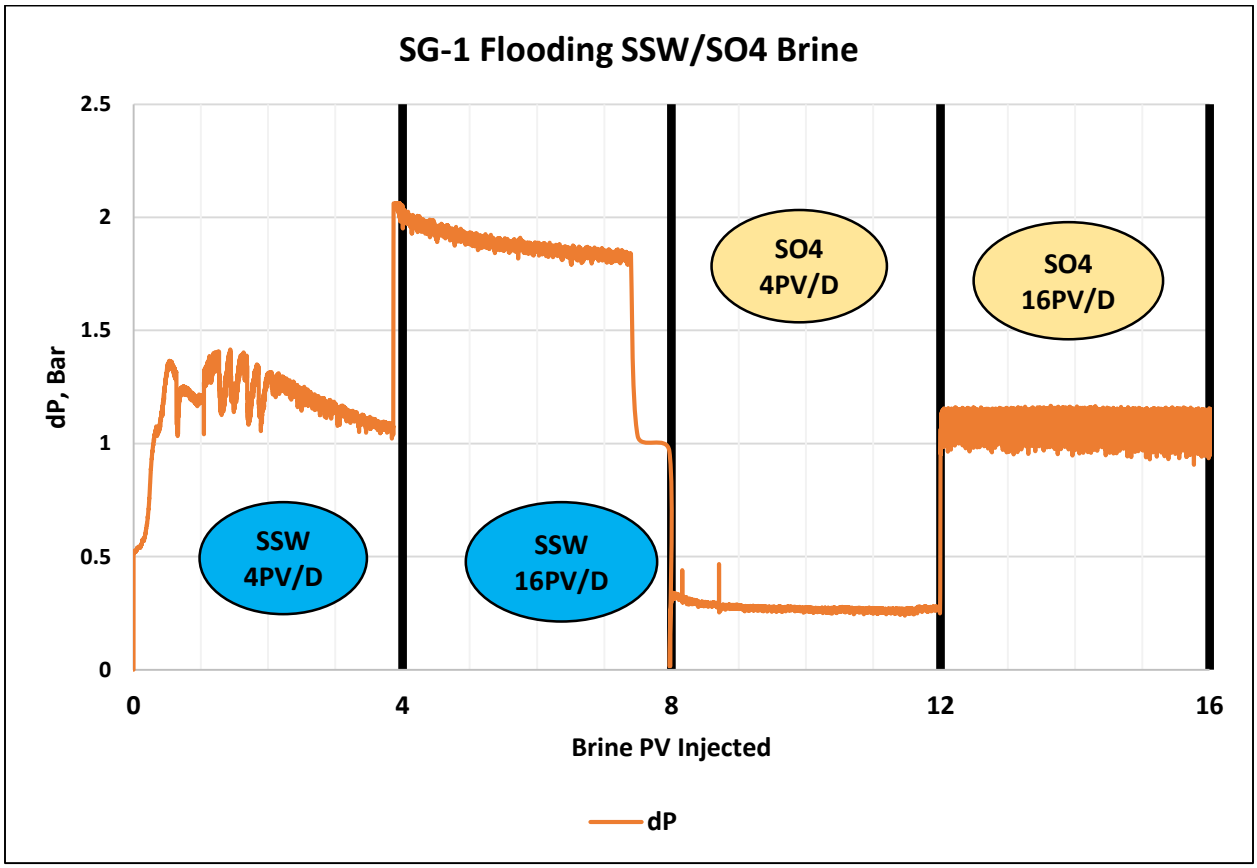

Figure 23: dP measured during flooding with SSW and SO4 brine in Core SG-1.

At the beginning of dP curve, we saw an increase in pressure drop in terms of peaks. These peaks could also be defined by dispersion of particles/fine migrations. Due to Mobilization of fines, a reduction in permeability could occur. Migration of fines block the pore throats; this shows

an increase in pressure drop across the core. Increase in resistance diverts the flow of water into the un-swept region (Alireza RezaeiDoust, 2011).

When injecting SSW at 4PV/day, we can see various peaks in the dP curve (Figure 23). These peaks may signify the movement of water resisted by other phase, i.e. synthetic oil. Pressure drop value stabilized gradually at the end of 3 PV. Similarly, when increasing the rate to 16PV/day, increasing in rate increases the dP initially. This increase in rate was able to overcome the capillary pressure in the pores which leads to displacement of oil and increases the sweep efficiency. At the end of 6^{th} PV dP stabilized, with small peaks of pressure drop.

In the second phase of experiment SSW was switched with SO_4^{2-} brine to check the hypothesis and suggested mechanisms of Low salinity flooding. After switching injecting brine with SO_4^{2-} brine, we observed following things:

- A sharp increase in pH values.
- Exchange between divalent ions take place. [HCO_3^-] increases while concentration of other ions decreases rapidly.
- Decrease in dP value by half of the value during injection with SSW.

Increase in pH may consider as an effect of low salinity water. A local increase in pH was observed by various researchers (Hamouda et al, 2014b, Fathi et al, 2010, RezaeiDoust et al, 2010). This increase in pH could be explained by following events.

Due to dissolution of cementing materials, in this case calcite, leads to release of hydroxyl ion (OH^-). Addition of OH^- increases the basic nature of effluents, thus increases the pH. Dissolution of calcite mineral can be expressed by (Dang et al, 2013):

$$CaCO_3 + H_2O \rightarrow Ca^{+2} + HCO_3^- + OH^- \quad (10)$$

This theory can be supported by the results from ion analysis (Figure 23). Dissolution of carbonate leads to increase in concentration of Ca^{2+} and HCO_3^-. The alkalinity of water/calcite can be expressed by following equation (Hamouda et al, 2014b):

$$alkalinity = 2[CO_3^{2-}] + [HCO_3^-] + [OH^-] - [H^+] \quad (11)$$

During the mixing of SSW- SO_4^{2-} brine at 8-10 PV, [Ca^{2+}] stabilized at a value of 0.16-0.17 times SSW. Though in the SO_4^{2-} brine only Na_2SO_4 was present. The only reason which explains the presence of Ca^{2+} in effluents, is dissolution of calcium from the precipitated sulfate salt during SSW flooding (Hamouda et al, 2014a). Similarly, [HCO_3^-] was stabilized at 10 times the concentration in SSW. After the 11th PV, pH increased very sharply and reached a value of 9. This high value of pH signifies high amount of interaction between rock and brine and calcite dissolution.

From the ion chromatograph results, if we observe closely the decline curve slope for all ions except HCO_3^- was higher in SO4 brine flooding than the SSW flooding. Rates of declining curve for [Na^+], [Ca^{2+}], [SO_4^{2-}] and [Mg^{2+}] are 0.035, 0.002, 0.00332 and 0.004. This showed that Na^+ fastest among all the active ions, means that Na^+ interacts with the rock surface in very low amount. It is very interesting to observe that SO_4^{2-} declines at about 1.5 times faster than Ca^{2+}. This may lead to lower contribution of SO_4^{2-} in $CaSO_4$ dissolution. Which means that in-case of flooding with SO_4^{2-} brine other processes take place, such as Sulfate adsorption. It has been demonstrated that sulfate adsorption and wettability alteration of chalk surface are interlinked processes (Gomari and Hamouda, 2006). It has been shown that sulfate can alter the surface wettability to more water wet. This could be one of the prominent mechanism for enhanced oil recovery (Gomari and Hamouda, 2006).

Another observation we can make from the ion chromatograph results by analyzing [Mg^{2+}]. Declining rate of [Mg^{2+}] was fastest than Ca^{+2} and SO_4^{2-}, which may suggest very low interaction of the Mg^{+2} from/to surface and brine. This may be due to the absence of $MgCl_2$ salt in SO_4^{2-} brine, [Mg^{+2}] decreased due to dilution of the brine. Early stabilization of [Mg^{2+}] and [Ca^{2+}], from figure 22, we can state that there may not be any formation of dolomite or magnesite and no exchange between Mg^{2+} and Ca^{2+}.

During SO_4^{2-} brine flooding, dP measurements showed a drop in average value by about half of the SSW flooding (Figure 23). When flooding SO_4^{2-} brine at 4PV/day, dP value was 0.6bar at 8th PV and it stabilized at 0.25bar after 9th PV with small fluctuating peaks. But between 8th and 9th PV we saw an increase in dP to 0.5bar. These peaks may be due to removal of fines from the rock. Migration of fines leads to blocking of pore throats and blocks the path of fluid flow. Because of the resistance in flow we observe an increase in pressure drop. This resistance in flow forces

brine to divert the flow direction in non-swept region, increase the permeability of rock with respect to injected brine. Therefore, increases the sweep efficiency. This mechanism supports why we observe an increase in recovery of about 4% in between 8^{th} and 9^{th} PV.

But when increasing the rate to 16PV/day, dP increases to 1.3 bar and remain constant throughout the flooding. Increasing rate did not increase the oil recovery. It could be because increase in rate wasn't able to overcome the capillary pressure in the pores which leads to displacement of oil and increases the sweep efficiency.

Results and analysis from the experiment supports that low salinity mechanism are more prominent in case of single brine injection than SSW injection. Interaction between rock and brine leads to mineral dissolution, pH increase and fines migration which improves the sweep efficiency and enhances oil recovery. Torrijos et al, 2016 has shown that for sandstone reservoirs, addition of Na^+ has an influence on SO_4^{2-} reaction. But results observed in case of chalk are quite opposite to this. From figure 22, the fastest declination of sodium indicated that sodium might have not involved in ion exchange with calcium. Hence, no effect of sodium in sulfate reaction.

A total recovery obtained from the SSW flooding is 64.2% of OOIP and injection of SO_4^{2-} brine gives a significant increase in recovery of 4%. Thus ultimate recovery obtained from the flooding process is 68.2%.

4.3. Flooding in Core SG-2 with SSW/Mg^{2+} Brine (1:10):

The core dimensions for SG-2 are already shown in table 10. The only difference is that core was flooded with Mg^{2+} Brine as a secondary injection brine. The flooding sequence remained same as the previous sample and results obtained: pH of effluents, dP measurements, ion analysis of effluents and oil recovery are shown in below figures.

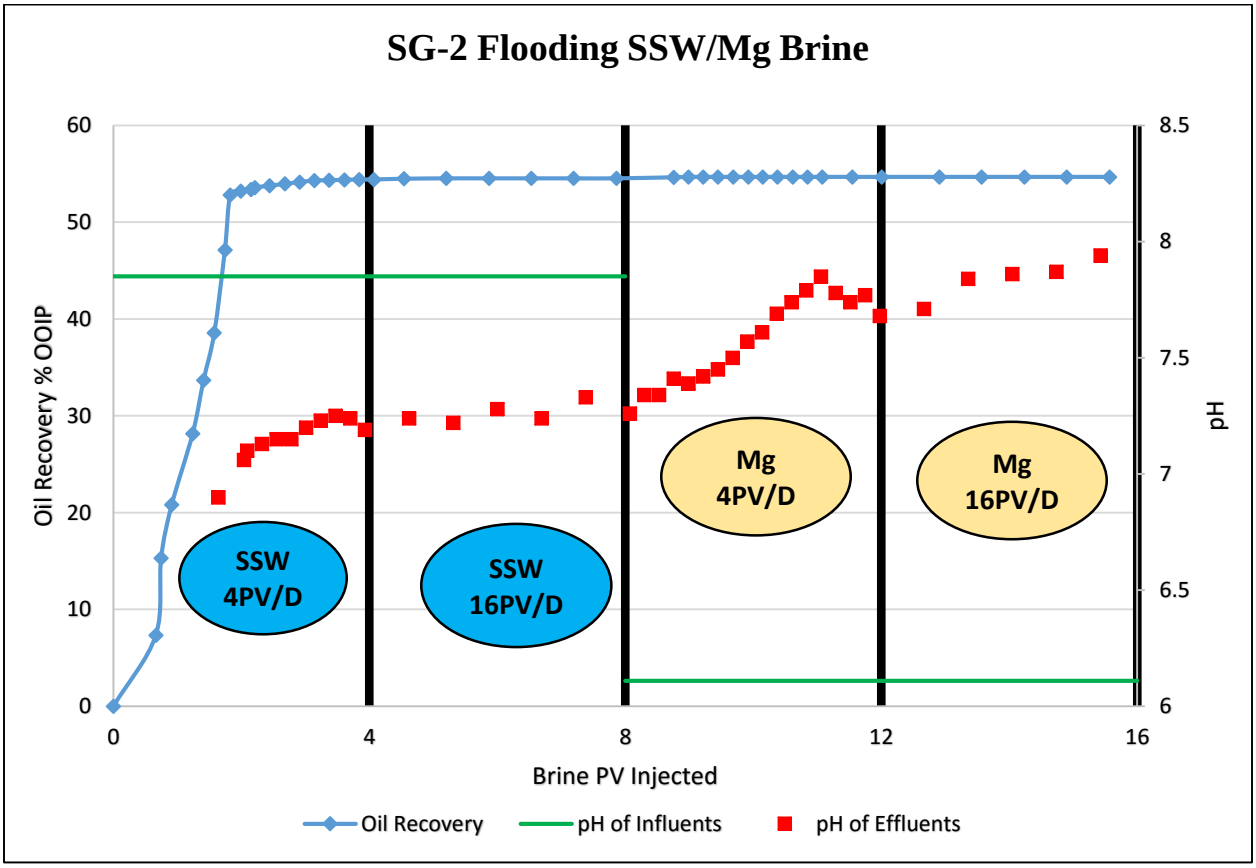

Figure 24: Oil Recovery, pH of effluent and influent measured during flooding with SSW and Mg brine in Core SG-2.

This flooding sequence in SG-2 core held in two phases, similar to the flooding in core SG-1 but the only difference was Mg brine injection as the secondary brine. Theoretically, the results obtained in case of SSW flooding should be similar as in case of flooding in SG-1, except the ion ranking.

pHs of effluents increased during injection of SSW at 4PV/day. At 4PV/day, pH remained almost constant with an average value of 7.25 but lower than pH of the influent, i.e. 7.85. It was

proposed that decrease in pH during SSW flooding may be due to hydration of Magnesium ions. On the other hand, if we look into the pH measurements during flooding Mg brine, we can see a sharp increase in the pH values. The pH values of effluents went up from 7.25 to 8, which was higher than the pH of influents, i.e. 6.11.

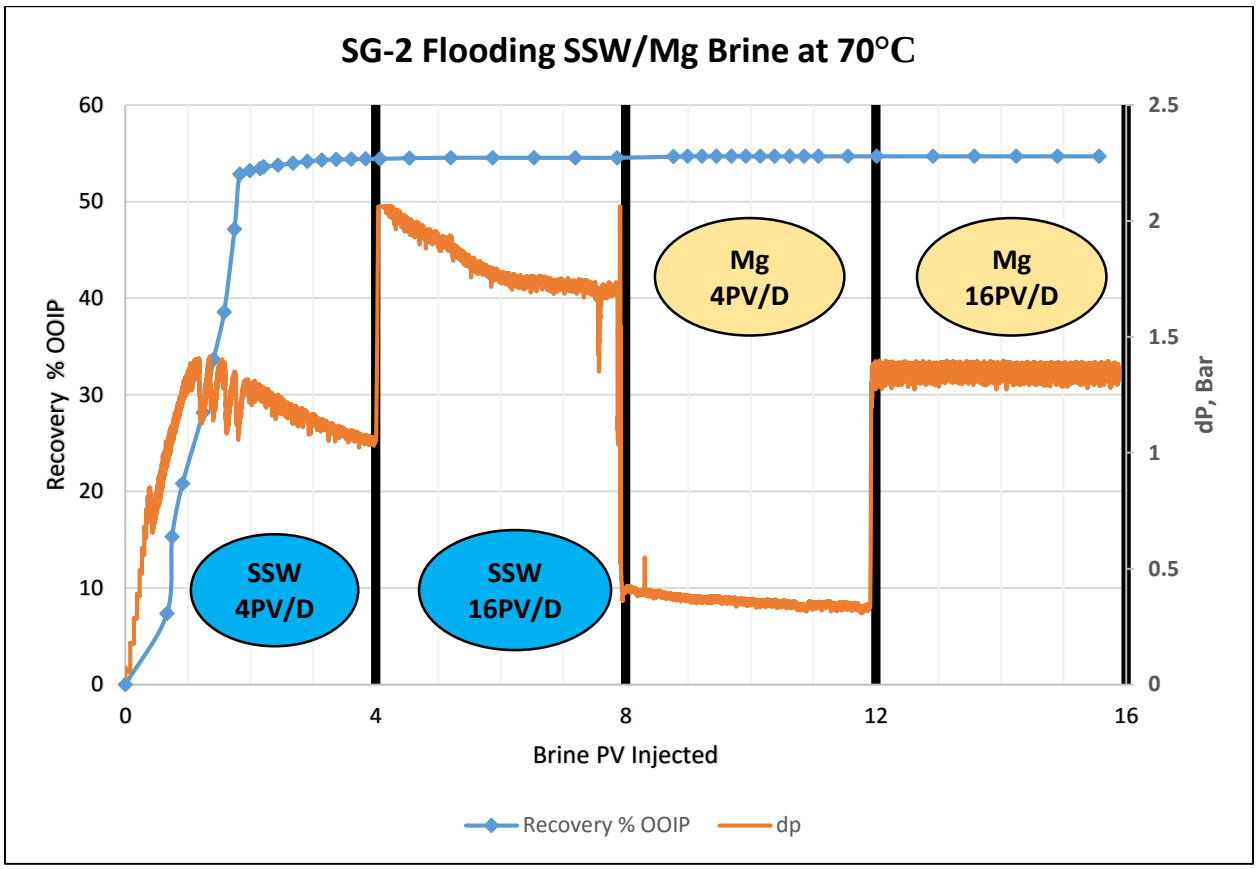

Figure 25: Oil Recovery and dP measured during flooding with SSW and Mg brine in Core SG-2.

This increase in pH may be due to dissolution of calcite and precipitation of sulfate ions, as explained in section 4.2 in detail. The pH results conform to the results observed by other researchers (Hamouda et al, 2014a and b, RezaeiDoust et al, 2011) and we have also observed in case of flooding in core SG-1, during injection of SO4 brine.

Pressure drop (Figure 25) gives a clear understanding of oil recovery as the flooding continues. The pressure drop at the start of SSW flooding with 4PV/day, dP reached at the peak of 1.3 bar after 1.5PV and started stabilizing after 2PV. When injection rate changed to 16PV/day, dP increased to 2.03 bar and later stabilized at 1.68bar after 10PV. The rate was increased to

overcome the capillary effects in the rock. When flooding was switched with Mg^{2+} Brine, the dP values decreased by half of the dP measured during SSW flooding. At 4 PV/day, dP decreased to 0.396 bar at the start and stabilized at 0.32 bar after 8.5PV. dP increased to 1.348 bar when brine was injected at 16PV/day and remained constant throughout the flooding.

The oil recovery can be justifying by analyzing the dP plot. Large number of peaks showed a significant amount of resistance while SSW flooding. Around 54.35% of OOIP was recovered from SSW flooding. But only 0.3% of oil recovery was observed at 16PV/day, possibly because of high capillary effects in the pores. After changing the brine Mg^{2+} Brine, overall increase in oil recovery is about 0.1%.

The reason for such a low recovery of 0.1% during Mg^{2+} brine might be easier to explain from Ion tracking of the effluents (Figure 26). For first phase, the ion concentrations in effluents remain same as in SSW. Similar to Ion tacking in case of SG-1 core (SSW/SO4 injection), in this case also we noticed an opposite trend of Ca^{2+}, Mg^{2+} and SO_4^{2-}. Decline curves of the ion concentrations give a better deduction of their interactions with the rock. Decline rates for Mg brine flooding of [Na^+], [Ca^{2+}], [Mg^{2+}] and [SO_4^{2-}] are 0.18, 0.002, 0.01 and 0.005 mole/L PV, respectively. Decline of Na^+ was the fastest than any other ion. This may indicate very low interaction/ ion exchange contribution by Na^+. Mg^{2+} declines at a faster rate than Ca^{+2} and SO_4^{2-}, despite the injected brine contains only $MgCl_2$ salt. Since injection brine does not contain sodium, presence of sodium in effluent may be due to dilution/mixing of brine.

As it has been described that dissolution of calcite is not the only reason of increase in calcium concentration. Magnesium concentration in the injected Mg^{2+} Brine is 0.01 relative to SSW. But from figure 26 we can see that after injection 2.3 PV (of Mg^{2+} Brine), [Mg^{2+}] started decreasing to value lower than the injected value and went down to 0.0005. This uniform deficiency in [Mg^{2+}] in the effluent compared with the injected brines may indicate possible exchange between Mg^{2+} and Ca^{2+} ions (Hamouda A.A., Evgeny Maevskiy, 2014). So this ion exchange phenomenon between Mg^{2+} and Ca^{2+} leads to formation of Magnesian or dolomite. This

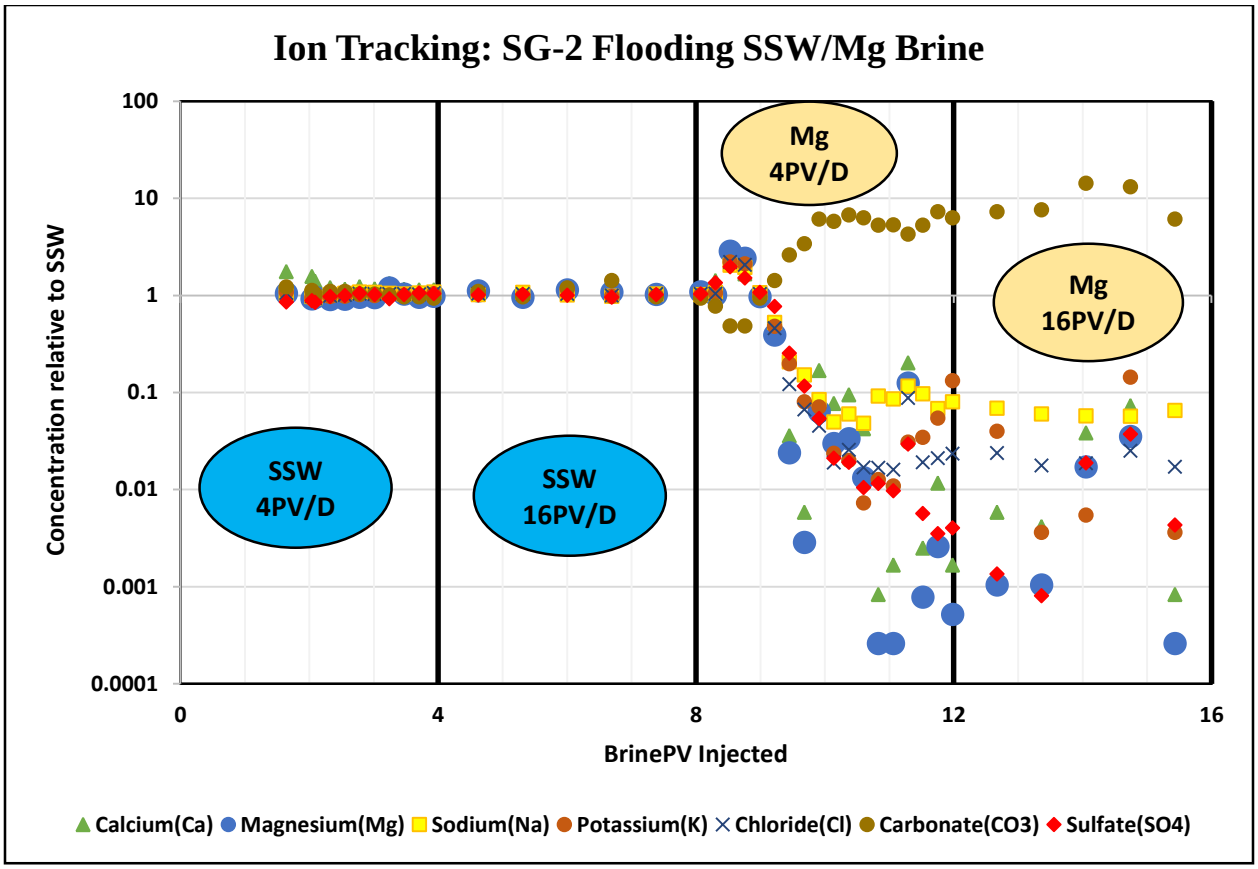

Figure 26: Ion concentrations of effluents relative to SSW taken while flooding with SSW-Mg brine in core SG-2.

has been explained by Hamouda et al, in the form of following reaction:

$$2CaCO_3(S)\ (Calcite) + Mg^{+2} = CaMg(CO_3)_2(S) + Ca^{+2} \quad (12)$$

Due to exchange of Ca/Mg a higher value of Calcium ion in effluents than magnesium was observed. As expected, due to dissolution of calcite, concentration of carbonate ion increases in the influents (from figure 26).

It was practically confirmed that Ca/Mg ion exchange, enhances sweep efficiency of the rock (Hamouda A.A., Evgeny Maevskiy 2014). Perhaps, ion exchange between Ca/Mg alone is not enough to alter the wettability, presence of SO_4^{2-} ion also requires. Ca/Mg largely contribute to enhancing sweep efficiency in presence of SO4, and increase the permeability, hence, pressure drop increases.

4.4. Flooding in Core SG-3 with SSW=> LSW (1:50)

Al-Attar H.H. et al, 2013, performed experiments on samples taken from Bu-Hasa Field, which resulted that sulfate concentration has a substantial effect on LSW flooding. From their experiments it was also shown that sulfate beyond an optimum concentration can display a negative impact on the recovery. Based on the experiments performed on a field (H.H. Al-Attar et al, 2013), the optimum sulfate concentration, with a significant oil recovery, is 47ppm. On laboratory scale it can be achieved by diluting SSW by 50 times with DW. Studies of flooding with Low salinity brines with various compositions has been performed in the Laboratory (Hamouda et al, 2014b). But this particular brine composition has been used to assess the field results on laboratory scale.

Diluting the SSW by 50 times with DW was used as secondary injection fluid. Core SG-3 was flooded with SSW as a primary injection fluid and later with LSW as secondary injection fluid. Flooding with LSW 1:50 was also performed to compare the obtained results with the results of LSW 1:10, performed by Hamouda et al, 2014b, in our laboratory. All the results obtained are shown and explained as follows:

From Figure 27 Oil recovery after injection of SSW is 47.4% and increase in recovery from LSW flooding in second phase is 7%, which gives an overall recovery of 54% of OOIP. This Increase in recovery of 7%, after flooding LSW, may be due to a better rock/brine interaction than LSW 1:10, where increase in recovery was~1%. It can also be assessed by looking at the pressure drop measurements.

An initial increase in pressure drop of 1.39 bar after 1.3PV was observed probably due to early water breakthrough. With small fluctuations, dP stabilized at 0.46bar after injection of 2.5PV of SSW at 4PV/day. It is interesting to examine drop in pressure at higher rate of SSW injection.

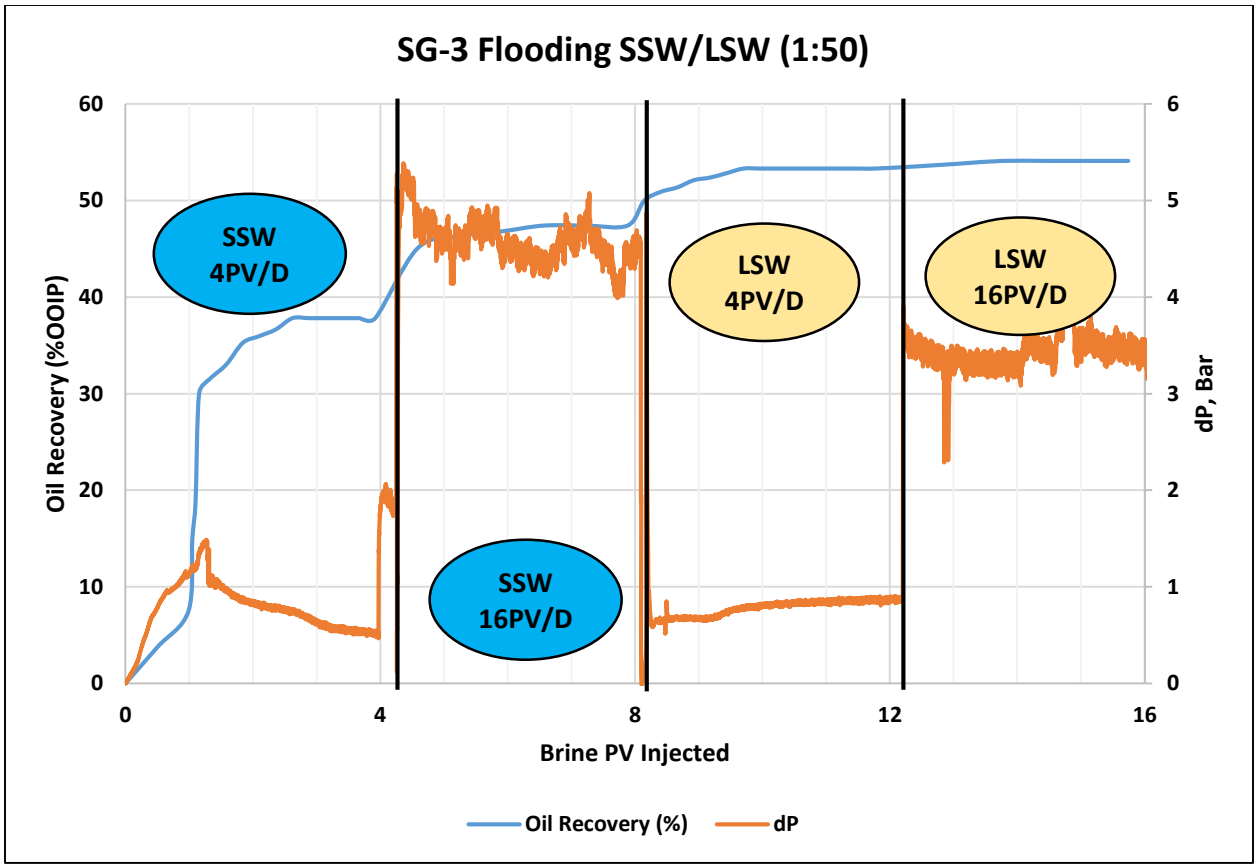

Figure 27: Oil Recovery and dP measured during flooding with SSW and LSW in Core SG-3.

dP varied from 5.2-4 bar and stabilizes at 4.5bar with a large fluctuation in between. This large fluctuation may be due to large rock-brine interaction and flow restrictions. A drastic increase in recovery of 10% at higher rate gives large indication of rock-brine interaction. As experienced in other experiments pressure drop decreases during the LSW injection. It could be because of low resistance in flow and flow through already swept area. LSW injection at 4PV/day, an initial increase in dP to 0.85bar at 8.5PV was obtained and after 9.3PV dP started stabilizing to 0.83bar with small peaks. But magnitude of fluctuation is much smaller than SSW, because LSW may flow through the channels created during SSW flooding, as in LSW follows the path of least resistant. While at higher rate dP stabilizes at 3.5bar with large increase in dP of 4.1bar at 13-14PV. Pressure drop values were calculated mathematically also. The calculated pressure drop values for LSW injection are 0.801 bar and 3.43 bar at 4PV/day and 16PV/day, respectively. The difference in pressure drop is approximately of 2%, which is very small. This could be due to error in calibration

of manometers. It has been stated before LSW injection leads to fines migration. Which leads to increase in pressure drop and diverts the flow of brine to the un-swept area, therefore, decrease the relative permeability for water. Hence, enhancement in the oil recovery.

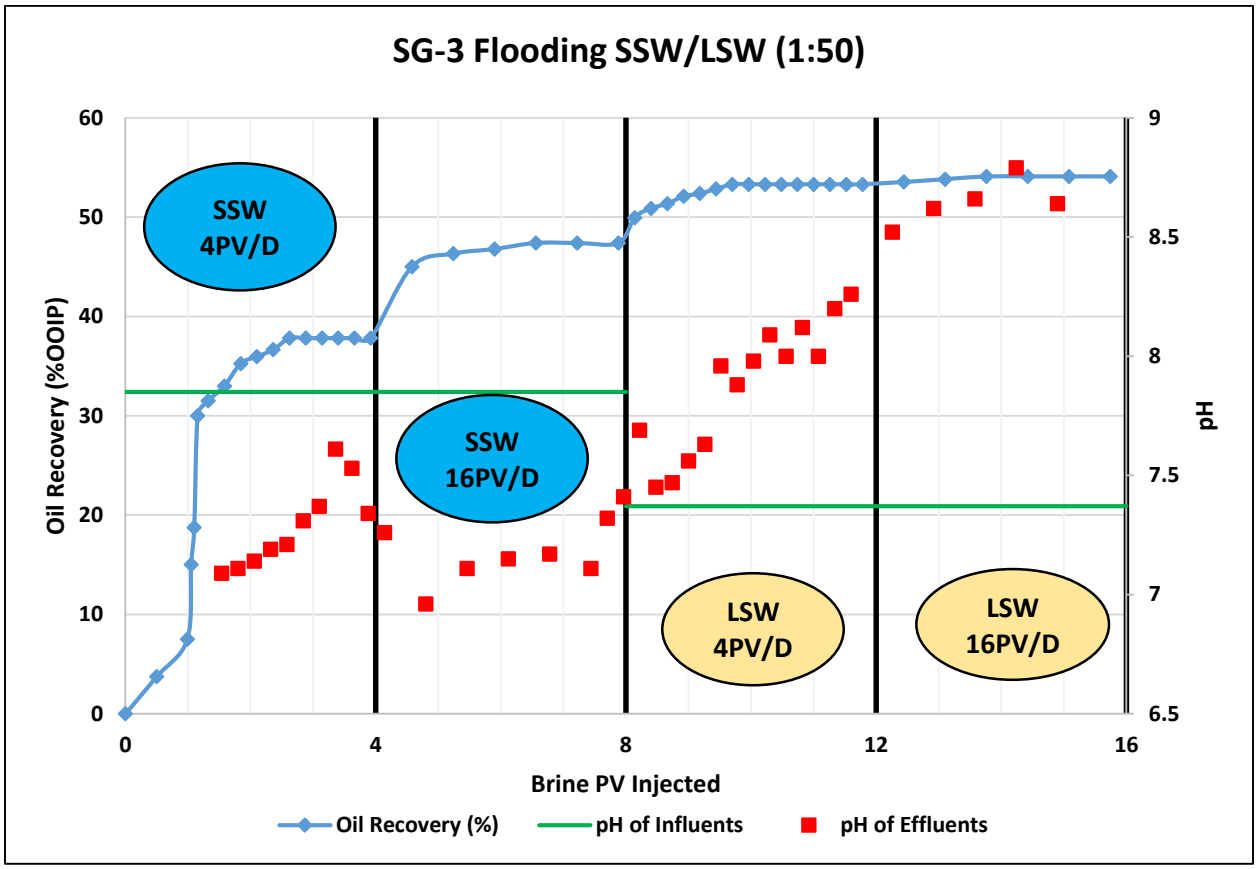

Figure 28: Oil Recovery, pH of effluents and influents measured during flooding with SSW and LSW in Core SG-3.

pH of effluents was measured for each sample during the process and shown in figure 28. Lower pH of effluents than the influent was observed in case of SSW injection and a gradual increase to a higher value than influent in case of LSW injection. The maximum pH reached during injection of LSW is recorded at a value of 8.3. These results are similar to what it was observed in the above experiments and observed by other researchers. As for the previous experiments discussed here, the possible explanation for the pH increase is dissolution of calcite minerals. A decrease in pH during injection of LSW at 16PV/day may be due to the equilibrium between rock and brine was reached at this stage of flooding. Hence, there may be less/no dissolution of calcite in the brine.

From the ion concentration results (Figure 29) for the first phase, all the ions have approximately equal concentrations to the SSW. While during LSW 1:50 flooding, all the ion curves except, concentration of HCO_3^- showed a decrease in slope. The decline rates of the ions for LSW 1:50 of [Na^+], [Mg^{+2}], [Ca^{+2}] and [SO_4^{2-}] are 0.04, 0.0044, 0.00044 and 0.003 mole/L PV. Rate of declination for [SO_4^{2-}] is 8 times greater than [Ca^{+2}]. This shows lower contribution of Ca^{2+} in $CaSO_4$ dissolution. Also, it was observed by other researchers (Gomari et al.) that sulfate is consumed in other processes such as adsorption. From Figure 29, [Ca^{+2}] & [SO_4^{2-}] follows the opposite trend initially (enlarged in circle). This observation was explained by Gomari et al., citing that if adsorption reflects a deficiency of [SO_4^{2-}], it may mean that chalk surface is continually renewed and dissolution of calcite contributes in stabilizing the calcium ion concentration. Calcite dissolution and alkalinity of the system has also been expressed in form of reactions (10) and (11).

As explained before, pH increases may be due to calcite dissolution, but it does not reflect in the [HCO_3^-] in Figure 29. The similar results were observed while experimenting with other LSW in the laboratory by Hamouda et al. They also explained that the water exposed to CO_2/air to some extent affects the pH and distribution of carbonate species (Hamouda et al., 2014b). This hypothesis is supports the results of [HCO_3^-] observed in case of LSW (1:50). Deficiency in [Mg^{+2}] could be due to ion exchange between magnesium and calcium which leads to deposition of dolomite/magnesian. Since the maximum pH measured is 8.3, it is very unlikely of brucite {$Mg(OH)_2$} to get deposited because brucite become stable at pH~10.7 (Hamouda et al., 2014b). Ion exchange between calcium and magnesium expressed in equation (12). Calcium and magnesium ion concentrations reaches its equilibrium at the starting of 11PV. But when LSW injection rate increases, we can see increase in Ca^{+2} and Mg^{+2} concentrations (encircled in black circle in figure 29). This may show increase in exchange of Mg^{+2} and Ca^{+2} and formation of magnesian.

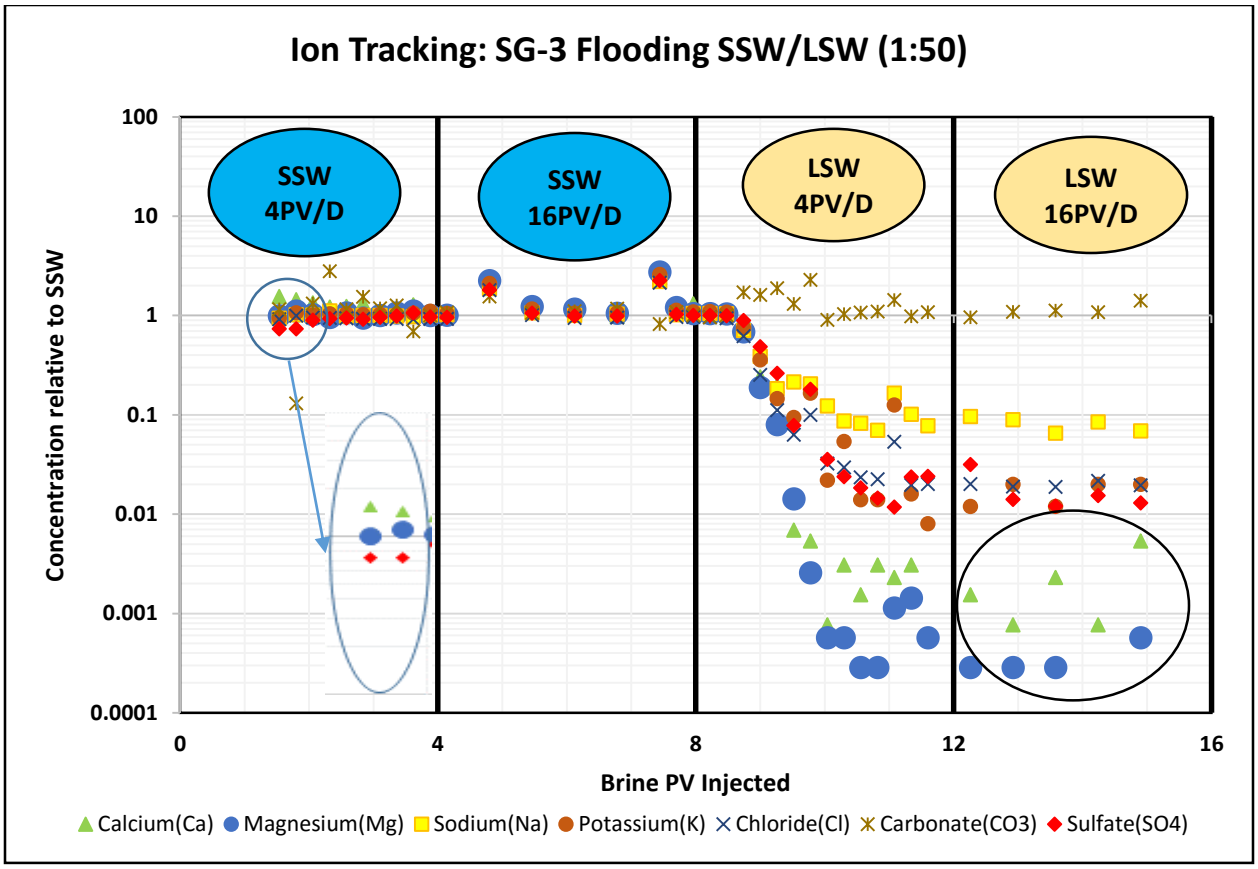

Figure 29: Ion concentrations of effluents relative to SSW taken while flooding with SSW-LSW in core SG-3.

From the experiments performed by Hamouda et al.[35], LSW 1:10 was considered as the best case with a recovery of 62%. While after flooding LSW 1:50 total recovery calculated is 54%. Despite having higher increase in recovery in case of LSW 1:50 (~7%) than LSW 1:10 (Hamouda et al, 2014b) (~0.3%), still LSW 1:10 will be considered as the best case.

From figure 30a, we can see that injecting LSW 1:10 at 4PV/day did not show any oil recovery but at 16 PV/day a 0.3% increase in oil recovery was obtained. The similar case was observed during flooding of LSW 1:50, in figure 27. A 7% increase in recovery was observed at

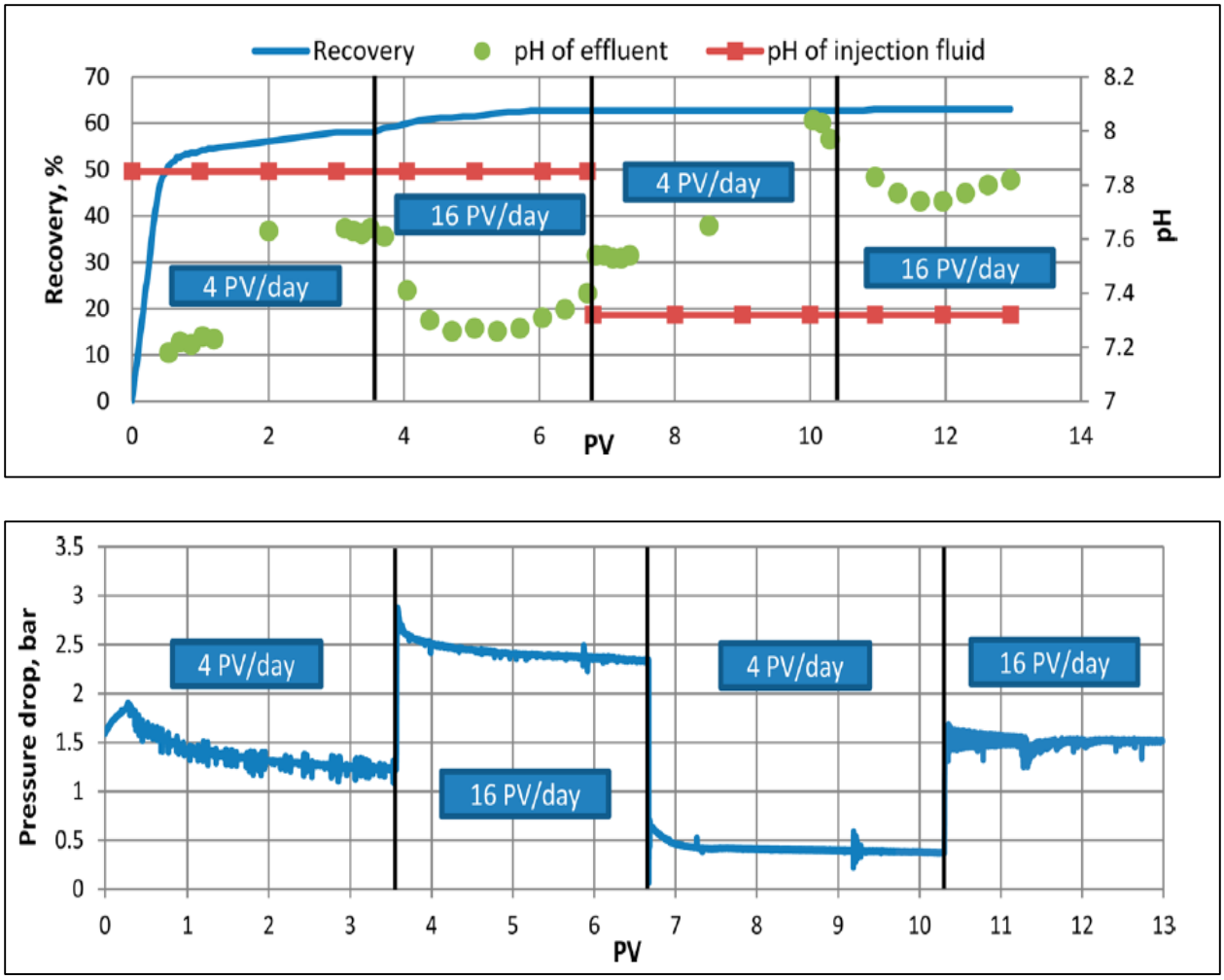

Figure 30: a) Recovery, pH & b) pressure drop during flooding with SSW/LSW 1:10. (Hamouda et al., 2014b)

higher rate. This may be explained with the help of pressure drop curves. From figures 27 and 30b, at 4PV/day drop in pressure is almost same ~0.5 bar, which indicates very low resistance in flow. While at higher rate average dP is 1.5 bar for LSW 1:10 (figure 30b) and for LSW 1:50 average dP is 3.5 bar (figure 27), which is higher than LSW 1:10. This higher dP in case of LSW 1:50 shows higher resistance in flow. Due to this high resistance, oil recovery is higher in case of LSW 1:50.

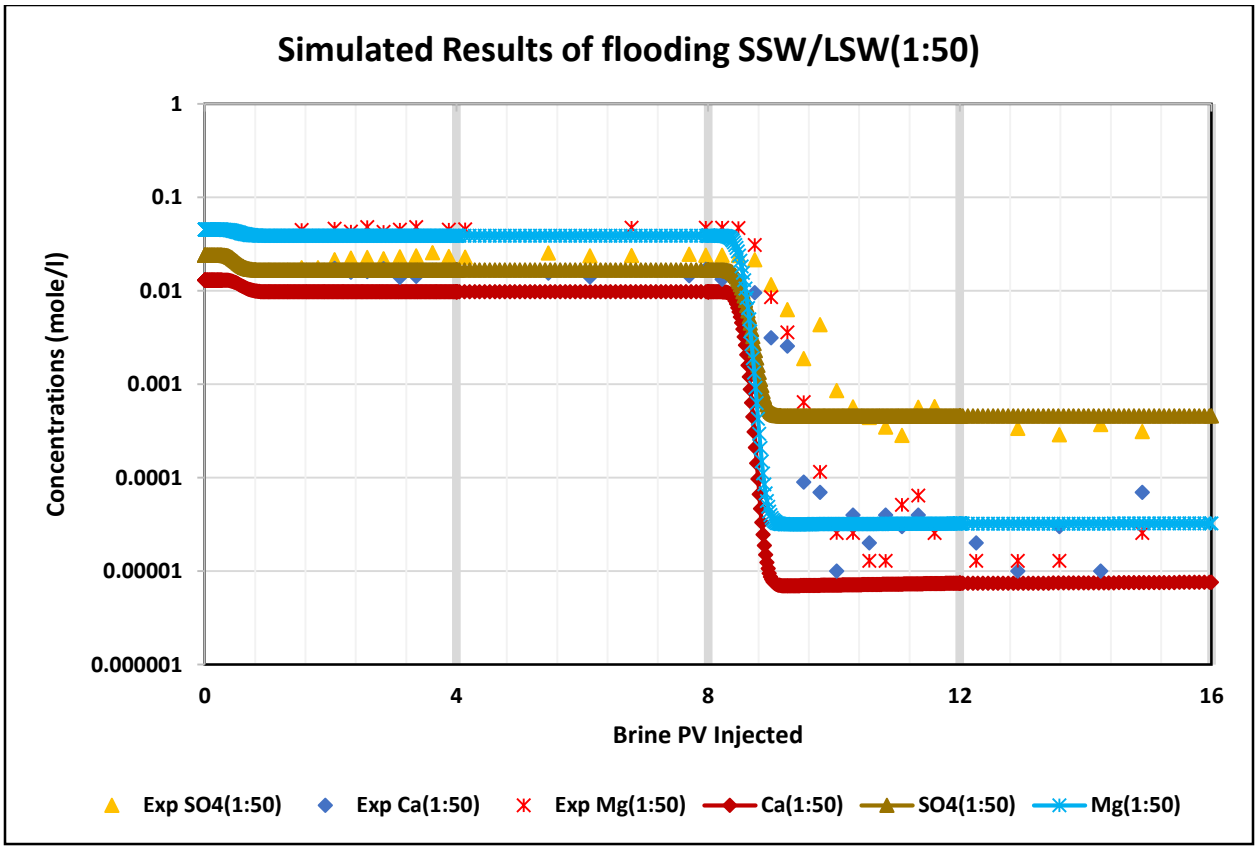

Figure 31: Comparison between experimental (points) and simulated (lines) ion concentrations (mole/l) for SSW/LSW.

Simulation (using CMG) and experimental ion concentrations are compared in figure 31. The simulation was also run for the 16PV, though the concentrations reached the equilibrium at 9PV. The decline trend and the concentrations for simulation and experimental data are in good agreement. The difference in starting of decline curves may be due to mixing of brines in experiment.

4.5. Flooding in Core SG-4 with SSW=> SO_4^{2-} Brine (1:50)

Al-Attar et al. performed flooding tests using samples taken from Bu Hasa field in Abu Dhabi. By varying the brine composition, they looked for an optimum effective sulfate concentration, which is sought to be 42ppm. In this experiment an attempt has been made to simulate the effect of SO_4^{2-} ion on oil recovery at this particular concentration. Also to compare the results obtained when core SG-1 is flooded with SO_4^{2-} brine (1:10), section 4.2.

In this case it was pre-assumed that the mechanism and qualitative interaction between rock/brine should be the same as flooding with SO4 1:10, but quantitative interaction could be different since the dilution ratio is different for both the cases. All the results and comparison with other experiments are discussed below.

Figure 32 shows measured pH and oil recovery calculated after flooding process. Oil Recovery from the first phase is measured about 62% (less than core SG-1). Whereas, increase in recovery from SO4 Brine is 2% at 4PV/day. But when brine was injected at 16PV/day, the increases in oil recovery was negligible. So total oil recovery calculated from the flooding is 64%. Recovery results may be explained by the dP measurements and Ion analysis given in below figures.

pH measurements of effluents showed a range of 6.9-9.21. The maximum observed pH in case of SO4 (1:50),9.5 was less than SO4 (1:10), 8.3. Higher pHs were observed by Hamouda et al (2014b) with higher dilution ratio. pH for LSW 1:25 was higher than LSW 1:5 and LSW 1:10 (Hamouda et al, 2014b).

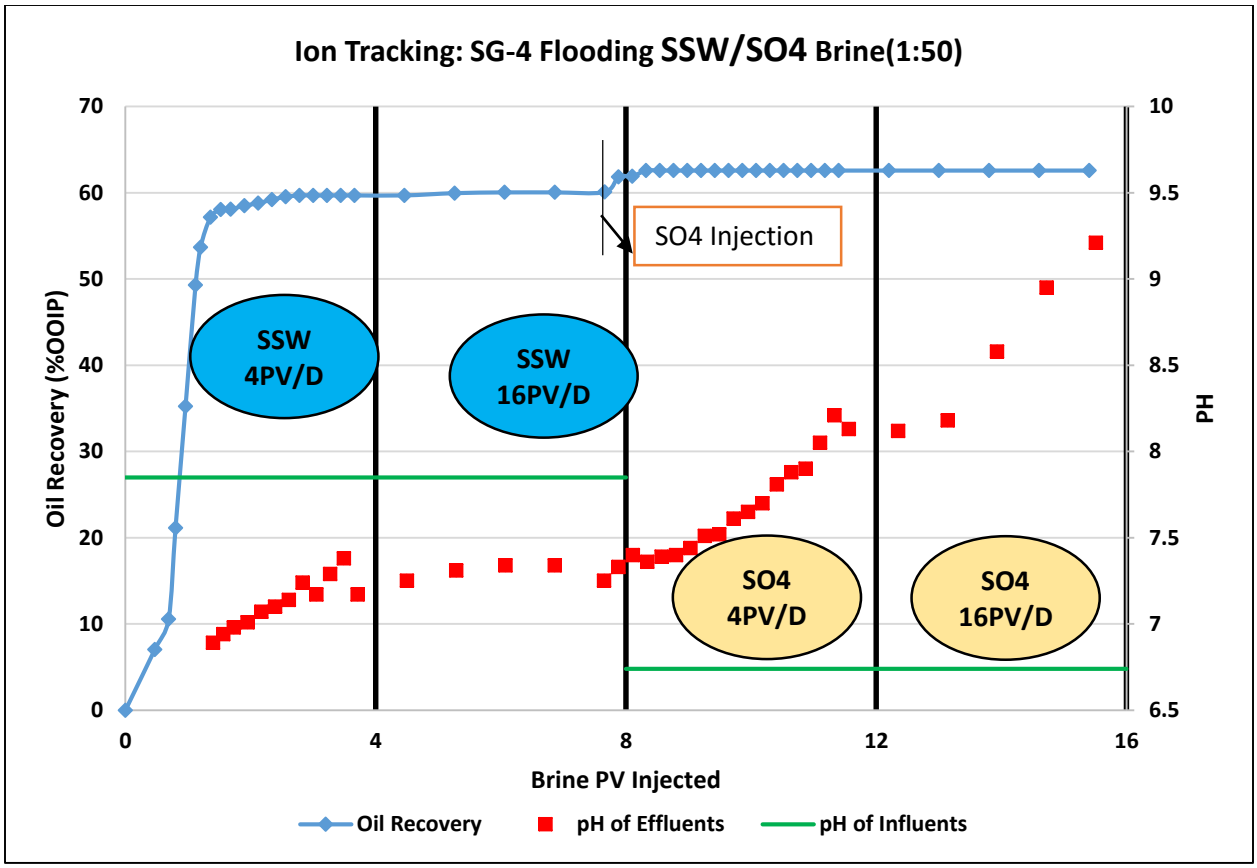

Figure 32: Oil Recovery, pH of effluents and influents measured during flooding with SSW and SO4 Brine in Core SG-4.

Higher values of pH were obtained may be due to higher dissolution of calcite in case of flooding with SO_4^{2-} brine (1:50) than flooding with SO_4^{2-} Brine (1:10). Higher pH values were also obtained in case of LSW 1:50 than LSW 1:10. From the Ion chromatograph results (figure 33), average concentrations of HCO_3^- is $3.9[HCO_3^-]_r$ssw in case of flooding with SO_4 brine (1:50) while flooding with SO4 (1:10) it was $9[HCO_3^-]_r$ssw (Figure 33) with respect to SSW. This confirms that quantitative calcite dissolution is more in case of flooding with SO4 (1:10).

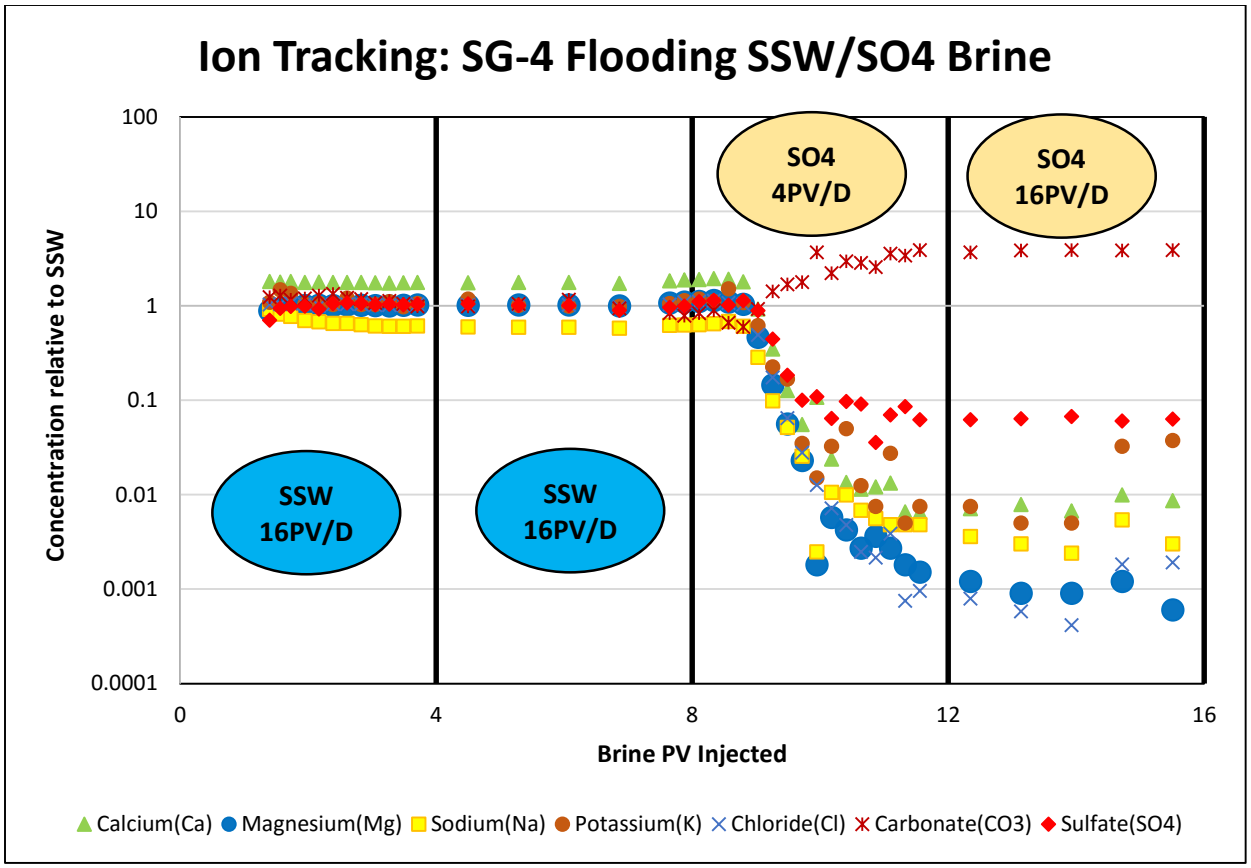

Figure 33: Ion concentrations of effluents relative to SSW taken while flooding with SSW-SO4 brine in core SG-4.

The declining rates of the ions [Na^{+}], [Ca^{+2}], [Mg^{+2}] and [SO_4^{-2}] are 0.039 0.0031, 0.0028 and 0.0026 mole/L PV, respectively, show that sulfate interacts more than Calcium, as it also was seen in case of flooding in SG-1 (flooding with SO4 brine). Which may lead to adsorption of $CaSO_4$ and alter the wettability to more water wet. That is why we observed an enhancement in oil recovery in second phase. Though we only have Na_2SO_4 in the injected brine, the presence of other ions may be due to mixing of brines and/or due to establishment of initial water saturation (S_{wi}) and the aging process. Higher decline rate of Mg^{+2} than Ca^{+2} shows negligible interaction between calcium and magnesium.

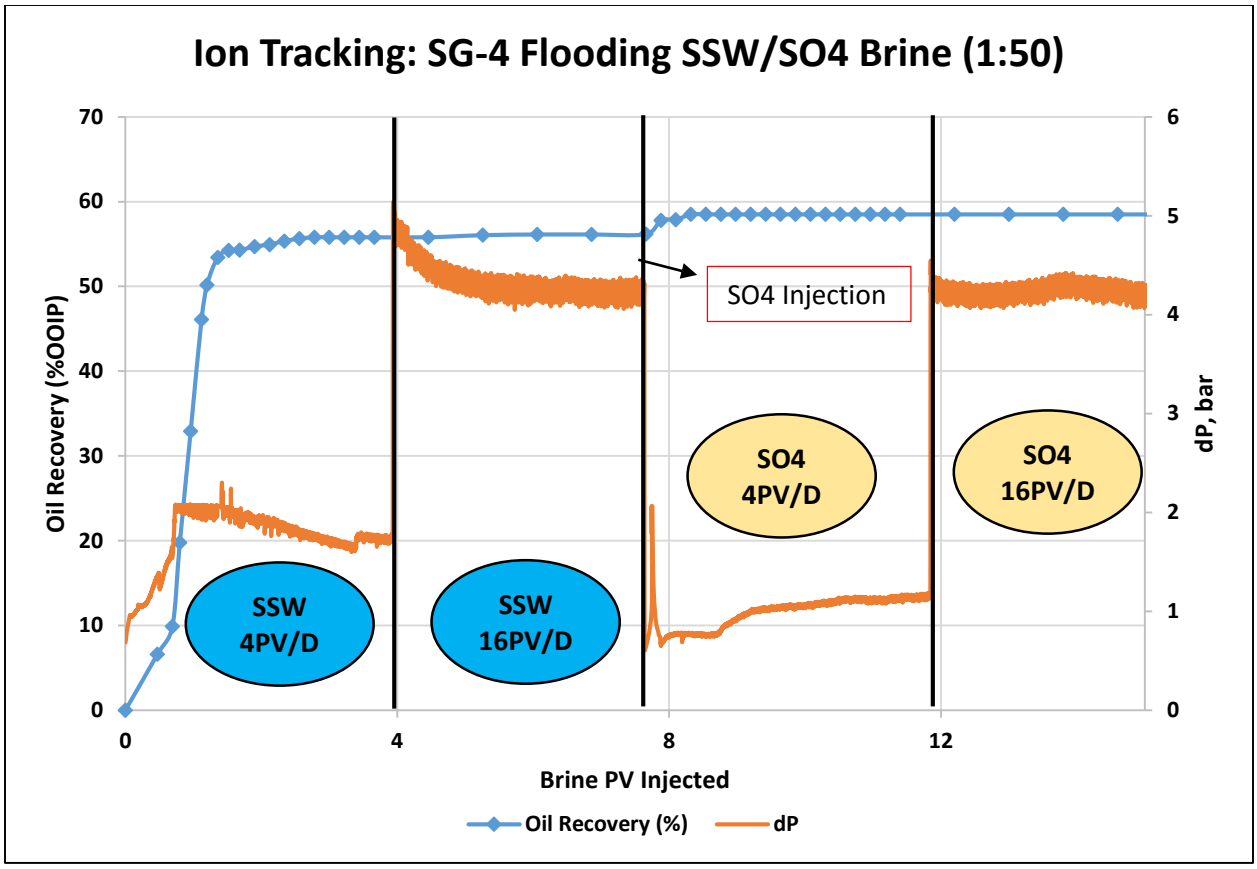

Figure 34: Oil Recovery and dP measured during flooding with SSW and LSW in Core SG-4.

Breakthrough occurred almost at the same time as in case of SG-1 (SO4 brine flooding), about 1PV. During SSW injection at 4PV/day, dP reached highest at 2.07 bar at 0.7PV and stabilized at 1.7 bar after 2PV. While at 16PV/day the average dP observed was about 4.1bar. With no variations in the peaks, zero increase in oil recovery has been observed at this rate. dP drops to an average value of 1 bar when injection brine switched to SO4 brine, may be due to flow of brine into the already swept area. Increase in dP at 4PV/day occurred may be due to displacement of mineral particles, which diverts the flow of brine to un-swept area. Thus increase in oil recovery. One more observation to note that after 1PV of SO4 brine injection, dP starts increasing and stabilized at 1.12bar. This result was also observed in case of flooding with LSW (1:50). Similar to SSW, injection of SO4 brine we observed no recovery at this rate. This may indicate less interaction between rock & brine and also capillary pressure in pores is high to overcome by this rate.

The increase in oil recovery was observed only at 4PV/day flow rate, which is less than what was observed in case of SO4 brine (1:10), section 4.2. From these results two conclusion can be made: (1) dilution by 10 times shows better results than any other dilution (Hamouda et al, 2014b), (2) sulfate concentration at 50 times dilution shows significant LS effects and recovery (Al Attar et al, 2013).

4.6. Flooding in Core SG-7 with SSW=> $MgCl_2$+NaCl Brine (1:10)

In section 4.3, it was observed that flooding $MgCl_2$ brine did not make a significant impact on oil recovery than injection Na_2SO_4 brine. The reason of higher recovery from SO4 brine than Mg brine was explained by Gandomkar et al. that due to less ionic radius of SO_4^{2-} than Cl^- leads to expand the double layers. Expansion of double layer increase the surface area of the divalent ions and leads to the more rock/brine interaction and sweep efficiency.

Nasralla et al, 2011, h performed experiments to understand the impact of cation exchange on oil recovery by LSWF in sandstone using single salt brine injection. They concluded that injection of NaCl and $MgCl_2$ brines leads to leaching of Ca^{+2}, which improves the oil recovery. This experiment was performed to assess the conclusion made by Nasralla et al, using NaCl & $MgCl_2$ in combination in chalk reservoir. Results are compared and analyzed later in this section.

Figure 35 shows pH measurements of influents and effluents with oil recovery obtained throughout the process. Here also difference between effluents and influents pHs were observed. pH of effluents ranges from 6.9-8.16. pH values decreased to 7 between 5-8 PV. After switching the brine to Mg+Na brine, pH increased drastically and reached to a maximum value of 8.2. Observed trend of pH values is similar to what was experienced in previous experiments. As it has already been discussed that variation in pH values are due to magnitude of calcite dissolution.

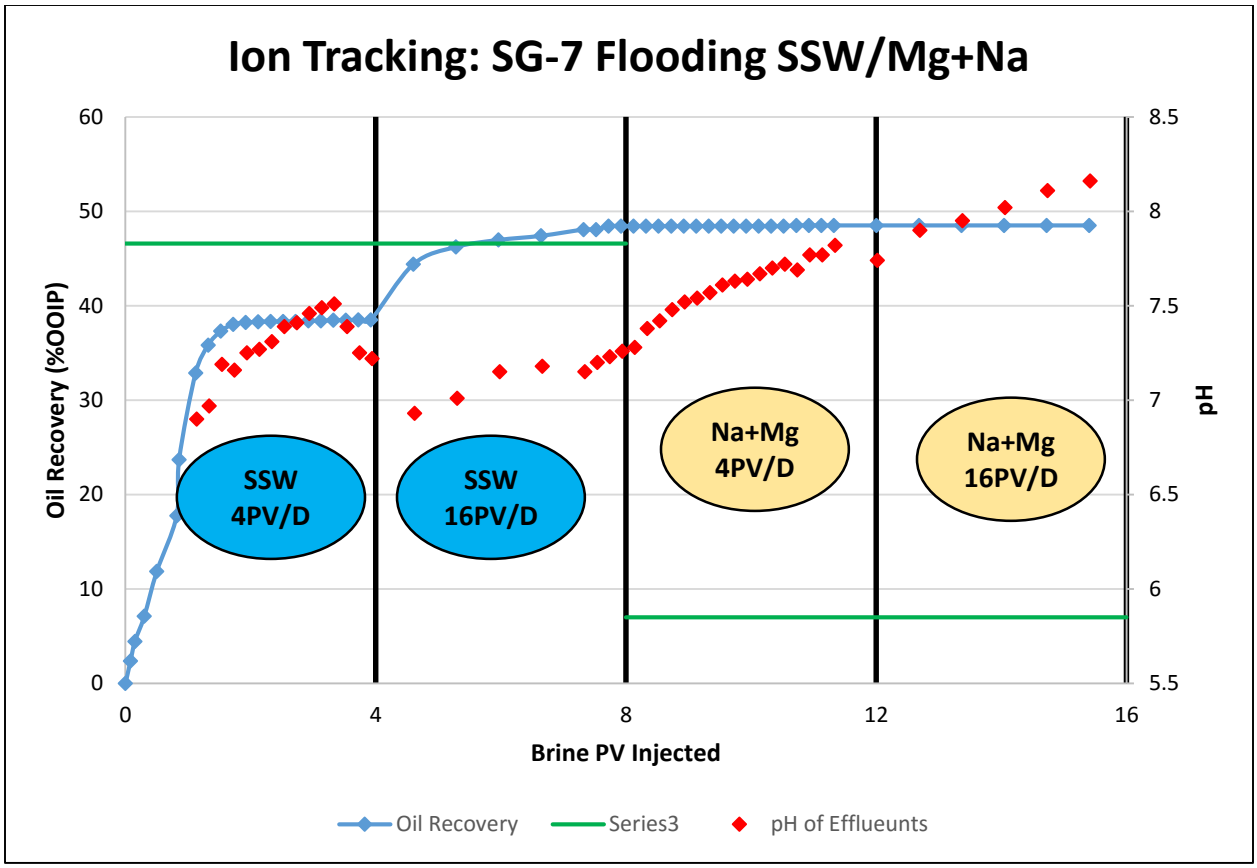

Figure 35: Oil Recovery, pH of effluent and influent measured during flooding with SSW and $MgCl_2$+NaCl brine in Core SG-7.

Figure 36 shows ion chromatograph results of the effluents. Effluent concentration during SSW flooding are almost same, which may imply very less interaction between rock and brine. For the second phase, the ion interaction can be explained with the help of declining rate. The declining rates of ions [Mg^{+2}], [Na^{+}], [Ca^{+2}] and [SO_4^{-2}] are 0.005, 0.05, 0.001 and 0.002 mole/L PV respectively. Decrease in concentration of ions other than sulfate and calcium may be due to the dilution of SSW by secondary brine as flooding proceeds. Dissolution of calcite shows increase in [CO_3^{-2}], shown in Figure 36. Mg^{+2} declines earlier than Ca^{+2}, which shows low interaction of magnesium. Nasralla et al. also experienced these observed results, in case of sandstone. Initial decrease in [Ca^{+2}] is due to dilution of core water after switching to secondary brine and later on constant concentration is due to leaching of Ca^{+2} (Nasralla et al., 2011). Ions present in effluents shows almost similar behavior as observed by Nasralla et al, 2011 and Gandomkar et al, 2015.

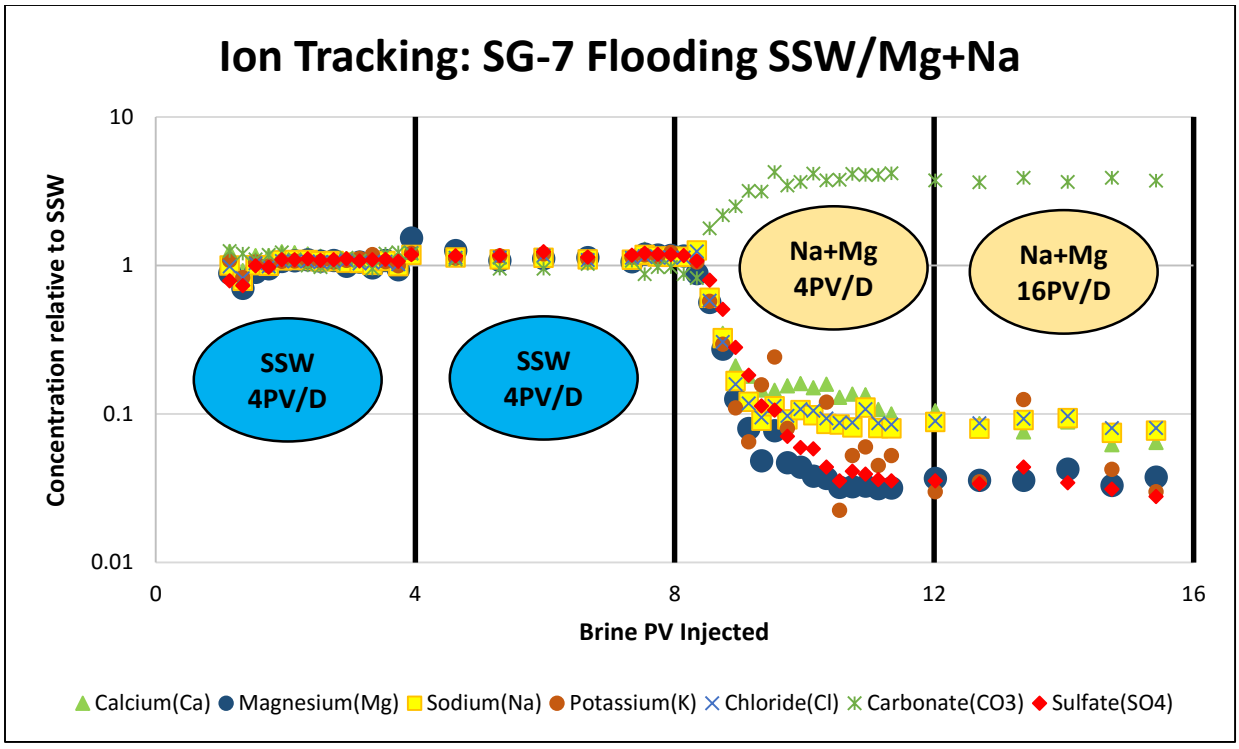

Figure 36: Ion concentrations of effluents relative to SSW taken while flooding with SSW-Mg+Na brine in core SG-7.

Figure 37 shows dP measurements in the core during flooding. As for all the experiments pressure drop curves follow exactly the same trends. From the oil recovery curve it can be compare that breakthrough occur at 0.67PV, gives a pressure drop of 2.5bars. Actual pressure drop in Mg+Na brine flooding ranges from 4.3-1.04 bars which is less than SSW flooding ranges from 6.1-2.08 bars. Sudden increase in dP may indicate diversion of brine to the un-swept area, leads to displacement of oil and increase in oil recovery.

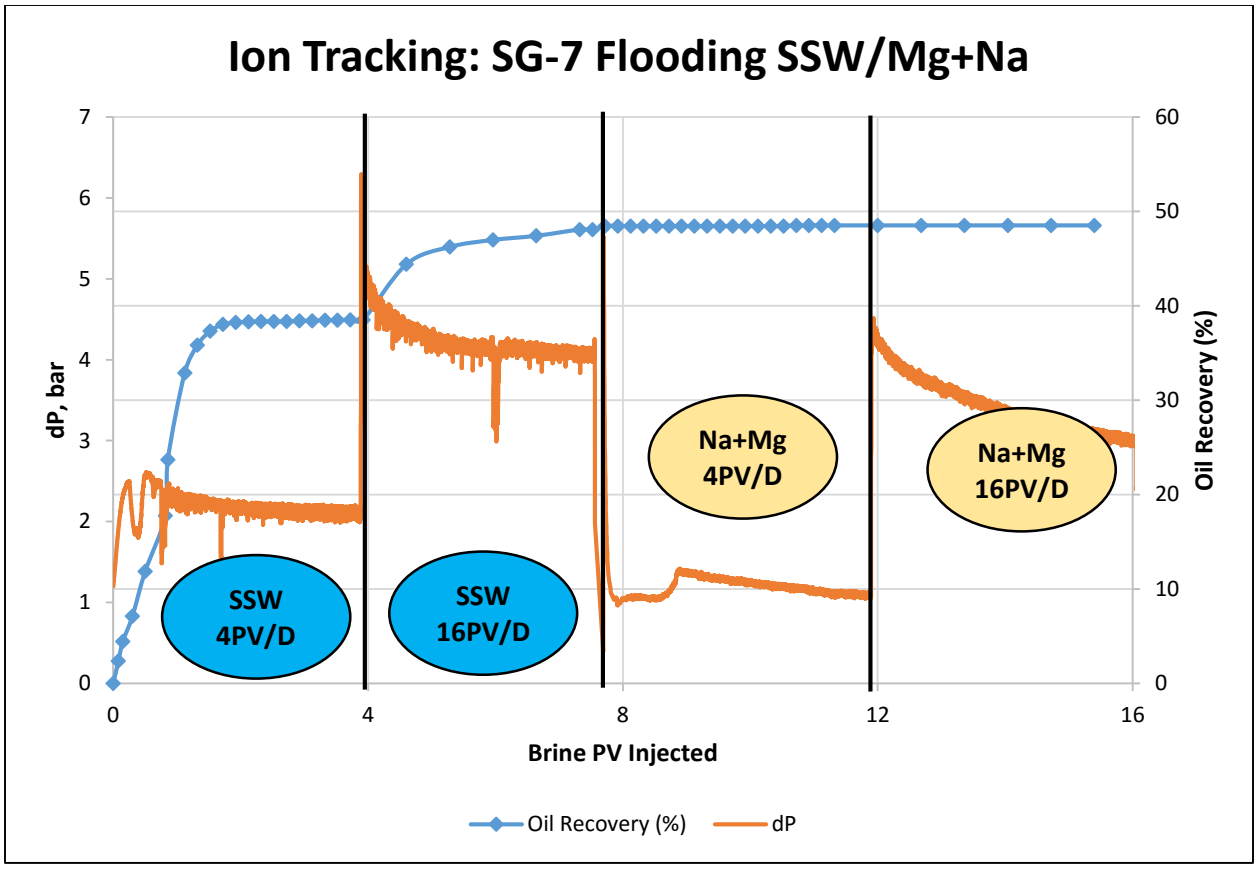

Figure 37: Oil Recovery and dP measured during flooding with SSW and Mg+Na brine in Core SG-7.

Investigation of LSWF performed by injecting $MgCl_2$ and NaCl salt brine shows a significant recovery from both the cases but a higher recovery from $MgCl_2$-brine (Nasralla et al, 2011, Gandomkar et al, 2015). Torrijos et al, 2016, observed increase in oil recovery by flooding with NaCl brine as a secondary injection fluid. Drastic increase in pH may reflected better interaction between brine/rock, ion exchange between Na^+/Ca^{+2} and wettability modification in the larger pores. In this experiment, though the increase in pH was observed but increase in recovery was zero. This may be due to very low interaction of sodium as it declined very fast compared to other ions. One hypothesis can be made from the oil recovery results that addition of NaCl with $MgCl_2$, decreases or prevent the expansion of double layer and in turn giving less increment in the electrostatic repulsion between rock and oil, which may not cross the threshold binding forces (Vander Waal forces) between oil and rock. Hence, oil molecules could not be able to release from

the surface (Gandomkar et al, 2015). Overall oil recovery measured from the experiment is 48.5% of OOIP. Increase in oil recovery is almost negligible after injection of Mg+Na Brine.

4.7. Flooding in Core SG-8 with SSW/ $MgCl_2$ (1:10) at 90°C:

In section, 4.3 flooding with Mg brine was performed at 70°C. Austad et al, have stated that affinity of Mg^{+2} towards surface is lesser at low temperature, because Mg^{+2} ion has a strong hydration energy. Zhang et al, performed experiments and observed that Ca^{+2} concentration in effluents is higher at high temperature than injected concentration, and Mg^{+2} in the effluent is lesser, due to the retardation.

Reactivity of Mg^{+2} with calcite surface can be explained by following reaction (by Hamouda et al, 2014b):

$$2CaCO_3(Calcite) + Mg^{+2} \leftrightarrow CaMgCO_3(s) + Ca^{+2} \quad (13)$$

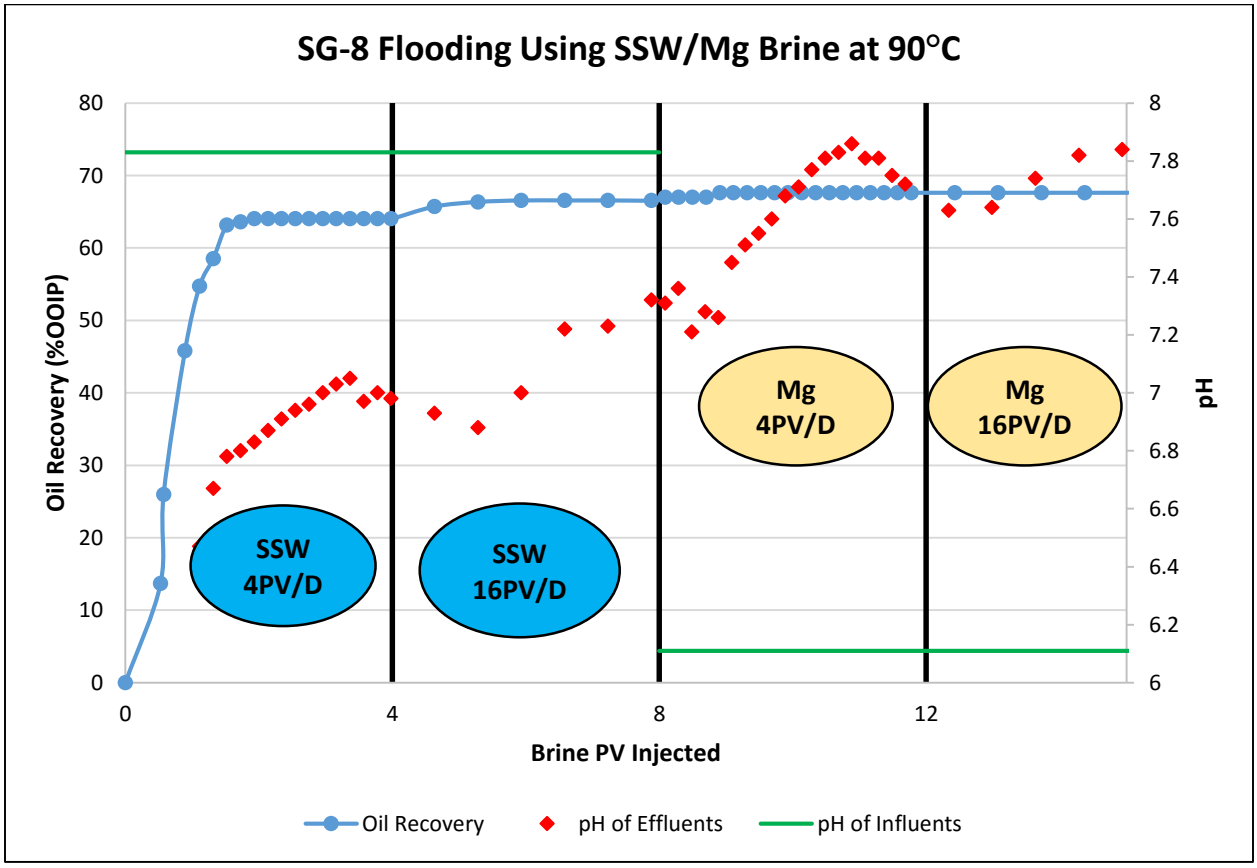

Figure 38: Oil Recovery, pH of effluent and influent measured during flooding with SSW and Mg brine (at 90°C) in Core SG-8.

Recorded pH, dP measurements and ion chromatograph results showed similar trend as it has been observed in the previous experiments. Figure 38 shows a sharp increase in pH of effluents while flooding Mg brine. pH ranges from 6.4-7.84 throughout the experiment. Lower pH of effluents than influent in case of SSW flooding shows less dissolution of calcite. pH of effluents while flooding with Mg brine at 70°C were almost same as pH during Mg brine flooding at 90°C. This may show no change in calcite dissolution with change in temperature.

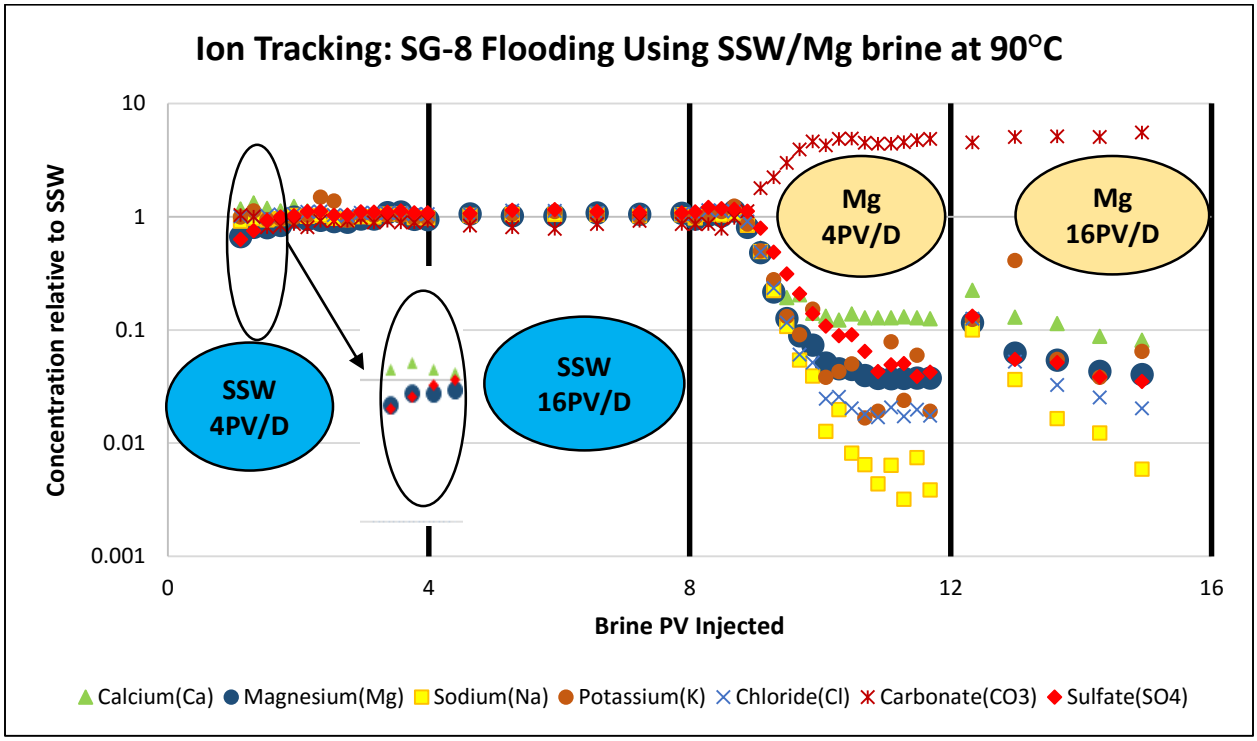

Figure 39: Ion concentrations of effluents relative to SSW taken while flooding with SSW-Mg brine (at 90°C) in core SG-8.

From the ion chromatograph results, initial rock/brine interaction was observed (shown in enlarged circle, figure 39). From Figure 39, declining rates of [Mg^{+2}], [Ca^{+2}] and [SO_4^{-2}] are 0.008, 0.003 and 0.009 mole/L PV, respectively. One more different and interesting observation is noticeable at higher temperature that there is one more decline curve at higher injection rate. This shows restoration of rock/brine interaction at higher rate. Increase in HCO_3^- concentration showed the dissolution of calcite. After switching to Mg-brine, calcium concentration in effluents at 90°C was higher than at 70°C (Section 4.3), throughout the Mg brine flooding and Mg^{+2} ion strongly

retarded, assessed from the decline rates (Figure 39 & 26). Higher concentration of calcium than magnesium may also due to leaching of Ca^{+2}.

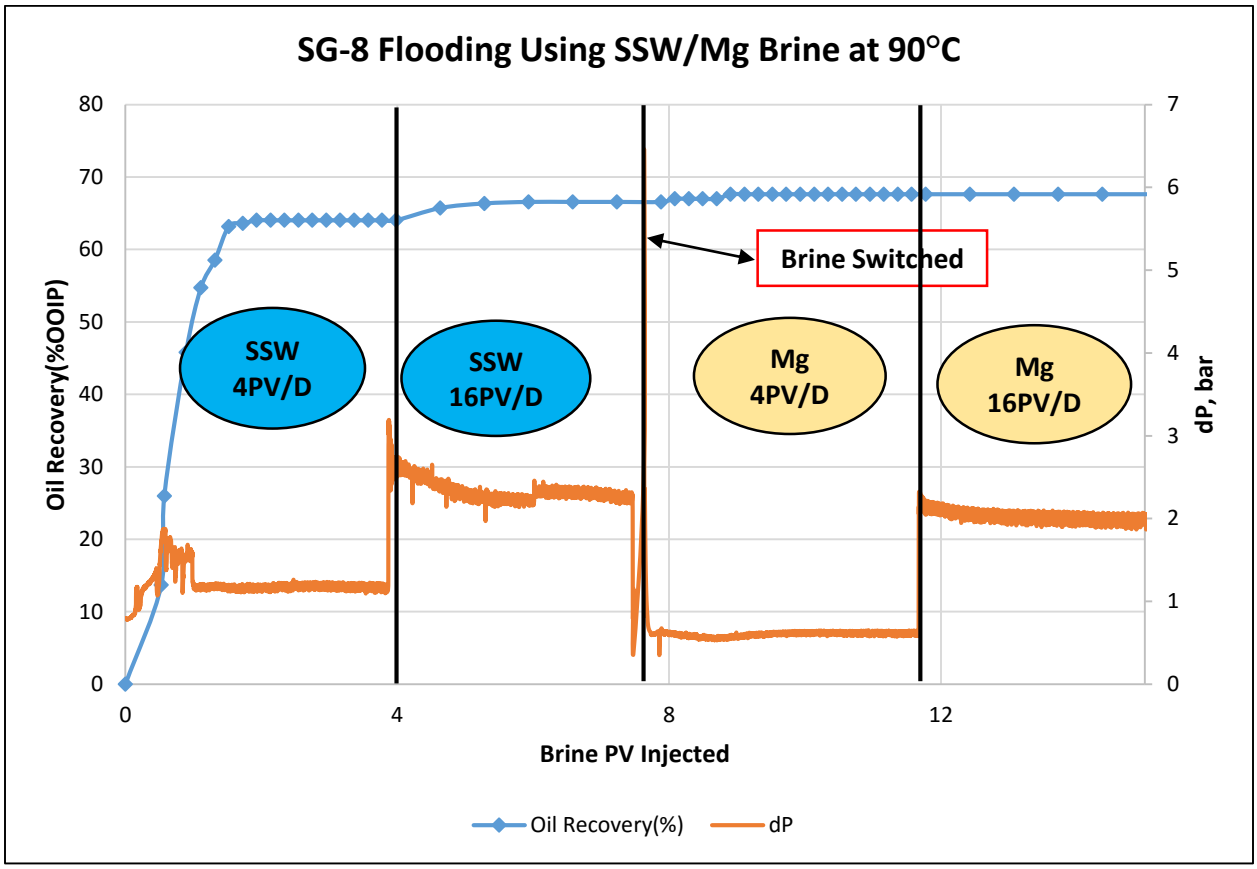

Figure 40: Oil Recovery and dP measured during flooding with SSW and Mg brine (at 90°C) in Core SG-8.

Interaction between rock/brine of higher magnitude ws observed at 90°C, which reflected by increase in oil recovery.

Pressure drop measurement can explain dynamic interaction inside the rock. Initial increase in peak (~2bar) shows water breakthrough at 1PV. As expected pressure drop was higher at 90°C, (3-0.5 bar) compared to 70°C (2.1-0.3 bar). The pressure drop was higher during SSW flooding reached a peak of 3 bar (at 4PV) than Mg brine flooding reached a peak of 2.5bar (at 11.5PV). Due to fine migration, increase in pressure drop experienced, which leads to increase in relative permeability and hence, improvement in oil recovery. Total oil recovery measured is 67.6% of OOIP with an increase in oil recovery 1.5% by flooding with Mg brine.

4.8. Flooding in Core SG-5 (saturated with crude X) with SSW/ LSW (1:10)

All the experiments performed previously, by Hamouda et al, 2014b. and also the experiments explained above, in the laboratory were performed on cores saturated with Model oil. In this case, the core was saturated with Crude Oil X. The composition of Crude Oil X is given in Table 5.

Most of the carbonate-oil reservoirs act as neutrally or preferential oil-wet, as discussed in details by Hirasaki and Zhang., Gomari and Hamouda, 2006 and Hansen and Hamouda, 2000. The oil-water interface becomes negatively charge due to presence of carboxylic groups, whereas the water-rock interface is positively charge due to presence of Ca^{+2} in brine initially. Presence of carboxylic groups increase the positive charge on surface. Thus, water wetness of the rock decreases as carboxylic group increase in Crude Oil. Amount of Carboxylic groups is expressed by AN.

Motives for performing this experiment was to,1) assess the difference between the magnitude of LSW mechanisms and, 2) Best outcome obtained by flooding LSW 1:10, irrespective of oil present in the core. Flooding sequence is similar to the other experiments and core details are shown in Table 10. Results obtained such as Effluents' pH, pressure drop during flooding and oil recovery are explained in comparative manner.

Figure 41 shows relative variation of effluents' pH with respect to the injection brine. pH trend, during SSW injection, observed in this case is similar to the results obtained in previous experiments and also explained in Hamouda et al., 2014b.

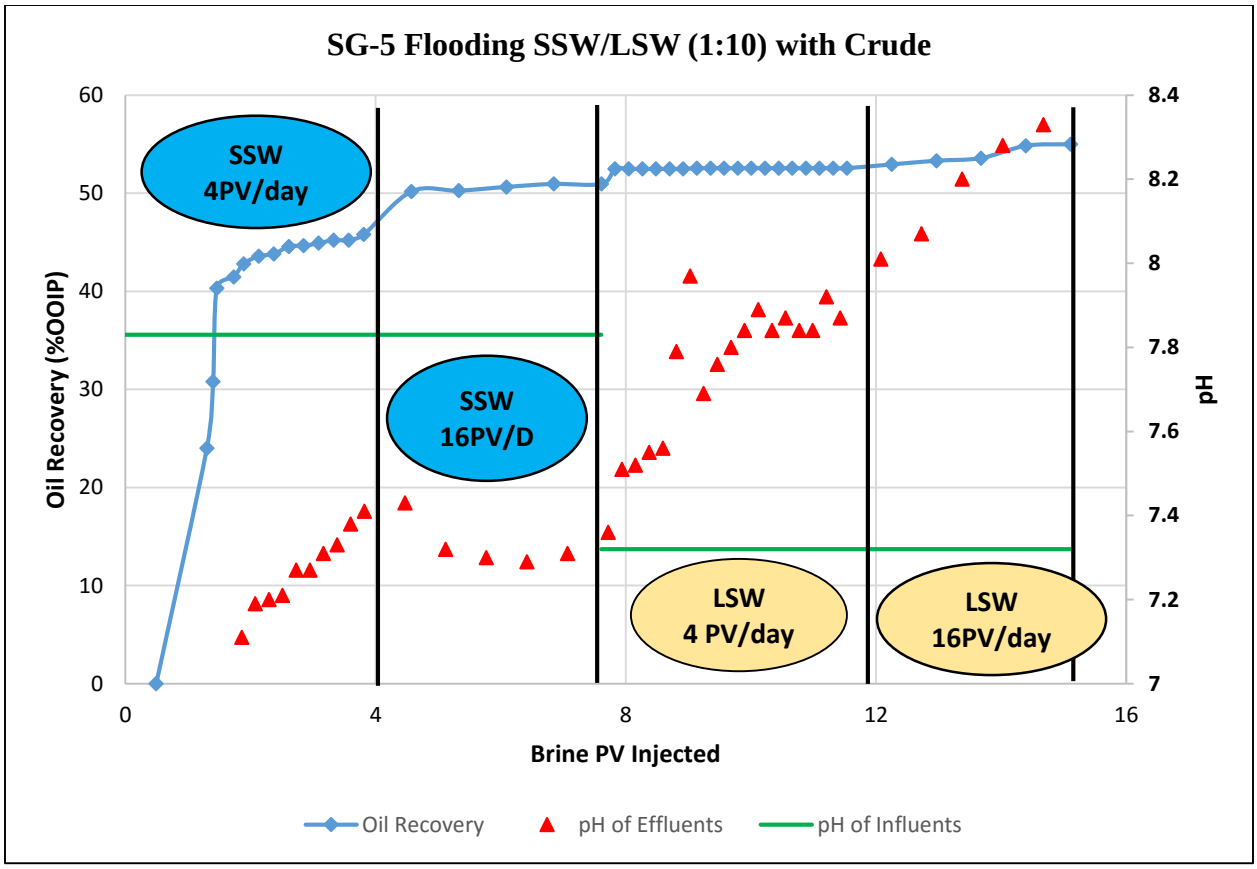

Figure 41: Oil Recovery, pH of effluents and influents measured during flooding with SSW and LSW in Core SG-5.

pHs of effluents were higher in LSW flooding than the injected brine and also than the effluent pHs of effluents during SSW flooding (figure 41). pH increase was observed as a LSWF mechanism, as explained in section 2.6. A sharp increase in pHs was detected during the LSW injection (7.61-15.11PV), Figure 42. Maximum pH observed during secondary flooding (LSWF) was 7.97 and 8.33 at 4PV/day and 16PV/day, respectively. Ion tracking results showed that may be due to calcite dissolution, concentration of OH^- increases in brine, hence pH increase.

Lager et al, 2008 had shown that in presence of high salinity brine rock forming minerals are undisturbed and retain their oil wet nature. While in case of low-salinity brines, surface particles get detached from the surface. So it's almost negligible to observe migration of fines during SSW injection. In figure 42, may be due to early water breakthrough, pressure drop peak observed at 1.12(1.23) bar(PV). Frequent increase in pressure drop was observed during SSW injection. This may be due to presence of two phases in the pore, where oil phase provides resistance to the flow

water. As the injection pressure overcomes the resistance, oil molecules starts moving and oil produces.

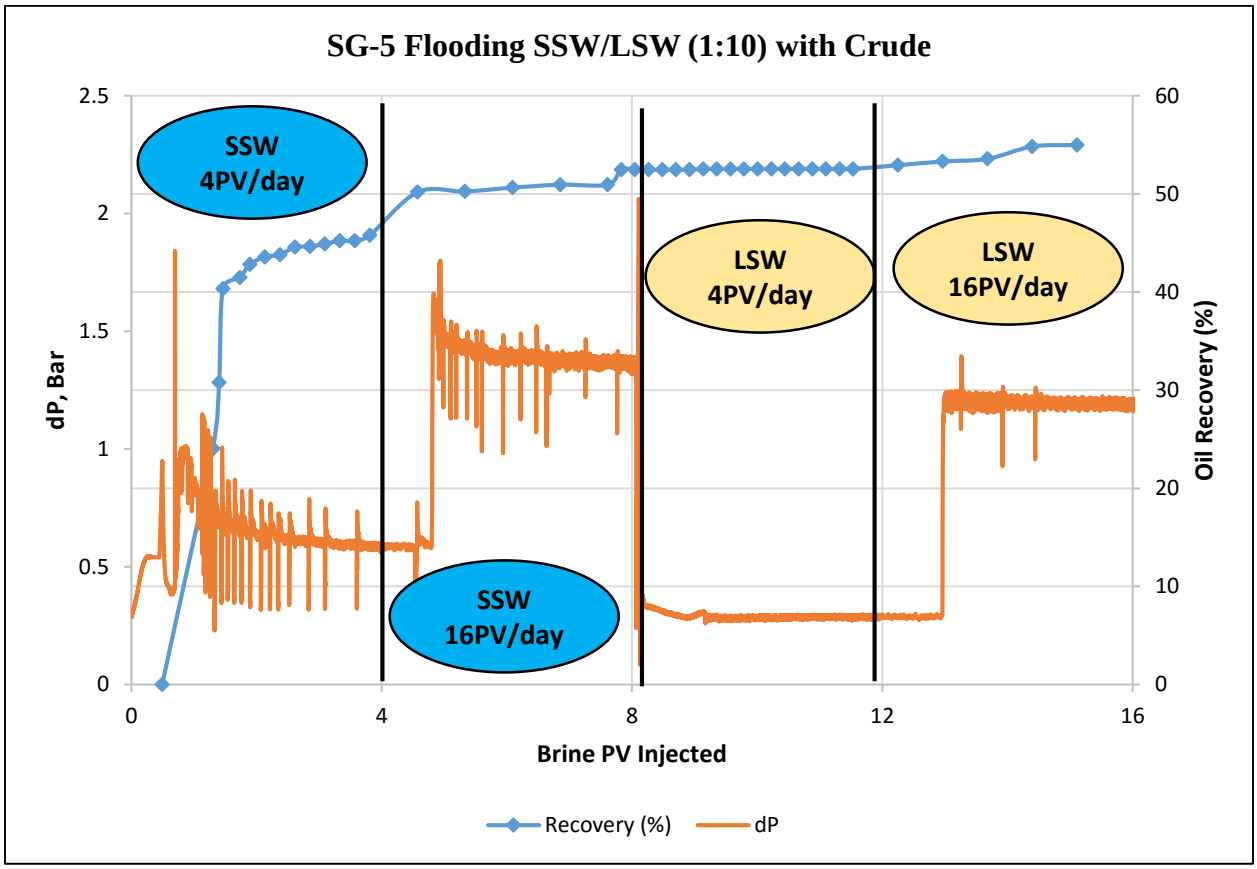

Figure 42: Oil Recovery & dP measured during flooding with SSW and LSW in Core SG-5.

In case of low salinity brine, oil particles detach from the pore surface. The pressure drop varied from 0.32-1.25 bar during LSW flooding, which was less than the pressure drop recorded in case of SSW injection, 0.5-1.79bar. From figure 42, injection of LSW at 4PV/day gives initial increase in pressure drop to 0.3bar (at 9.15 PV). Later on, as flooding proceeded, the pressure drop remained constant to 0.27bar. It may be because injection rate 4PV/day was not enough to overcome the capillary forces and colloidal forces, which keep the particles attached to the surface. It also reflected in the oil recovery results i.e., 2% increase in total recovery. By increasing the injection rate to 16PV/day, various pressure drop peaks were observed such as 1.33bar at 13.12PV. This may be due to migration of fines at higher rate, gives increase in pressure drop, and increase in sweep efficiency. A 3% of increase in recovery was obtained and this could be due to fine migrations from the rock surface and which enhanced the sweep efficiency.

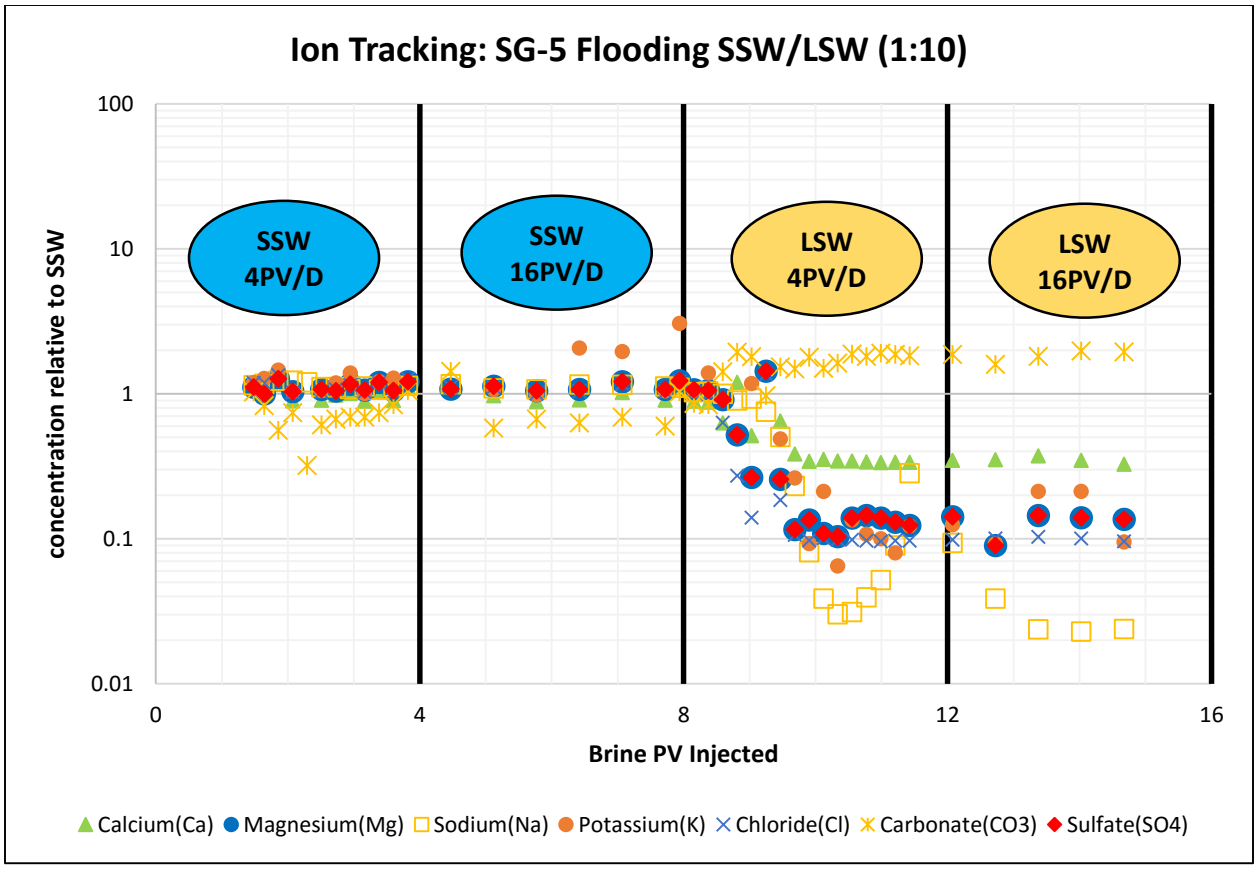

Figure 43: Ion concentrations of effluents relative to SSW taken while flooding with SSW-LSW in core SG-5.

Interaction between rock and brine can be analyzed by ion chromatograph results (Figure 43). The AN is very low for this crude oil, which means that carboxylate groups in the crude are very less (Section 3.1.2.1). MIE is negligible in case of SSW injection, that's why the concentrations of ions in effluents are same as in SSW. The injection of LSW containing low concentration of Ca^{+2} and Mg^{+2} which causes ion exchange between adsorbed polar components and cations. Ion exchange is discussed by looking at the decline rates of the ion concentrations. Decline rates for [Ca^{+2}], [Mg^{+2}] and [SO_4^{-2}] are 0.005, 0.02 and 0.027 Mole/ L PV, respectively. This shows calcium declined very fast which implies low interaction with rock surface. Due to less interaction of calcium and magnesium at low injection rate, cations were unable to remove the organo-metallic complexes from the surface. This why there is no increase in recovery at later stage.

If we closely observe in figure 43, average [Ca^{+2}], [Mg^{+2}] and [SO_4^{-2}] are approximately 0.32, 0.14 and 0.15, respectively. These values are higher than the value observed at lower

injection rate. The similar results were obtained by Hamouda et al., 2014b. Lower value of Mg^{+2} than Ca^{+2} shows ion exchange between them. In addition, low salinity cations removed the organo-metallic complexes from the surface. This reflected by the increase in the oil recovery at the later stage. This leads to formation of magnesian, also observed in section 4.4. Dissolution of calcite shows increase in concentration than in SSW.

Hamouda et al., 2014b suggested that LSW 1:10 gives the highest recovery than brines with different dilution ratio, LSW 1:5, 1:15 & 1:25. That is why, in the next section (section 4.9) flooding was done by injecting LSW 1:50. By comparing results of these two flooding confirms that recovery is higher, overall 55% with 5% increase with LSW, in case of LSW 1:10.

Simulation (using CMG) and experimental ion concentrations are compared in figure 43. The simulation is also run for the 16PV, though the concentrations reached the equilibrium at 9PV.

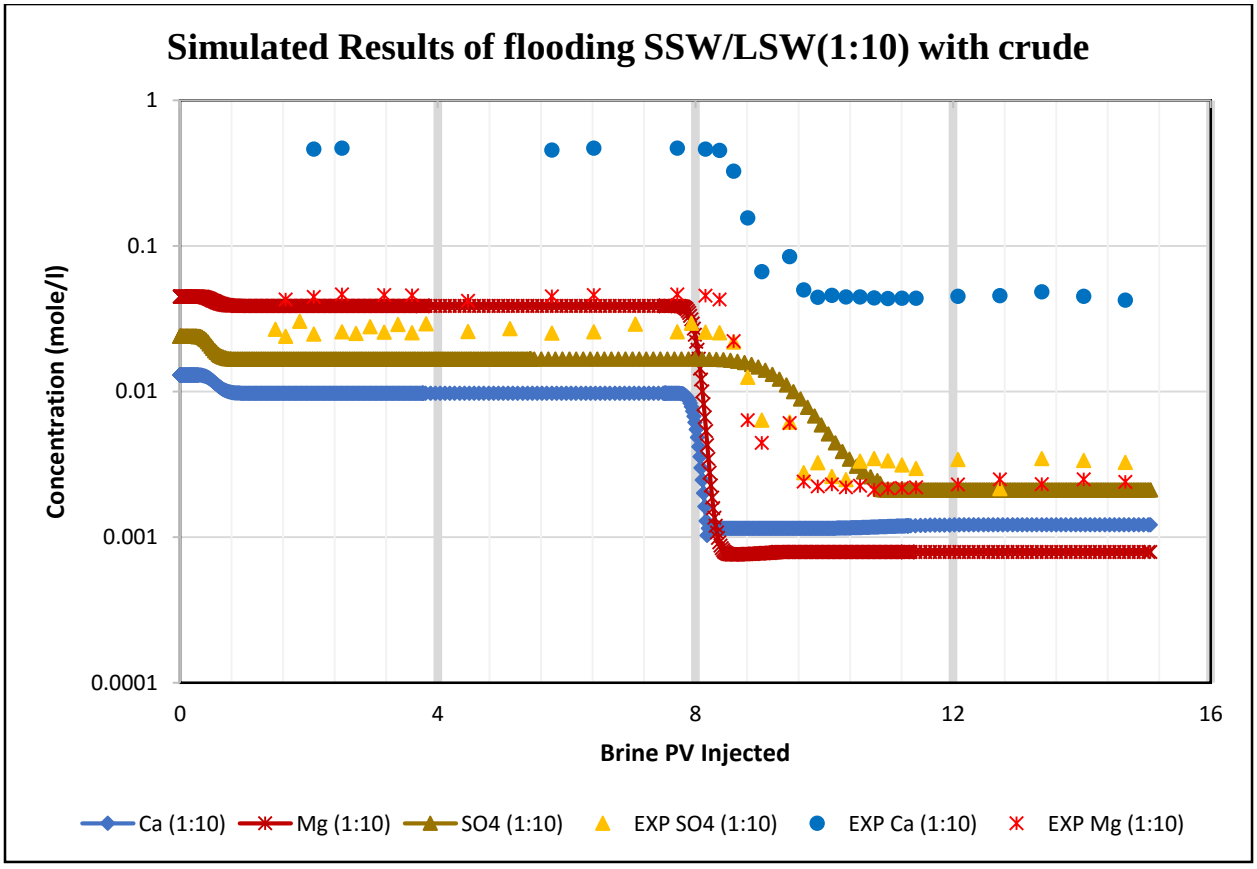

Figure 44: Comparison between experimental (points) and simulated (lines) ion concentrations (mole/l) for SSW/LSW.

The decline trend and the concentrations for simulation and experimental data are in good agreement. The difference in starting of decline curves may be due to mixing of brines in experiment. Calcium concentrations are higher in case of experiments. This may be due to the dissolution of calcium sulfate during establishing initial water saturation and aging process[34]. Also may be because of inability of the software to simulate the exchange between calcium and magnesium which leads to formation of magnesian.

4.9. Flooding in Core SG-6 (saturated with crude X) with SSW=> LSW (1:50)

Similar to section 4.4, core saturated with crude oil was also flooded with LSW 1:50. The results i.e. pH, oil recovery and pressure drop, obtained are compared with the results obtained after flooding with LSW 1:10. Hamouda et al. (2014b) confirmed that injecting LSW 1:10 gives the best outcome. When their results were compared with results from section 4.4, the statement

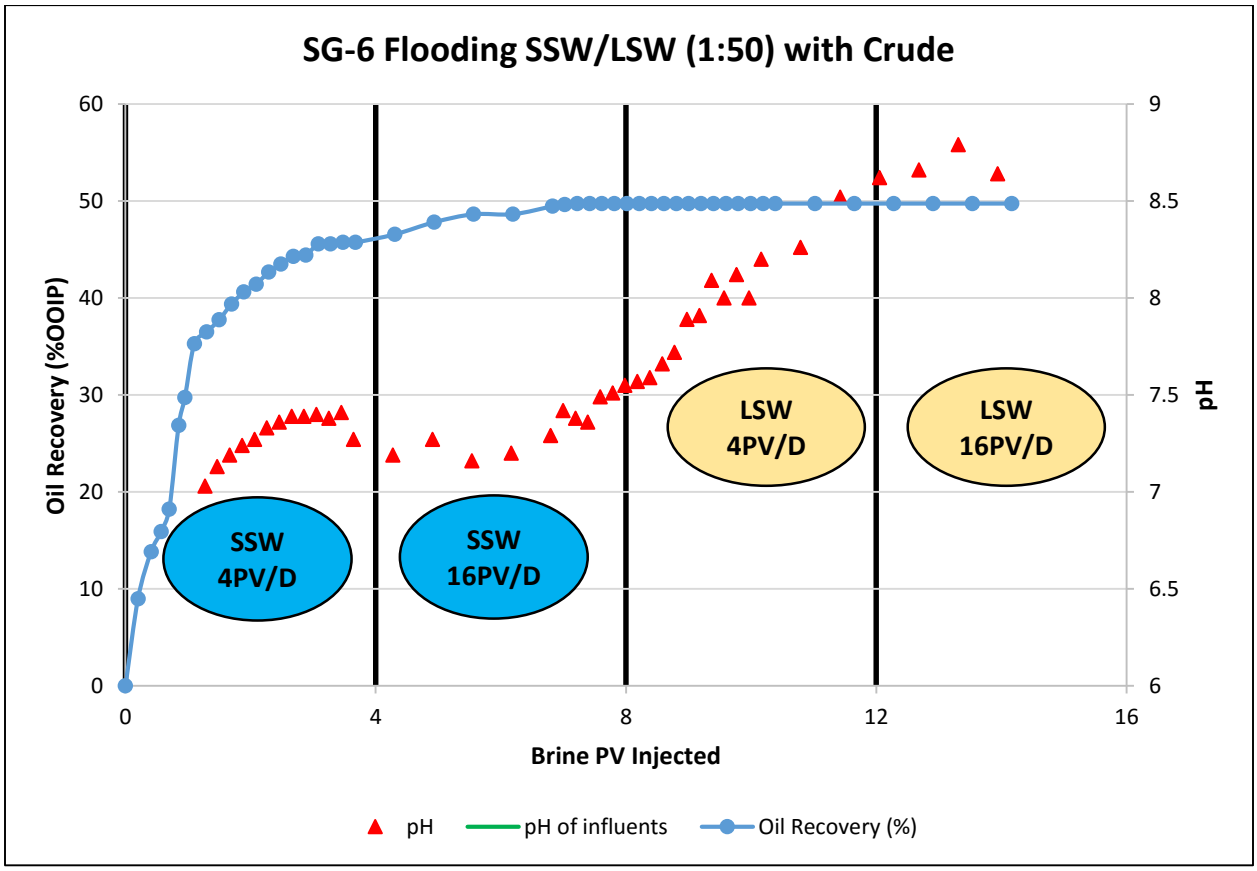

Figure 45: Oil Recovery, pH of effluents and influents measured during flooding with SSW and LSW in Core SG-6.

found to be rigid. Similarly, results were obtained and compared with cases where cores saturated with crude. Results are shown and explained later in this section5Likewise, all the experiments effluents' pH, oil recovery and pressure drop were recorded. Core details and flooding sequence is shown in Table 5.

pHs of effluents were measured and shown in figure 45. pH trends were conforming to the pH behavior observed in previous experiments mentioned in this work. pHs of effluents was lower than the influent during primary flooding with SSW. pHs of effluents varied from 7 to7.55. However, in second phase, during LSW injection, pHs increased sharply and were higher than influent. Maximum pH reached to 8.8, which was slightly higher than LSW 1:10 (section 4.8). This shows higher dissolution of calcite in injected brine.

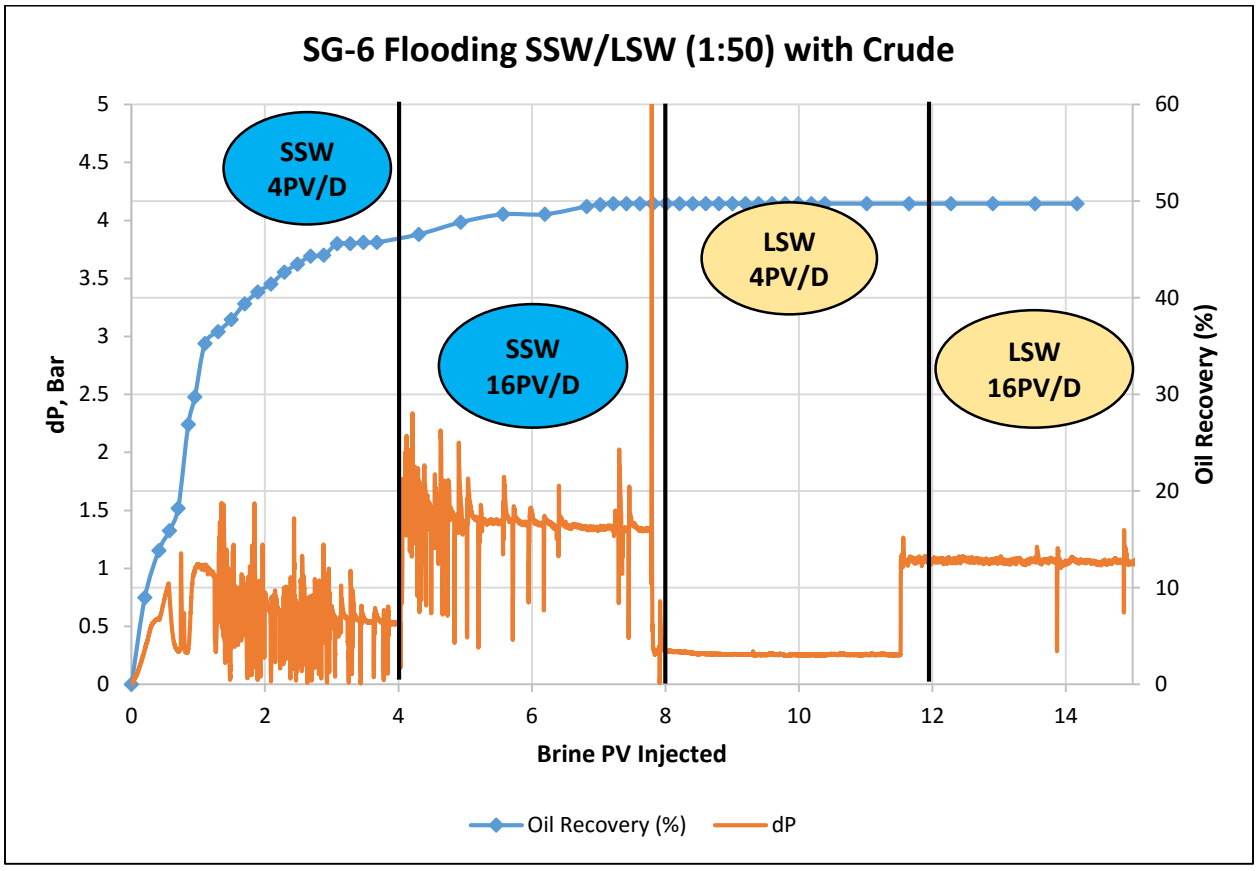

Figure 46: Oil Recovery & dP measured during flooding with SSW and LSW in Core SG-6.

Early breakthrough observed at 1.38 PV of SSW injection, when the pressure drop increased to 1.5 bar. Pressure drop varies from 2.33-0.5 bar, with various peaks representing increase in pressure drop. As explained before, these peaks reflected displacement of oil

molecules, hence, oil production. While injection of LSW, the average pressure drop recorded was lower than SSW. In second phase, pressure drop varies from 0.25 to 1.09 bar. From figure 47, pressure drop at low injection rate is almost constant, 0.25bar throughout the injection of 4 PV. It was also experienced and explained in case of flooding with LSW 1:10 (figure 42). Few peaks were observed between 14 and 15PV of brine injection with increase in dP to 1.5 bar. This indicated increase in pressure drop may be due fine migration which leads to increase in sweep efficiency, hence, increase in oil recovery.

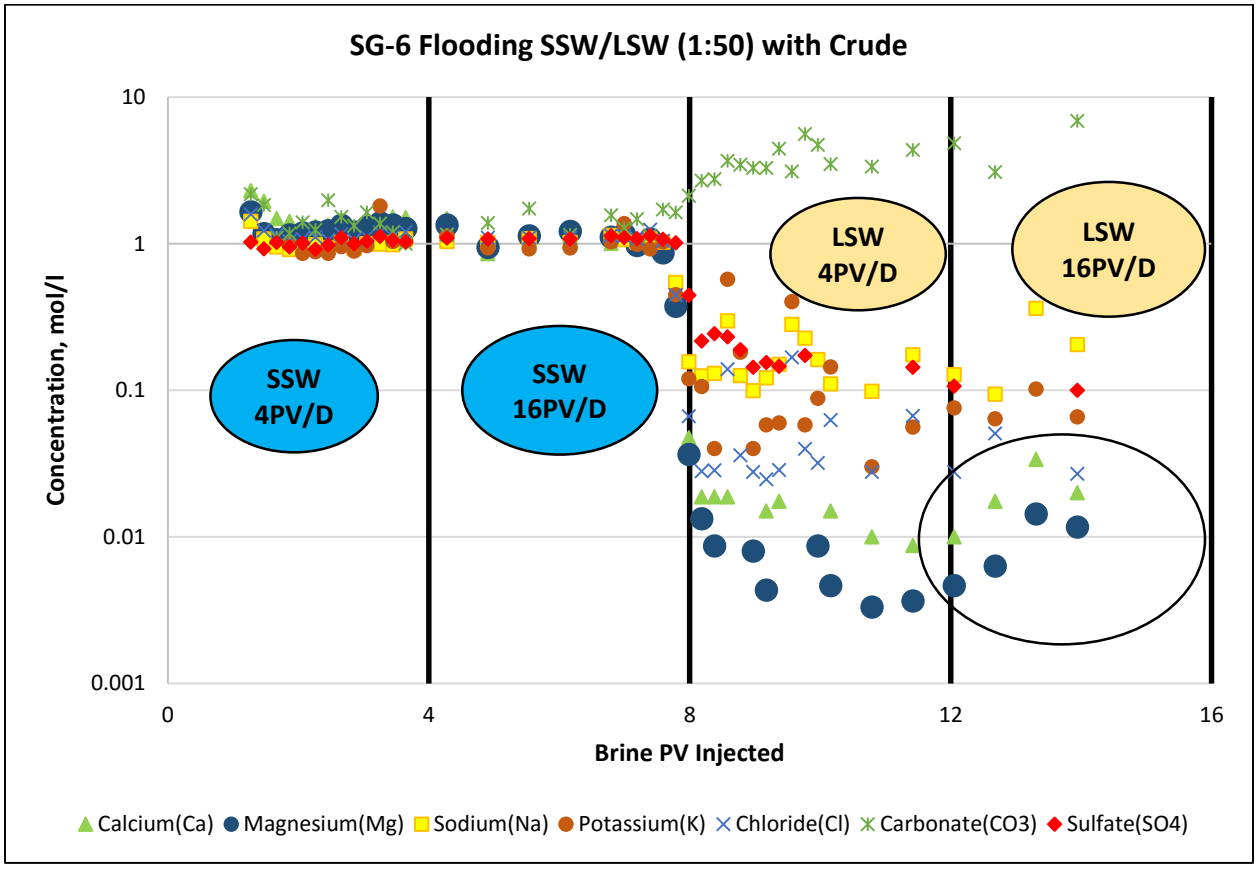

Figure 47: Ion concentrations of effluents relative to SSW taken while flooding with SSW-LSW in core SG-6.

From the ion concentration results (Figure 47) for the first phase, all the ions have almost same concentration as was in SSW. During LSW 1:50 flooding, all the ion curves except, [HCO_3^-] shows a decrease in slope. The declining rates of the ions for this part for [Na^+], [Mg^{+2}], [Ca^{+2}] and [SO_4^{2-}] are 0.06, 0.007, 0.003 and 0.004 Mole/L PV. This shows a lower contribution of SO_4^{2-} in $CaSO_4$ dissolution than Ca^{+2}. In addition, it was observed by other researchers (Gomari et al.)

that sulfate has been consumed in other processes such as adsorption. Calcite dissolution and alkalinity of the system has also been expressed in form of reactions (10) and (11).

As explained pH increase may due to calcite dissolution, as explained in previous experiments mentioned here, but it does not reflect in the [HCO_3^-] in Figure 47. The similar results were also observed while experimenting with other LSWs in the laboratory by Hamouda et al., 2014b. They also explained that the water exposed to CO_2/air to some extent affects the pH and distribution of carbonate species (Hamouda et al., 2014b). This hypothesis supported the results of [HCO_3^-] observed in case of LSW (1:50). Deficiency in [Mg^{+2}] could be due to ion exchange between magnesium and calcium which leads to deposition of dolomite/magnesian. Exchange of Mg^{+2} and Ca^{+2} increases the water wetness of the chalk surface and contribute in increment in oil recovery (encircled in figure 47).

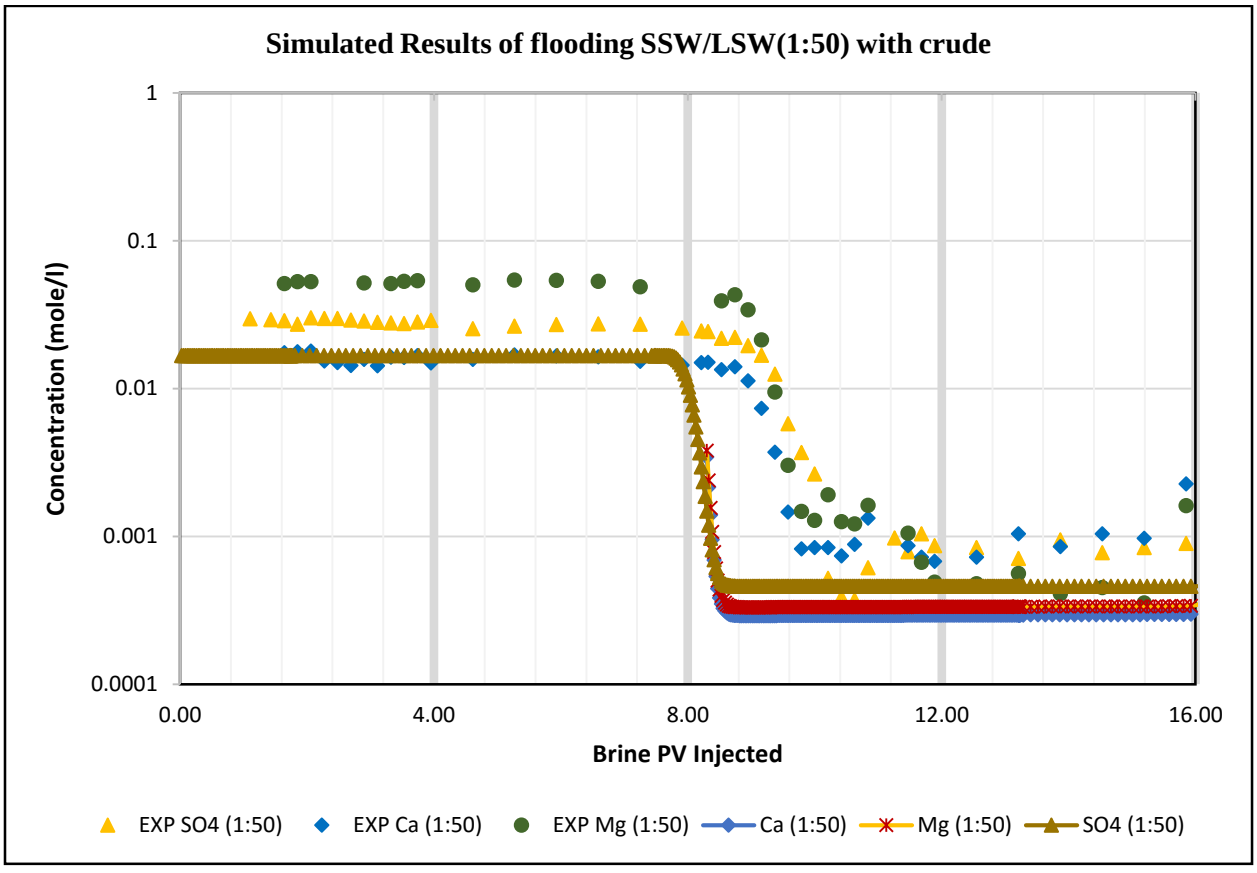

Figure 48: Comparison between experimental (points) and simulated (lines) ion concentrations (mole/l) for SSW/LSW.

Two results were observed from this experiment. First, LSW 1:10 gives better recovery (54%) than LSW 1:50 (49%). A 5% increase in recovery was observed in case of LSW 1:10. Second, results obtained conform to the results in case of flooding with LSW 1:50 when core wa saturated with model oil (section 4.4).

Simulation (using CMG) and experimental ion concentrations are compared in figure 48. The decline trend and the concentrations for simulation and experimental data are in good agreement. The difference in starting of decline curves may be due to mixing of brines in experiment. Calcium and magnesium concentrations are higher in case of experiments. This may be due to the dissolution of calcium sulfate during establishing initial water saturation and aging process (Hamouda et al, 2014b). But ionic concentrations are almost equal at equilibrium.

4.10. Simulation Part

Simulation was done to compare the results obtained from the experiments and results generated from the numerical model. Numerical models were generated in the CMG (2014 Version). Data obtained from the experiments were used to generate the relative permeability curves in CMG.

Relative permeability curves give an idea of relative movements of fluid inside the core during flooding and change in relative permeability after the flooding ends. The ion tracking, oil recoveries and relative permeability curves were monitored using CMG GEM simulator for simulating the fluid rock interactions.

When simulating the LSW using CMG GEM simulator, the fluid and grid models were first established. CMG modelling was performed for LSW 1:10 (core saturated with model oil), LSW 1:10 and LSW 1:50 (core saturated with crude oil X) The inputs required to these models are given as:

- **Fluid modelling**
    - Oil Composition: Composition of model oil and crude oil which was used as input is given in Table 3 & 4.
    - Ion concentrations of injected brines are presented in Table 6.
    - Required reactions:

Aqueous reactions	Mineral reaction
$CO_2(aq)+H_2O=H^+ +(HCO_3^-)$	$Calcite+(H^-) = (Ca^{+2}) + (HCO_3^-)$
$(OH^-)+(H^+) = H_2O$	
$(CaCH_3COO^+) = Ca^{+2}+(CH_3COO^-)$	
$CaSO_4 = Ca^{+2} + SO_4^{2-}$	
$MgSO_4 = Mg^{+2} + SO_4^{2-}$	

Table 12: Selected reactions (Hamouda and Pranoto, 2016)

- **Grid modelling**

This is a horizontal, one-dimensional model with 50 blocks in I direction. This core model is consisting of one injector (in block 1) and one produce (in block 50), see figure 48. Reservoir properties inserted in the model are shown Table 13.

Rock Properties (field unit)	Value
Grid	50,1,1
Length i	0.003937 ft.
Length j	0.269148 ft.
Length k	0.269148 ft.
Porosity (core SG 3, 5 & 6)	0.49, 0.50, & 0.51
Permeability	3.9 mD
Reservoir Temperature	158°F
Mineral fraction of Calcite	99%

Table 13: Reservoir/Grid properties

- **Ion Exchange**

Ion exchange reactions considered in the modelling cover sodium and calcium ions. The reaction indulging exchange between sodium and calcium is expressed by Dang et al. as:

$$Na^{+} + \frac{1}{2}(Ca - X_2) \leftrightarrow (Na - X) + \frac{1}{2}Ca^{+2} \quad (14)$$

4.10.1. Simulation Results and discussions

- **Ion Tracking**

The effluent concentrations of Divalent Ions Ca^{+2}, Mg^{+2} and SO_4^{-2} are expressed for all the three cases as a dimensionless concentration relative to the SSW, as shown Figure 31, 44 & 48. The simulation is run for 16PV. The simulated data are plotted together with the experimental data. Both the data are in correlation with each other. From these figures, we can see that deviation between experimental and simulated data. These deviations and difference in decline curve stabilization is explained in respective sections.

- **Oil Recovery**

The flooding sequence is same as it was performed in the experiments. Out of 16 PV of brine injected, for first 8 PV SSW was injected at 4PV/day and 16 PV/day, with 4PV at each rate. For second 8PV LSW was injected at the similar injection rates. Overall oil recovery with SSW was approximately same i.e. 40.8%, see figure 49. It is interesting to observe that simulation shows that LSW 1:10 gives a faster response than LSW 1:50. The same results were obtained by Hamouda et al., 2016. They observed that recovery from higher dilution ratio brine shows a lag in response. From an oil recovery standpoint, LSW 1:10 gave 1.9% increase in recovery while LSW 1:50 gave 1.7% increase in recovery.

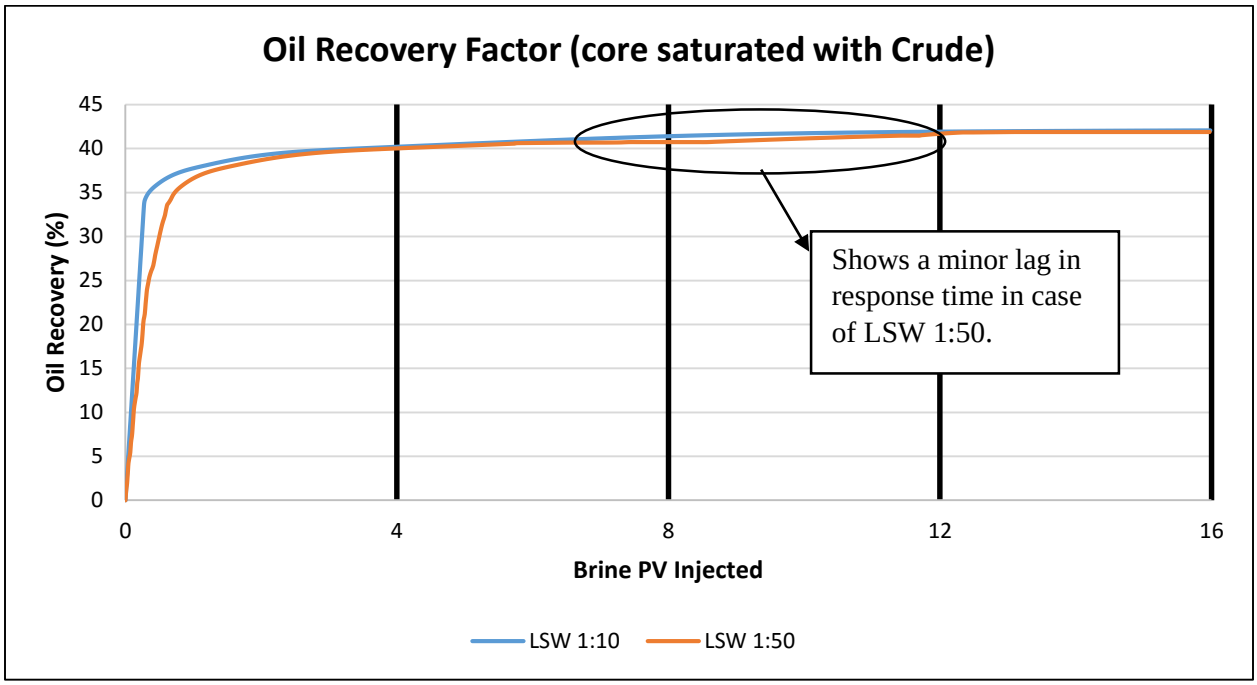

Figure 49- The recovery factor for different LSWs.

Figure 49 shows different time response when injecting LSW 1:10 and LSW 1:50 in a core saturated with Crude Oil X.

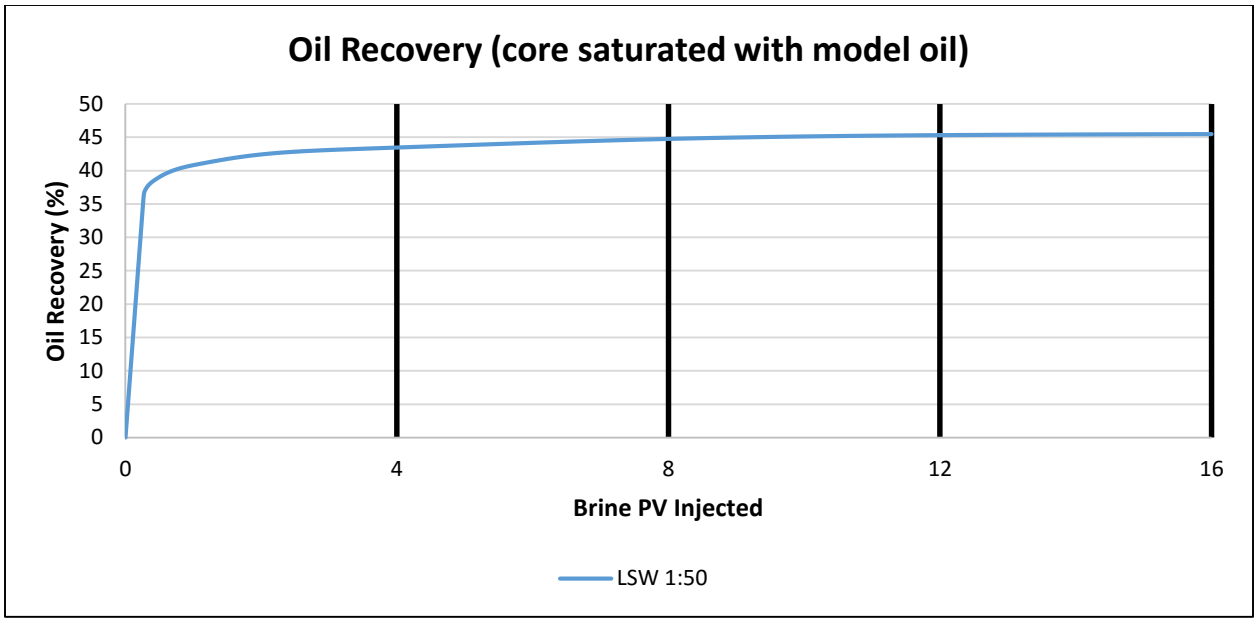

Figure 50- Simulated recovery factor for LSW 1:50 (core SG-3)

Hamouda et al (2014b) obtained the highest oil recovery from chalk cores (SK chalk) by flooding with LSW 1:10. It is also seen in figure 50 overall recovery observed is 45% which is less than recovery obtained in case of LSW (1:10), as shown in paper by Hamouda et al (2014b).

Relative movement of fluids in the pores and change in relative permeability of rock as the flooding proceeds is represented by relative permeability curves. To generate the relative permeability curves we used Corey's correlation, a widely used approximation of relative permeability. This correlation represents power law in the water saturation S_w. If S_{wi} is the irreducible (minimal) water saturation, and S_{or} is the residual (minimal) oil saturation after water flooding, we can define a normalized (or scaled) water saturation value (Wikipedia, Relative permeability):

$$S_{wn} = \frac{S_w - S_{wi}}{1 - S_{wi} - S_{or}}$$

Where, S_{wi} irreducible water saturation

S_{or} Residual oil saturation.

Then relative permeability of oil and water is given as (Wikipedia, Relative permeability):

$$K_{ro} = (1 - S_{wn})^{N_o}$$

$$K_{rw} = K_{rw}^{o} \cdot {S_{wn}}^{N_w}$$

Where, K_{ro} relative permeability for oil,

K_{rw} relative permeability for water,

K^{o}_{rw} the end point of the water relative permeability.

Since CMG is not designed for simulating the flooding for modified brines such as single salt brines. So only experiments with LSW injections are modeled here. Relative permeability curves can also be generated using Sendra but Sendra takes into account only injection rates, not the rock/brine interactions. So it does not show any relative change with change in injected LSW.

Relative permeability curves for chalk core (SG-5) flooded with SSW and LSW 1:10 are shown in figure 50. Vertical axis shows values for relative oil/water permeability; horizontal axis shows water saturation values. On figure 51 red line is relative permeability for water (wetting phase) and blue line for oil (non-wetting phase). From the experimental data, we have residual water saturation around 0.19. Movement of fluids from the pore depends on the saturation of the fluids in the rock. Presence of water has small effect on movement of oil in beginning due to very small water saturation, that's why initial relative permeability of oil and water is 1 and 0 respectively.

As water injection continues, the saturation of water increases in the pores, which leads to movement of water, hence increase in water permeability. This is shown in figure 51. From Figure 51 we can see that cross point is corresponding to water saturation value 0.42. Zone which is before crossing point (mobility ratio less than 1) indicates effective oil displacement. So values which are higher than 0.42 can indicate later water breakthrough, hence, higher recovery.

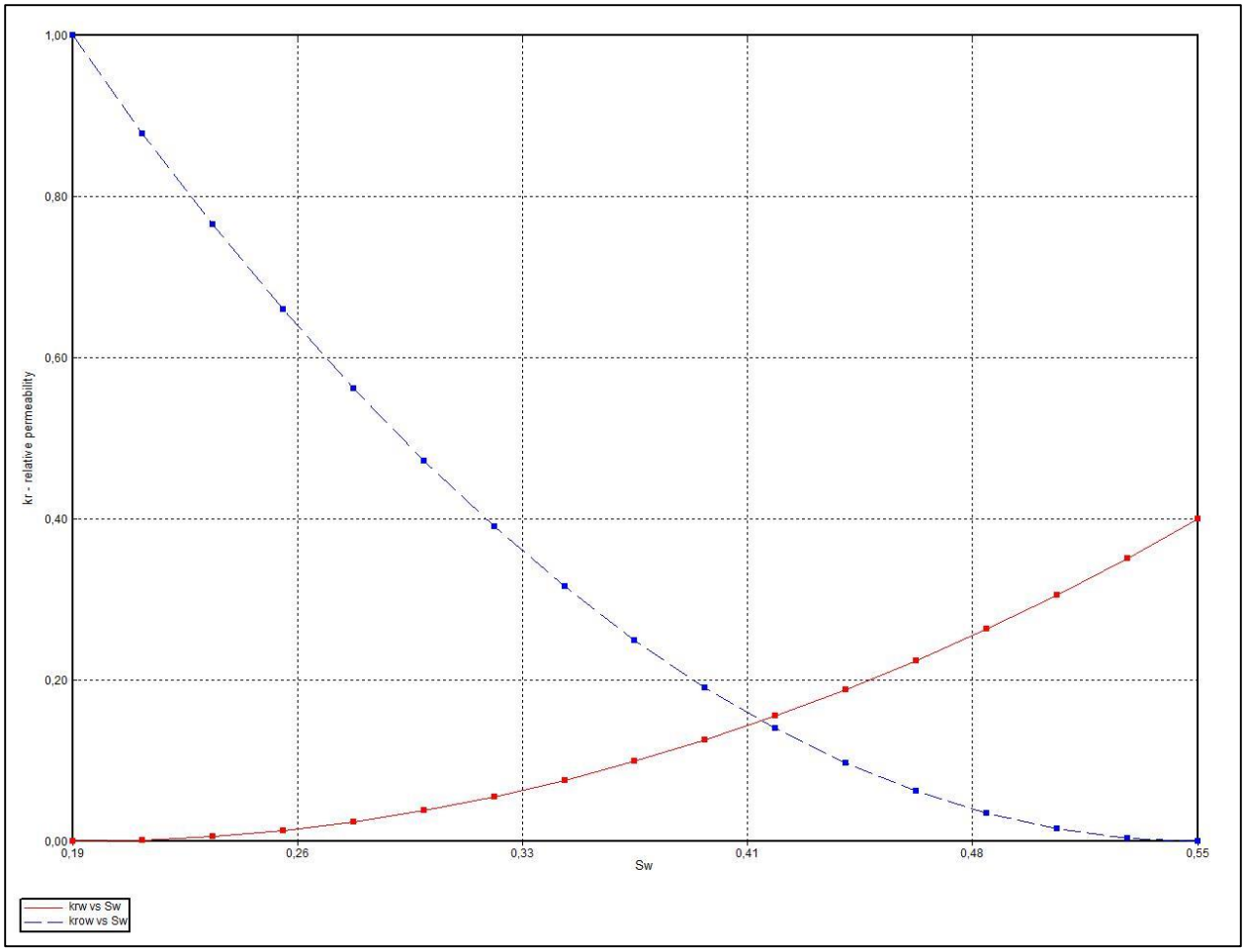

Figure 51: Simulated relative permeability curves for LSW 1:10 (SG-5, saturated with crude oil).

Similarly, for core (SG-6) flooded with SSW and LSW 1:50, the relative permeability curve is shown in figure 52. The cross point value is 0.39, which is less than 0.42 (observed in case of LSW 1:10). This indicates early water breakthrough and lower oil recovery than in case of LSW 1:50. These results were confirmed by the oil recovery curves (figure 49).

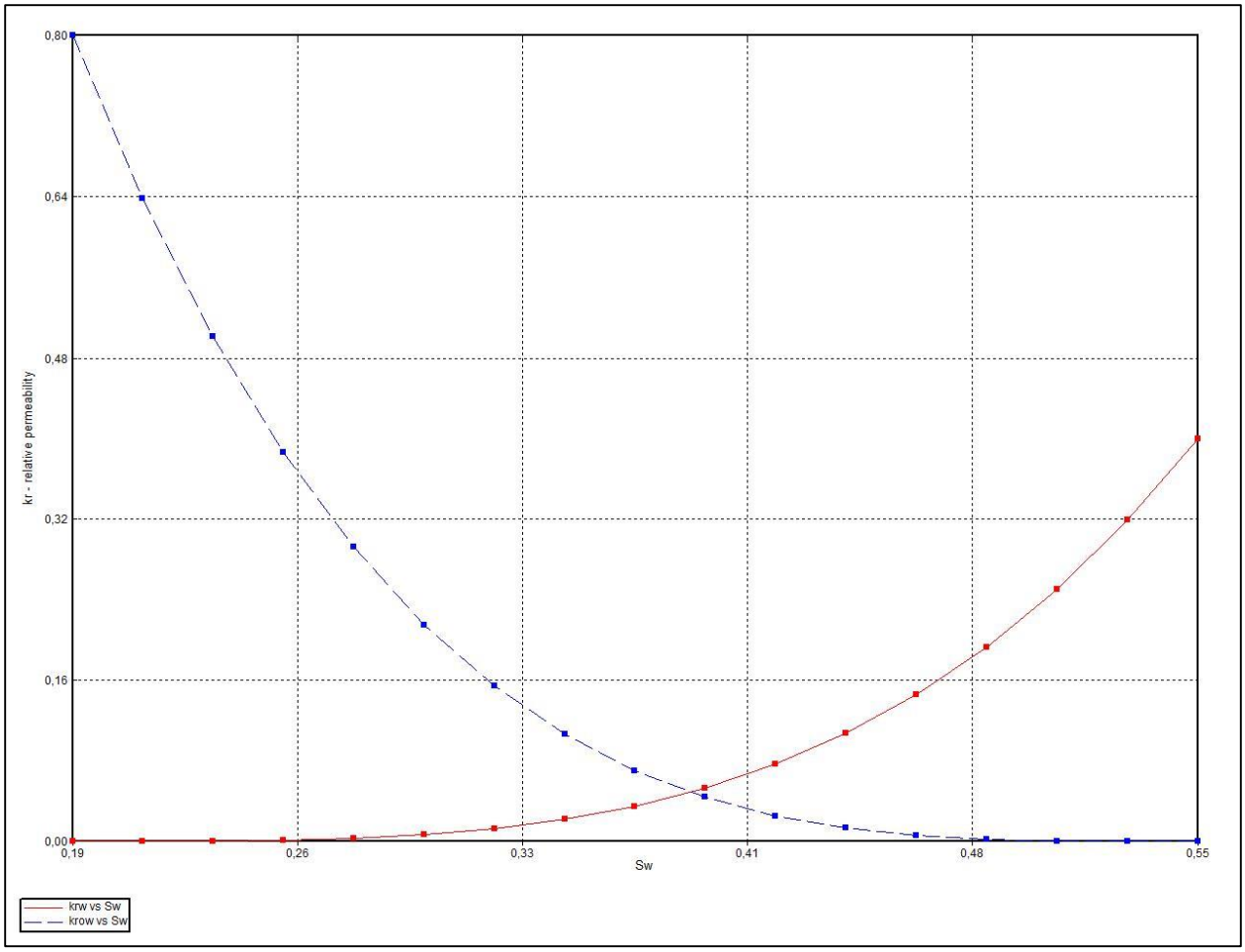

Figure 52: Simulated relative permeability curves for LSW 1:50 (SG-6, saturated with crude oil).

Oil recovery observed in case of LSW 1:10 is 42.8% which is slightly higher than LSW 1:50 (42.6%).

Core SG-3 was initially saturated with model oil (N-decane +stearic acid). Figure 53 shows the relative permeability curves generated by CMG GEM simulator. From figure 49 & 50 shows that recovery obtained is higher when core is saturated with model oil. It could be due presence of very less carboxylate group. Presence of carboxylate groups is linked to the wettability of the rock and So water wetness of the rock increases as the AN of oil decreases.

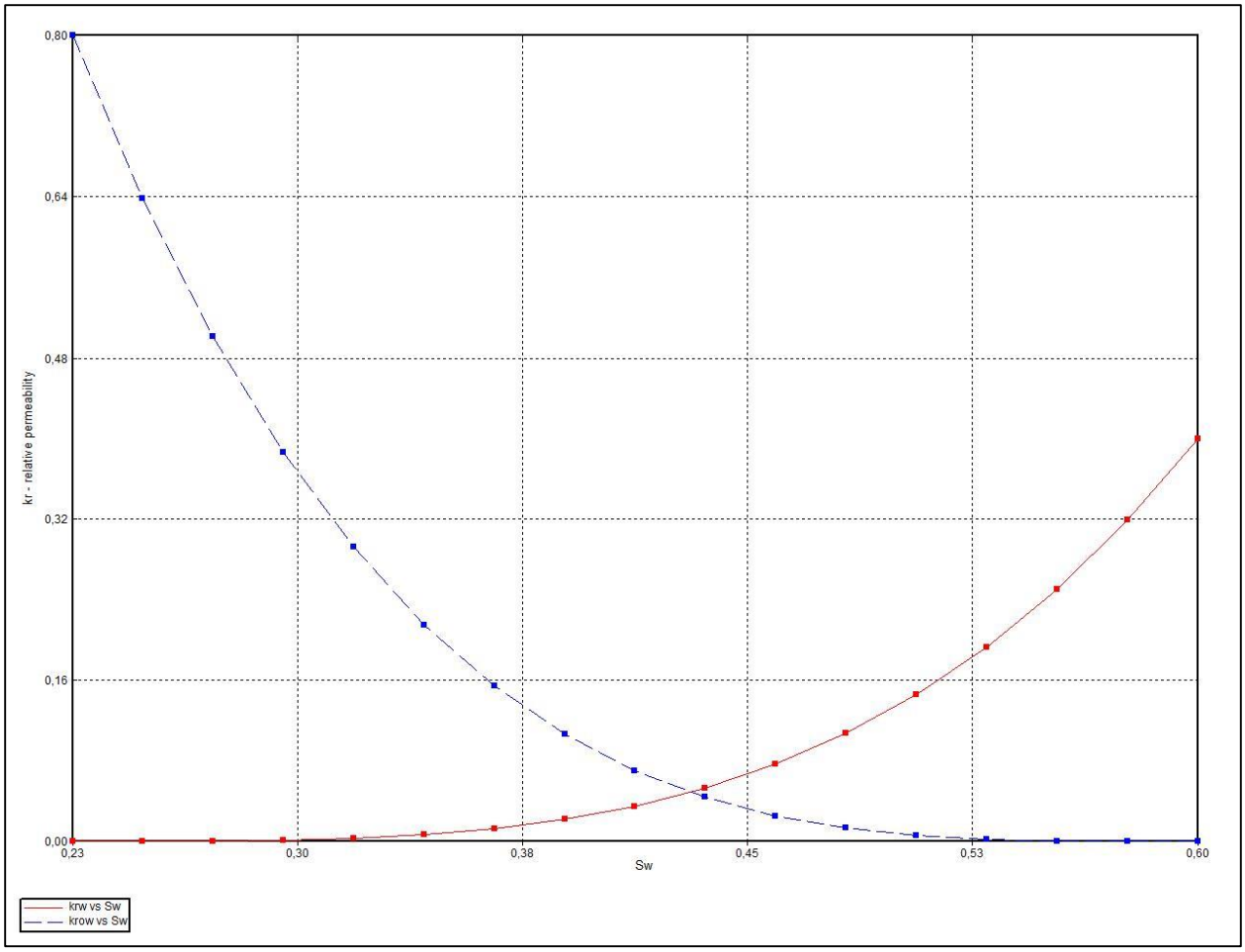

Figure 53: Simulated relative permeability curves for LSW 1:50 (SG-3, saturated with model oil).

From figure 53, the cross point lies at ~0.43 which is higher than 0.42, obtained in case of flooding with LSW 1:10 (Figure 52). This clearly indicates higher oil recovery in case of LSW 1:50 (when core is saturated with model oil) that LSW 1:10 and 1: 50 (when core is saturated with crude oil). These results are also experienced in experimental work also.

5. SUMMARY

In this work results were measured and analyzed during secondary injection of LS brines and single salt brines.

5.1. Oil Recovery from Secondary Flooding with LS.

All the cores were flooded with SSW as primary injection fluid and then flooded with different LS brines as secondary injection fluid. In figure 54, oil recoveries after injection of LSWs, single and two salts brine into saturated cores are plotted. The cores were flooded with two injection rates: 4 PV/day (0.09ml/min) and 16 PV/day (0.36 ml/min). For all the cores there were differences in oil recovery by SSW. The reason for the differences may be caused by the differences in the pore size distribution. This may be indicated by the lower S_{wi} for cores #5, #6, and #4 than compared to the others (Table 10&11). Ultimate recovery after secondary flooding with LSW 1:10, LSW 1:50, SO4 1:10, SO4 1:50, Mg at 70°C & 90°C and Mg+Na brines at 4PV/day were 52.9, 51.1, 68.2, 58.4, 54.6, 67.6 and 48.5%, respectively. The additional incremental oil recovery of 1, 0.2, 3.8, 2.3, 0.11, 1.1 and 0.5% from the primary recovery by SSW flooding, respectively. After switching the injection rate to 16PV/day, no recovery was observed in any of the cases.

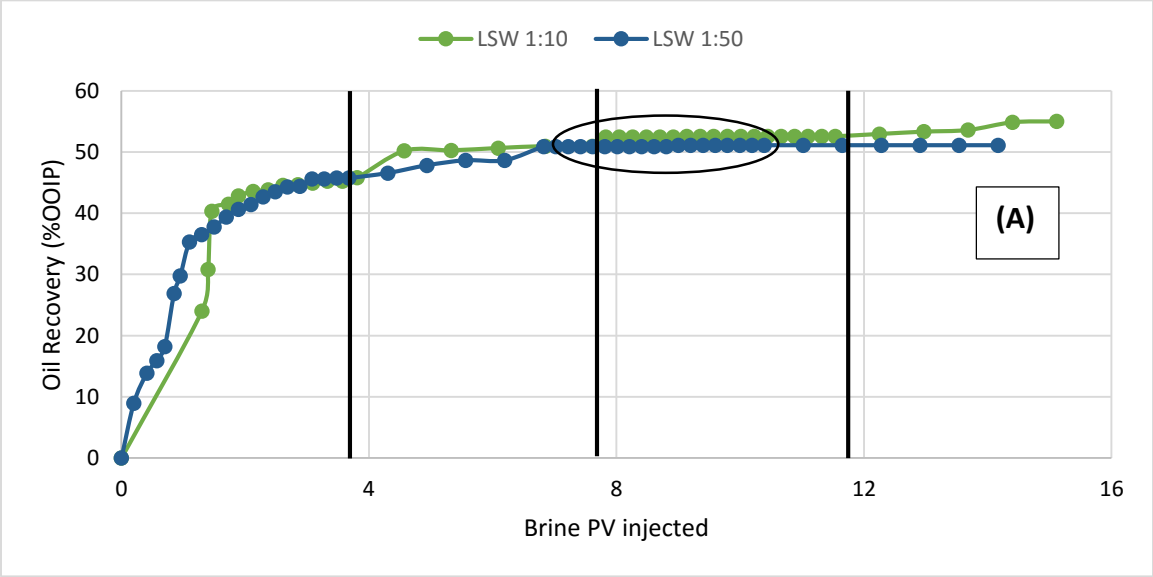

Figure 54A). Recovery during flooding with SSW/LS brines.

From figure 54A), the recovery response time for LSW 1:50 is different from LSW 1:10. LSW 1:50 gives slower response as well as lower recovery than LSW 1:10 (encircled in figure 54A).

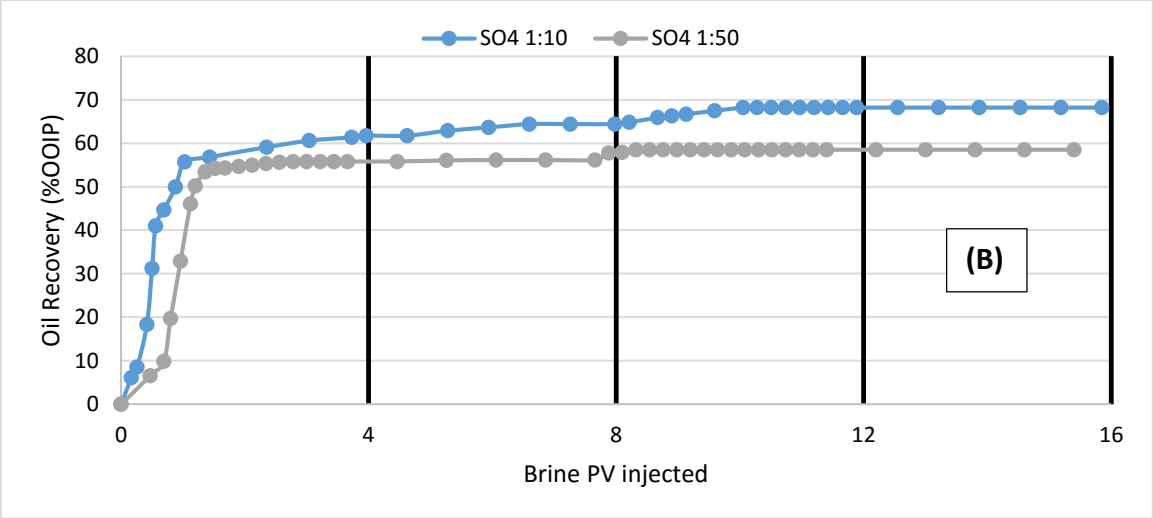

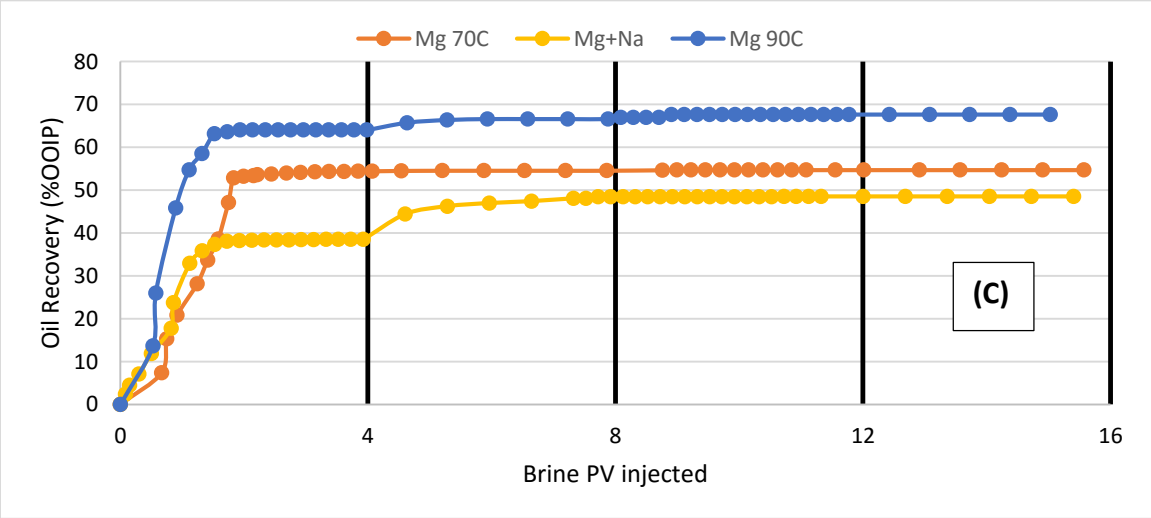

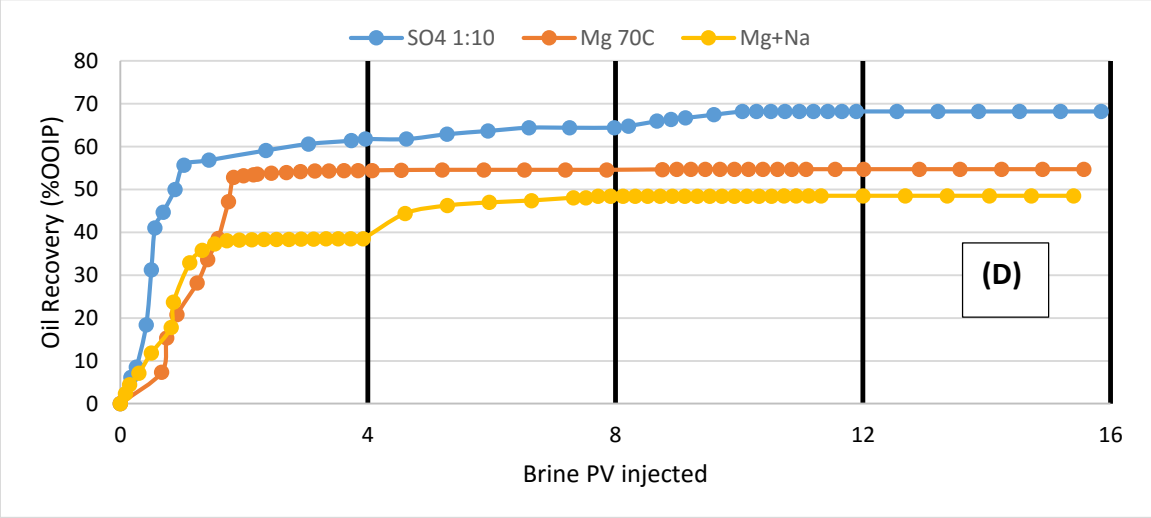

Figure 54B), 54C), & 54D). Recovery during flooding with SSW/LS brines.

From figure 54A), the recovery response time for LSW 1:50 is different from LSW 1:10. LSW 1:50 gives slower response as well as lower recovery than LSW 1:10 (encircled in figure 54A). This was also observed by Hamouda et al, 2016, while simulating LSW flooding in chalk using CMG-GEM simulator that oil recovery response was slower during injection of brine with higher dilution i.e. LSW 1:25 showed slower oil recovery response than LSW 1:5 and 1:10. Oil recovery response obtained while injection with single salt brines (SO4 brines) with different dilution ratios (figure 54B) were similar to the response observed while flooding with LSW 1:10 and 1:50. Oil recoveries from flooding with Mg salt brine (at 70°C & 90°C) and Mg+Na salts brine is compared in figure 54C). Oil recovery was the highest in case of Mg90 (67.6%) and lowest in case of Mg+Na brine (48.5%). This difference in oil recoveries may be due to differences in affinity of Ca^{+2} and Mg^{+2} ions towards surface at different temperatures[5]. Interaction of ions are explained later in this paper. Figure 54B) to 54D) shows higher oil recovery in case of SO4 1:10 (68.2%) compared to Mg70 (54.68%) and Mg+Na (48.5%). The only reason which could explain this difference in oil recovery is ion interaction, which is explained later in this paper.

Pressure drop curves for each flooding is shown in figure 55. During the flooding, pressure drop peaks were observed at various PVs flooding. From figure 55A), 55B) at the start of SSW flooding pressure drop(dP), at 4PV/day, reached a peak of 1.8(0.69) and 1.5(1.3) bar (PV) for LSW 1:10 & LSW 1:50, respectively. Continuous pressure drop peaks were observed at this rate and later dp stabilized at almost same point, i.e. 0.62(3.8) for LSW 1:10 and 1:50. When the rate was increased to 16PV/day, dP increased to 1.3(4.9) and 2.3(4.6) bar (PV) for LSW 1:10 & 1:50, respectively, after that dP stabilized at 1.33(6.7 PV) for LSW 1:10 and 1:50. When brine was switched to LSW at a rate of 4PV/day, dP showed a constant behavior and stabilized roughly at 0.3 bar after 0.5PV (equivalent to a total of 8.5PV from start) for both LSW 1:10 and 1:50. When rate was increased to 16PV/day, dP rose to 1.25(13) and 1(11.8) bar PV respectively for LSW 1:10 and 1:50. Higher dP in case of LSW 1:10 than LSW 1:50 shows higher resistance in flow during injection of LSW 1:10 than LSW 1:50.

From figure 55C) at the beginning of SSW flooding at 4PV/day pressure drop reached a peak of 1.33(0.59) & 2.064(0.9) bar (PV) for SO4 brine 1:10 and 1:50, respectively. After some fluctuation, dP stabilized at 1.13(2.8) and 1.14(2.7) bar(PV), respectively for SO4 1:10 and 1:50. When rate increased to 16PV/day, dP spiked up to 2(4.1) and 5(4.2) bar(PV), after that dP

stabilized at 1.9(5) &4(5.5) bar(PV) respectively for SO4 1:10& 1:50. Early dP peak observed in all cases may indicate early water breakthrough, therefore low sweep efficiency. At 16PV/day very less fluctuations in dP were observed during flooding with SO4 1:10 and 1:50. Constant dP may reflect negligible resistance in flow of brine, hence, decrease in sweep efficiency in the pores. This was also reflected in oil recovery curve. When brine was switched to SO4 brine at a rate of 4PV/day, less fluctuations were observed in case of SO4 1:50 than SO4 1:10. dP stabilized roughly at 0.3 bar after 0.7PV (equivalent to a total of 8.7PV from start) and 1 bar after 1 PV (equivalent to a total of 9PV from start) respectively for SO4 1:10 and 1:50. When rate was increased to 16PV/day, dP rose to 1.16(11.7) and 4.2(11.8) bar PV respectively for SO4 1:10 and 1:50, with no fluctuations. The higher oil recovery was observed in case of SO4 1:10 (68.2%) than SO4 1:50 (58.4%). Three observations were made from injection of LSWs and SO4 brines (1:10 &1:50): 1) Higher fluctuations were observed at 16PV/day than 4PV/day in case of LSW1:10 and 1:50 flooding, 2) magnitude of dP was higher in case of dilution ratio 1:50 than 1:10, and 3) increase in recovery was higher in case of dilution ratio 1:10 than 1:50 in both the cases, LSW as well as SO4 brines flooding, this is in agreement with Yousef et al.

Similarly, from Figures 55D) & 55E) Mg brine was injected at 70°C & 90°C and $MgCl_2$+NaCl brine was injected as a secondary injection fluid. From figures 55D) & 55E) at the beginning of SSW flooding at 4PV/day pressure drop reached a peak of 1.33(0.98), 1.7(0.58) & 2.42(0.46) bar (PV) for Mg70, Mg90 and Mg+Na, respectively. After some fluctuations, dP stabilized at 1.1(2.3), 1.14(1.1) and 2.11(1.84) bar (PV), respectively for Mg70, Mg90 and Mg+Na. When rate increased to 16PV/day, dP spiked up 1.9(3.8), 3(3.91) and 5.9(3.8) bar PV, and it stabilized at 1.7(5.8), 2.2(6.05) and 3.9(5.8), respectively for Mg70, Mg90 and Mg+Na. At 16PV/day very less fluctuations in dP were observed than 4PV/day. When brine was switched to LS (Mg70, Mg90 &Mg+Na) brines at a rate of 4PV/day, dP showed smaller fluctuations in all the cases than SSW. In case of Mg70, the magnitude of dP was constant (figure 55D) and dP stabilized roughly at 0.3 bar after 2.86PV (equivalent to a total of 10.86PV from start), 0.56bar after 1 PV (equivalent to a total of 9PV from start) and 1.2bar after 2.04 PV (equivalent to a total of 10.04PV from start) respectively for Mg70, Mg90 and Mg+Na brines. When rate was increased to 16PV/day, dP rose to 1.2(12), 2.05(11.83) and 3.11(11.8) bar(PV) respectively for Mg70, Mg90 and Mg+Na, with no fluctuations in pressure.

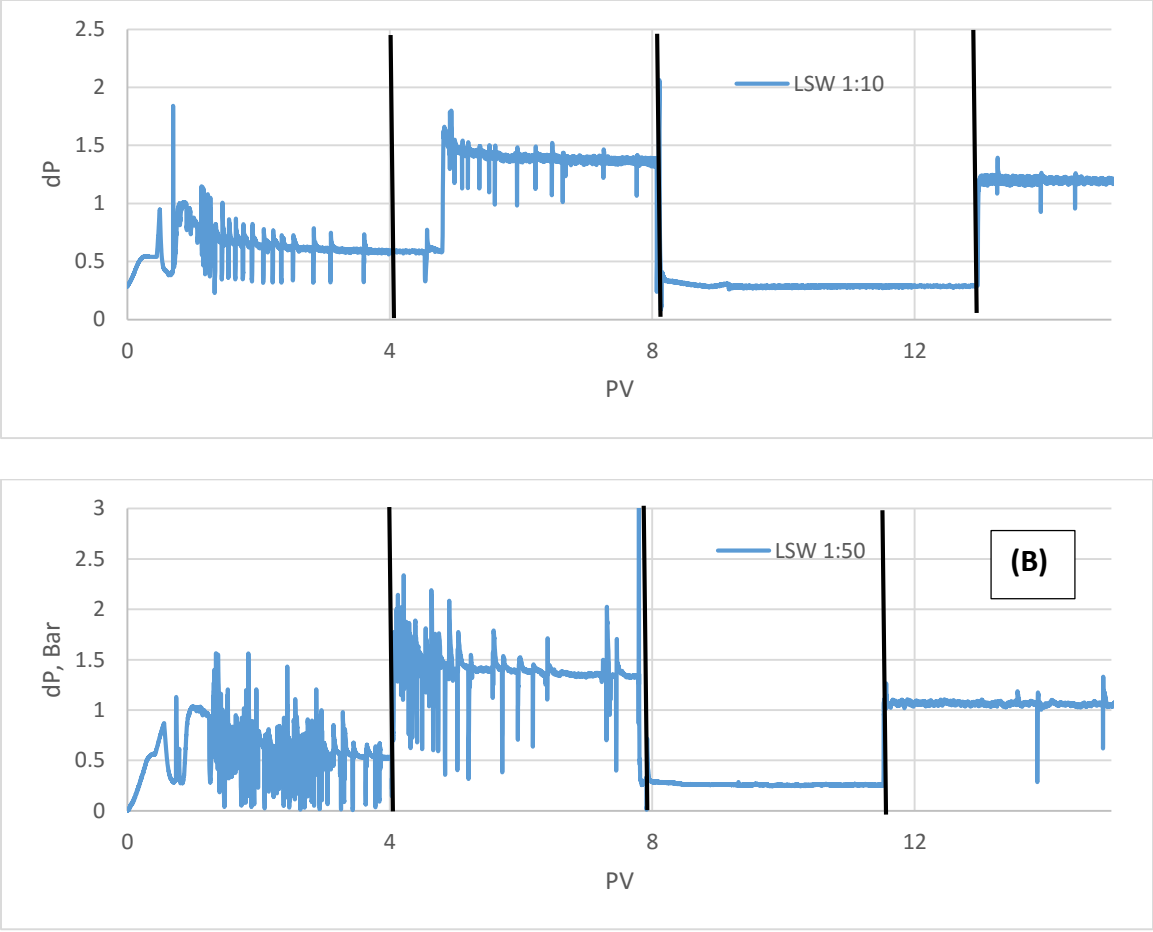

Figure 55A) & 55B). Pressure drop across the core during SSW/LS brine flooding.

At 4PV/day, 0.11, 1.1 and 0.5% increase in recovery was obtained respectively for Mg70, Mg90 and Mg+Na brines. Since there was no increase in pressure drop at 16PV/day of LS brine injection, no resistance in flow occurred. This could be the reason of no additional oil recovery at higher rate. The highest oil recovery was observed in case of Mg90 (67.2%) brine than Mg70 (54.6%) and Mg+Na (48.5%) brines.

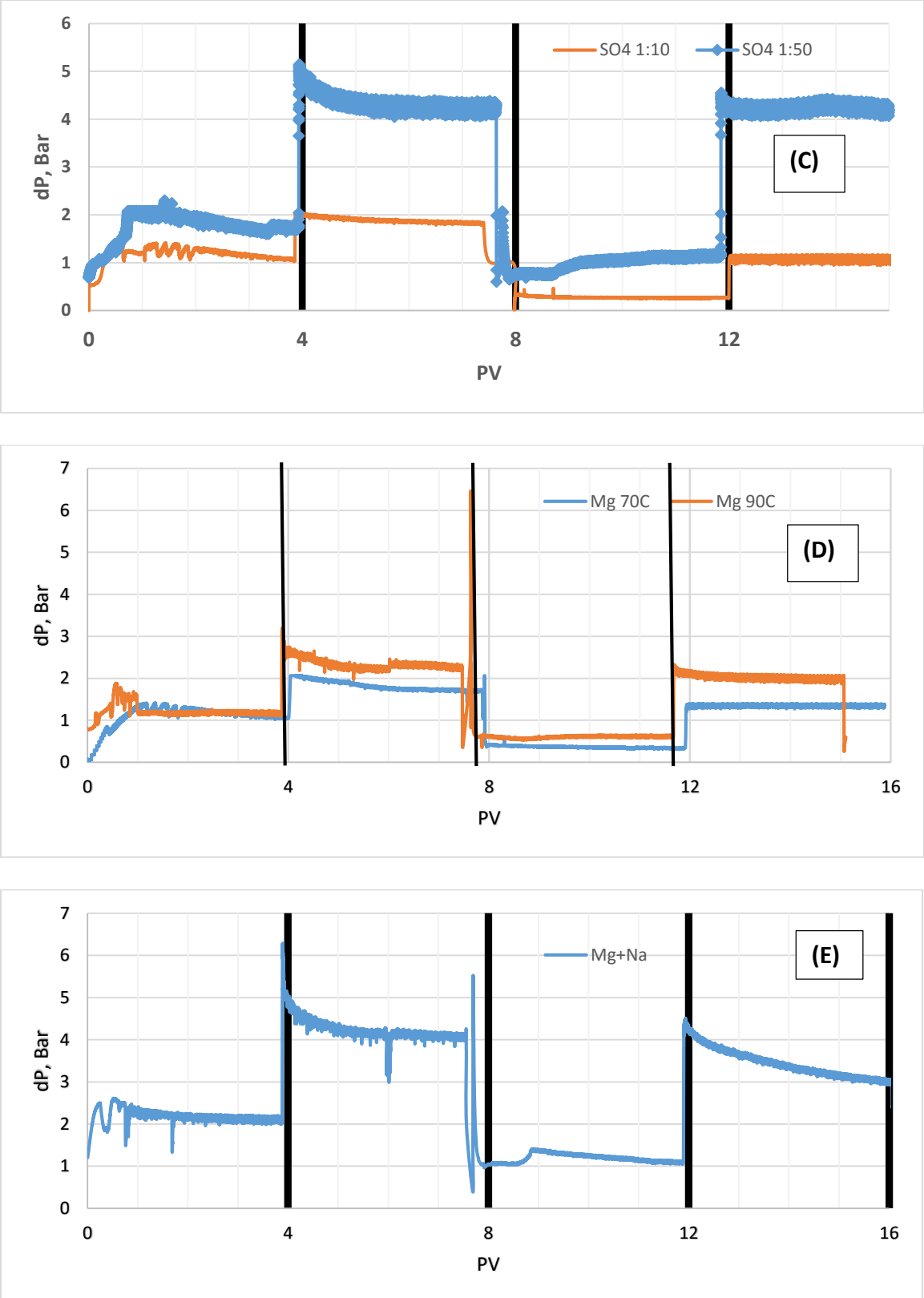

Figure 55C), 55D) &55E). Pressure drop across the core during SSW/LS brine flooding.

Figure 56 showed effluents' pH during SSW injection. The effluent pH for LSW 1:10 and 1:50 increased from 7.32 and 6.74 to 7.92 and 8.52 at 4PV/day, respectively. Further increase in rate from 4 PV/day to 16 PV/day, showed an increase in pH to 8.33 and 8.8 for LSW 1:10 and 1:50, respectively. For SO41:10 and 1:50 flooding, effluents' pH increased from 7.5 to 8.2 and 7.4 to 8.1 at 4 PV/day, respectively. When flooding rate increased to 16PV/day, pH increased to 8.7 and 9.2 for SO4 1:10 and 1:50, respectively. So far, it was seen that highest change in pH occurs in case of higher diluted LS brines, i.e. LSW1:50 and SO4 1:50. These results were also observed by Hamouda et al, 2014b during flooding with LSW 1:5, 1:10, 1:15 and 1:25.

Similarly, for Mg^{+2} flooding pH of effluents increased to 7.8 at 4 PV/day. When rate switched to 16PV/day, pH increased to 7.9. The difference in pH for both rates was about 0.1. Almost similar pH values were obtained when flooding Mg^{+2} at 70°C and 90°C. When flooding Mg+Na brine pH increased to 7.74 and 8.1 at 4PV/day and 16PV/day, respectively. Difference in pHs in case of Mg brine and Mg+Na brine may be due to ion exchange between Mg/Ca and Na/Ca. This may increase the dissolution of calcite and increase the amount of OH^- during injection of Mg+Na brine, thus increase in pH.

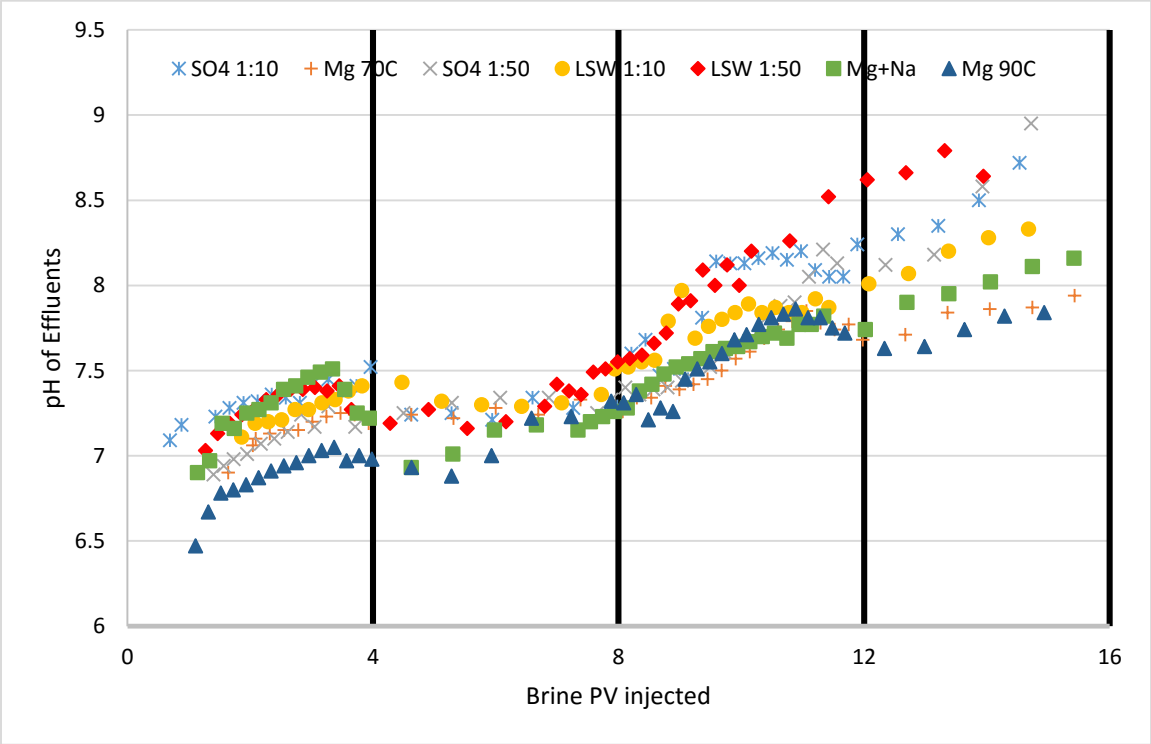

Figure 56. Effluent's pHs.

5.2. Ion Tracking from Secondary Flooding by LS brines.

Ion tacking from the flooding gives an idea of fluid/rock interaction. Below figures 57&58 show the concentration of tacked ions in the effluents during flooding with various brines with respect to SSW. Dimensionless ion concentration is estimated as the ratio between the measured ion concentration in effluents to the ion concentration in SSW. Theoretically, ion concentrations of secondary brine should reach the value 0.1/0.05 depending upon the dilution ratio with SSW, assuming no interaction.

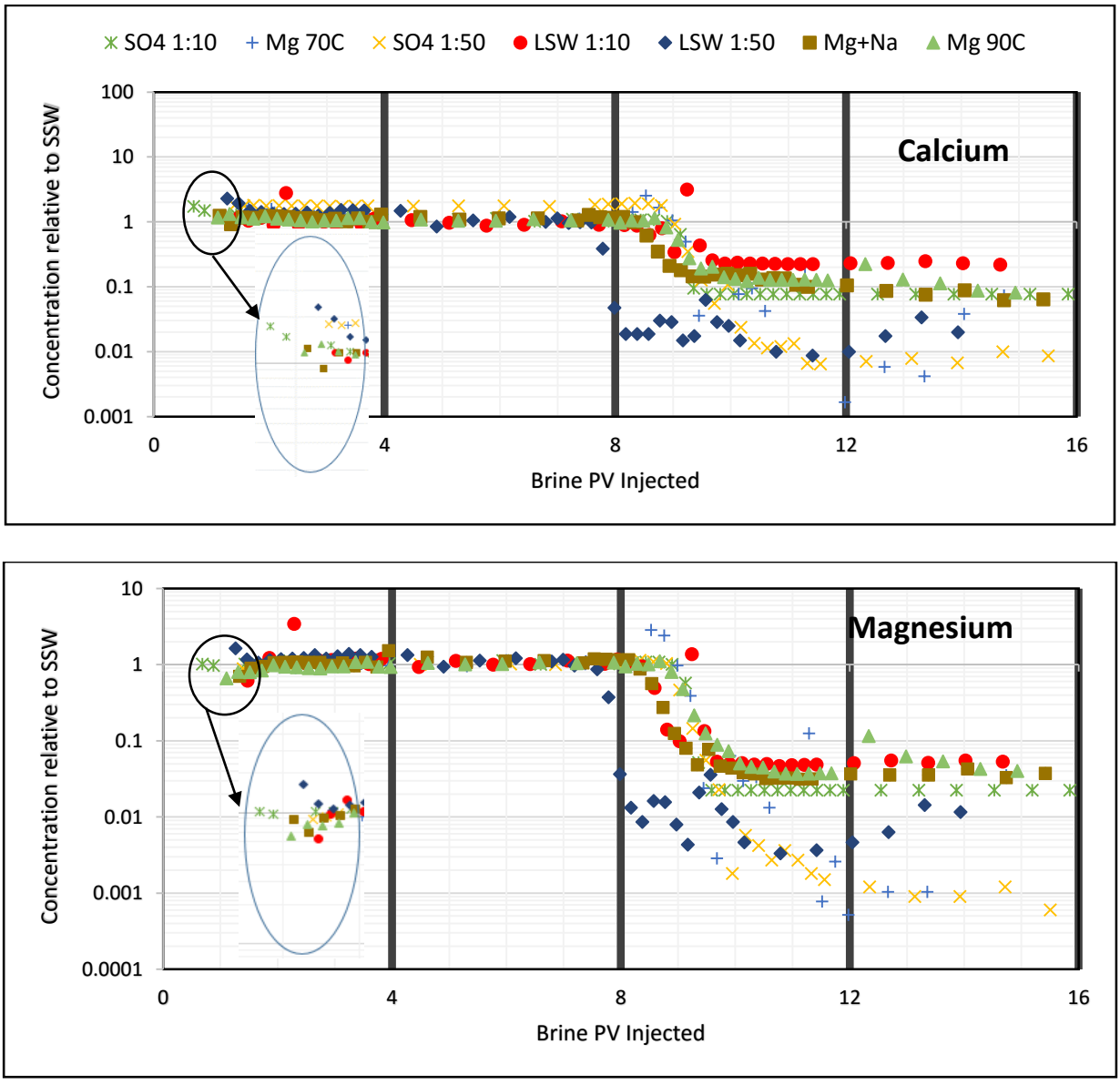

Figure57. Ion tracking, with ion concentrations relative to SSW in effluents.

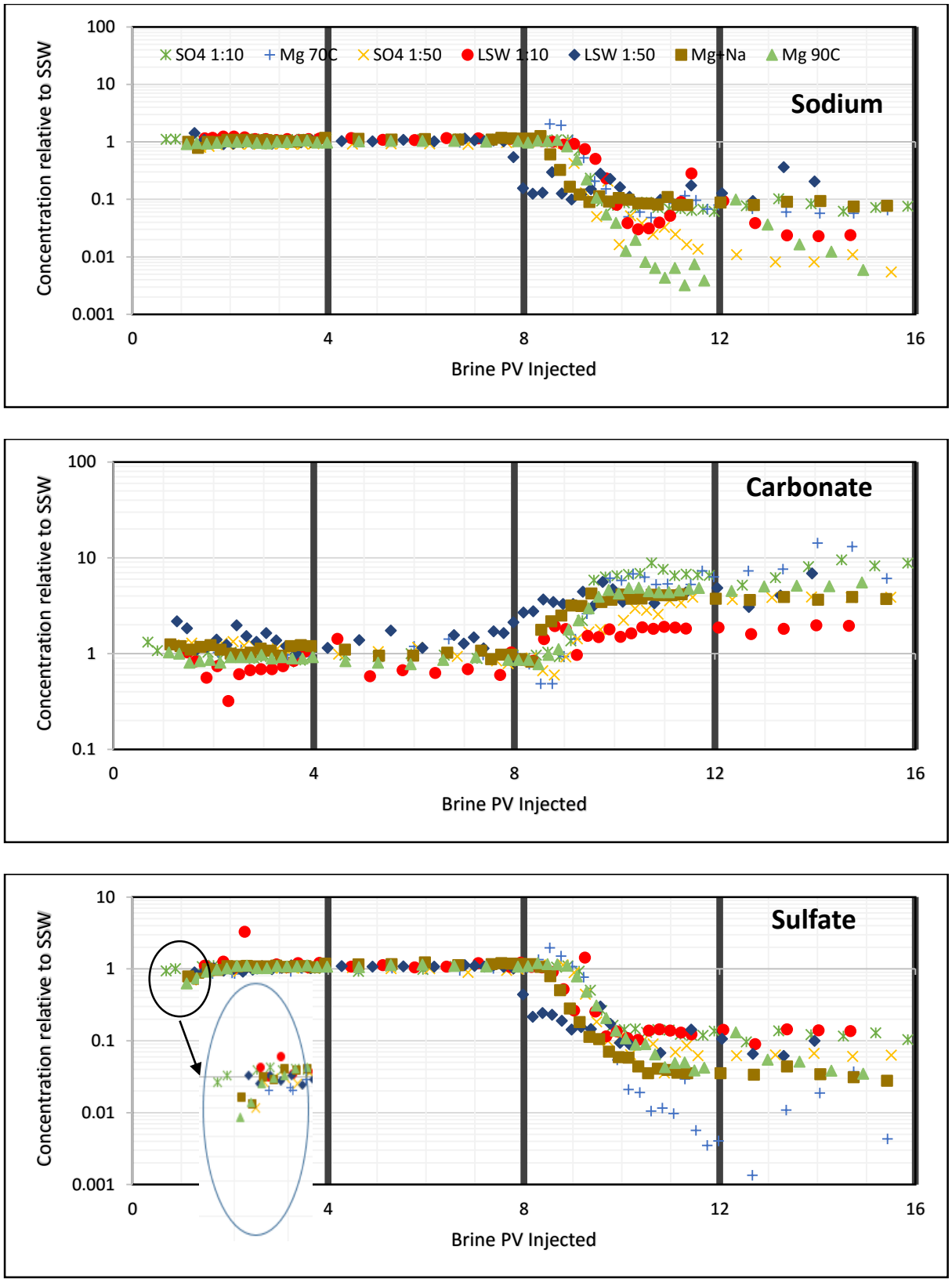

Figure58. Ion tracking, with ion concentrations relative to SSW in effluents.

During the SSW injection for the first 8PV, effluents' ion concentration remained same as in SSW (figure 57&58), except [Ca^{+2}], [Mg^{+2}] and [SO_4^{2-}]. At the start of flooding, [Ca^{+2}]$_r$ssw was about 1.9(0.88PV), 1.8(1.7PV), 1.9(1.4PV), 1.17(1.64PV), 2(1.27PV), 1.16(1.14PV) and 1.32(1.11PV) times [Ca^{+2}]ssw respectively for SO4 1:10, Mg70, SO4 1:50 LSW 1:10, LSW 1:50, Mg+Na & Mg90 and declined to 1[Ca^{+2}]ssw at ~3PV for all the cases. On the hand, [Mg^{2+}]$_r$ssw and [SO_4^{2-}]$_r$ssw increased from 0.98(0.88PV), 0.66(1.11PV), 0.9(1.64PV), 0.62(1.48PV), 0.8(1.34PV) & 0.66(1.11PV) times [Mg^{2+}]ssw and 0.94(0.69PV), 0.85(1.64PV), 0.68(1.11PV), 1(1.52PV), 0.78(1.14) &0.68(1.11PV) times [SO_4^{2-}]ssw to 1[Mg^{2+}]ssw and 1[SO_4^{2-}]ssw at ~1.8PV respectively for SO4 1:10, Mg70, SO4 1:50 LSW 1:10, Mg+Na & Mg90 brine. These observations are in agreement with the results obtained by Hamouda and Petrovich, 1998.

Figure 57&58 shows decline rates of individual ions. Decline rates for [Na^+] are 0.035, 0.18, 0.039, 0.05, 0.38, 0.1, and 0.06 mol/L PV respectively for SO4 1:10, Mg70, SO4 1:50, LSW 1:10, LSW 1:50, Mg+Na & Mg90 brine. Compared to other ions [Na^+] declines at the fastest rate (decline rates for other ions are given later). Early decrease in [Na^+] was also observed by Hamouda et al, 2014b. The decline rates for [Na^+] in SO4 1:10, SO4 1:50, Mg+Na and Mg90 are lower than the other cases. Slower decline rate may indicate that presence of sodium in the injected single salt brines has involved in ion exchange Ca^{+2}. This could be in agreement by looking at decline rate of [Ca^{+2}] in SO4 1:10, SO4 1:50, are 0.002,0.003 and in Mg+Na, Mg90 are 0.003, and 0.002 mol/L PV, which are lower than LSW 1:10 & 1:50. Nasralla et al, also observed that may be continuous dilution of the injected brine cause a decrease in [Na^+]. They also concluded that [Na^+] and [Mg^{+2}] present during injection of NaCl, Na_2SO_4 and $MgCl_2$ causes leaching of Ca^{+2} from rock surface, hence increase in calcium concentration in effluents. Low decline rate of calcium in SO4 and Mg brine may indicate leaching of Ca^{+2} from the rock surface. It was clearly stated by previous researchers that removal of Na^+ and Cl^- ions helps in expansion of electrical double layer and increase in the reactivity of active ions (Ca^{+2}, Mg^{+2}, SO_4^{2-}). Thus, addition of Na in the injected Mg+Na brine did not make any positive impact on the process. Mg70 alone gave higher recovery than Mg+Na at 70°C.

Flooding with LS brines [SO_4^{2-}] has become <1, figure 58(Sulfate). This showed that there may be processes like sulfate adsorption and dissolution of $CaSO_4$ are taking place. Decline rate for [Ca^{+2}] was about 1.5, 1.3, 1.11 and 3 time greater than [SO_4^{2-}] in effluents during SO4 1:10

&1:50, LSW 1:10 & 1:50 flooding. Faster declination of [Ca^{+2}] may indicate less contribution by calcium in $CaSO_4$ dissolution (Hamouda et al, 2014b).

Al-Attar et al, observed an optimum concentration of SO_4^{2-} (50 times dilution of SSW), which gave the highest recovery. But in this paper SO4 1:10 gave higher recovery than 1:50. This may be due to less interaction of Ca^{+2} and Mg^{+2} ions in presence of lower sulfate concentration, in SO4 1:50. $[Ca^{+2}]_r$ssw & $[Mg^{+2}]_r$ssw concentrations were observed to be 0.07 &0.01 and 0.007 and 0.001 respectively for SO4 1:10 and 1:50. Increasing [SO_4^{2-}] in the injected brine tends to alter the wettability to more water wet and higher recovery, which is reflected as higher recovery from SO4 1:10 than SO4 1:50. Increase in recovery was ~3% higher for SO41:10 than SO4 1:50. Less recovery obtained from SO4 1:50 than 1:10 may indicate that optimum sulfate concentration is higher than 47ppm.

Gandomkar et al, compared the recovery results by flooding Na_2SO_4, NaCl, and $MgCl_2$ brines as secondary mode. They suggested that low salinity brine enriched in potentially determining ions (SO_4^{2-}) and depleted in monovalent ions is suitable in oil recovery. [SO_4^{2-}] decline rate was faster in case of Mg+Na flooding (0.005 mol/L PV) than SO4 1:10 (0.002 mol/L PV). Addition of SO_4^{2-} and removal of monovalent ion (Cl^-) in brine causes the double layer to expand and displacing the oil particles and alter the wettability.

Dissolution of calcite in the brine increase the pH as well as concentration of carbonate. Relation between calcite dissolution and increase in pH may be expressed by alkalinity of water/calcite system (Hamouda et al, 2014b):

$$alkalinity = 2[CO_3^{2-}] + [HCO_3^-] + [OH^-] - [H^+]$$

[HCO_3^-] s. Average value for [HCO_3^-] after LSW flooding, reached to 2 and 5 time the SSW for LSW 1:10 and 1:50, respectively. For all the brines [HCO_3^-] stabilizes after 10 PV, i.e. after 2 PV of LS brine injection to a value of 5 times the SSW. After injecting LS brines a continuous increase in concentration of bicarbonate ions was observed. Dissolution of calcite may be expressed by (Lehmann et al, 2013):

$$CaCO_3 + H_2O \rightarrow Ca^{+2} + HCO_3^- + OH^-$$

Gomari et al, noted that increase in calcite dissolution decreases the stability of lattice and produces fines. Flow of fines with injected brine increases the flow resistance and enhances sweep efficiency. Calcite dissolution also increases calcium concentration in the effluents. Also may be due to precipitation of $CaSO_4$ on surface and ion exchange with Mg^{+2} and Na^{+} changes in $[Ca^{+2}]$ takes place.

Calcite dissolution is not the only reason for increase in $[Ca^{+2}]$. Ion exchange between Ca/Mg affects the $[Mg^{+2}]$ and $[Ca^{+2}]$ in the effluents. For example, in case of flooding with Mg90, $[Mg^{+2}]$ stabilizes at $0.03[Mg^{+2}]ssw$ after 11.68PV at 4PV/day but when rate increased to 16PV/day, $[Mg^{+2}]$ increased to $0.11[Mg^{+2}]ssw$ at 12.33PV and declined to $0.04[Mg^{+2}]ssw$ at 14.28PV with a rate of 0.001 mol/L PV. Similarly, at 16PV/day $[Ca^{+2}]$ declined from 0.22(12.33PV) to 0.8(14.2PV). The consistent deficiency in the effluent concentrations may reflect deposition of Brucite. Highest pH obtained in this case was 8.79 but brucite is stable at pH~10 (Hamouda et al, 2014b). So the exchange between calcium and magnesium may lead the formation of magnesian/dolomite and can be expressed by (Hamouda et al, 2014b):

$$2CaCO_3(S)\ (Calcite) + Mg^{+2} = CaMg(CO_3)_2(S) + Ca^{+2}$$

Exchange between Ca/Mg was also observed in case of flooding with LSW 1:10, LSW 1:50, Mg+Na, and SO4 1:10 brine. At 16PV/day $[Mg^{+2}]$ increased to 0.01(13PV), 0.05(12.2PV), 0.04(14PV) and 0.02(12.1PV) for LSW 1:10, LSW 1:50, and Mg+Na brine, respectively. On the other hand, this trend was not observed during Mg70 flooding. At 70°C no detectable increase in Ca^{+2} concentration was observed. As temperature increases, less Ca^{+2} is available for adsorption[4]. Absence of SO_4^{2-} in the injected brine eliminated precipitation of $CaSO_4$ and Mg^{+2} acts as a wettability modifier at higher temperature. This shows that Ca^{+2} and Mg^{+2} reaction depends on temperature and at higher temperature reactivity of magnesium increases. This is in agreement with what it was observed by Austad et al, 2006. Ca/Mg reaction enhances the sweep efficiency in presence of sweep efficiency and increases the oil recovery.

6. CONCLUSION

The mechanism related to increase in oil recovery in carbonate reservoirs are still not completely explainable. A series of experiments were performed for this study to test the low salinity effects in chalk reservoirs. Core were flooded with SSW and modified brines (single & two salts brines and LSWs) as primary and secondary injection fluids, respectively. Results obtained from these experiments provide pillars to the observation made by other researchers. Based on the experimental and numerical results, few bulletin points are concluded:

- Divalent Ions have an effect in wettability alteration. Ca/Mg contributes largely in enhancing the sweep efficiency. But this effect increases in presence of SO_4^{2-}. Highest recovery obtained while Flooding with SO_4^{2-} brine than any other brine shows that presence of sulfate ion may contribute in wettability alteration.
- CMG simulator as well as experimental results showed, Oil recovery response time depends on the dilution factor of brine. Brine with higher dilution gives slower response. LSW 1:10 gives earlier response than the LSW (1:50).
- Increase in ion concentrations of Mg^{+2} and Ca^{+2} in the later part of modified brine injection confirms ion exchange between the ions and thus precipitation magnesian.
- Hamouda et al (2014b) concluded that LSW 1:10 gives best outcome than any other dilution. Results in this work confirms that LSW 1:10 gives higher recovery in case of core saturated with model oil as well as crude oil.
- Pressure drop increment in second phase of experiments gives a clear indication of fine migration during injection of single & two salts brines and LSW. Tough fines were not observed in samples during experiments. This may be due to size of the particles is very small or the migration took place in the core only or may be due to absence of enough pressure to overcome the trapping of particles.
- Slightly higher increase in recovery in case of Mg^{+2} injection at 90°C than at 70°C shows higher reactivity of magnesium at higher temperature.

7. REFERENCES

1. Abdulla, F., Hashem, H. S., Abdulraheem, B., et al. 2013. First EOR Trial using Low Salinity Water Injection in the Greater Burgan Field, Kuwait. Paper SPE-164341-MS proceedings of the SPE Middle East Oil and Gas Show and Conference, Manama, Bahrain, 10-13 March.
2. Ahmed Tarek, 2001, *"Reservoir engineering handbook. Second edition"*, Houston, Texas, USA, Gulf Professional Publishing is an imprint of Butterworth-Heinemann, ISBN: 0884157709.
3. Aladasani, A., Bai, B. and Wu, Y.-S. 2012. Investigating Low-Salinity Waterflooding Recovery Mechanisms in Sandstone Reservoirs. Paper SPE-152997-MS proceedings of the SPE Improved Oil Recovery Symposium, Tulsa, Oklahoma, USA, 14-18 April.
4. Al-Attar, H. H., Mahmoud, M. Y., Zekri, A. Y., Almehaideb, R. A., & Ghannam, M. T. (2013, June 10). Low Salinity Flooding in a Selected Carbonate Reservoir: Experimental Approach. Society of Petroleum Engineers. doi:10.2118/164788-MS
5. Amott, Earl: "Observations Relating to the Wettability of Porous Rock", SPE 1167-G, Los Angeles, California, Pages 156-157 (Oct-58)
6. Anderson, William G.: "Wettability Literature Survey - Part 2: Wettability Measurement", SPE 13933, Pages 1246 - 1258 (Nov-86)
7. Arnarson, T.S. and Keil, R.G., 2000. Mechanisms of pore water organic matter adsorption to montmorillonite. Marine Chemistry, 71(3-4): 309-320.
8. Austad, T. Water Based EOR in Carbonates and Sandstones: New Chemical Understanding of the EOR-Potential Using "Smart Water". Class Literature at University of Stavanger. 2014.
9. Bjørlykke, K., 2001. *Sedimentology and petroleum geology*. Gyldendal Norsk Forlag AS.
10. Burgot J.-L., 2012, *"Ionic Equilibria in Analytical Chemistry"*, Springer, Science+Business Media, ISBN: 1441983813.
11. Cotterill, Sam J. Low Salinity Effects on Oil Recovery. MSc Thesis, Impertial College London. 2014.
12. Dang, T.Q.C., Nghiem, L.X., Chen, Z. & Nguyen, Q.P., 2013. Modelling Low Salinity Waterflooding: Ion Exchange, Geochemistry and Wettability Alternation. Paper SPE 166447 presented at the 2013 SPE Annual Technical Conference and Exhibition; Jakarta, Indonesia, 22-24 October.

13. Deryaguin, B. V. and Lan dau, L. D., 1941, Theory of the stability of strongly-charged lyophobic sols and of the adhesion of strongly-charged particles in solutions of electrolytes: *ActaPhys.-Chim. USSR*, vol. 14, p. 633–662.
14. Donaldson, Erle C., Thomas, Rex D. and Lorenz, Philip B.: "Wettability Determination and Its Effect on Recovery Efficiency", SPE 2338, Pages 13-14, Bartlesville, Okla. (Mar-69)
15. Fathi, J. Water-Based Enhanced Oil Recovery (EOR) in carbonate reservoirs. PhD Thesis, University of Stavanger. 2012.
16. G Hansen, A. A. Hamouda, R Denoyel. The effect of pressure on contact angles and wettability in the mica/water/n-decane system and the calcite + stearic acid/water/n-decane system, Colloids and Surfaces A: Physicochemical and Engineering Aspects, Volume 172, Issues 1–3, 25 October 2000, Pages 7-16, ISSN 0927-7757.
17. Gandomkar, A., & Rahimpour, M. R. (2015). Investigation of Low-Salinity Waterflooding in Secondary and Tertiary Enhanced Oil Recovery in Limestone Reservoirs. *Energy & Fuels Energy Fuels*, *29*(12), 7781-7792. doi: 10.1021/acs.energyfuels.5b01236
18. Green, D. W., & Willhite, G. P. (1998). *Enhanced Oil Recovery* (Vol. 6, SPE Textbook Series). Henry L. Doherty Memorial Fund of AIME Soceity of Petroleum Engineers, Richardson, TX USA. 1998.
19. Hamouda, A. A., & Maevskiy, E. (2014b). Oil Recovery Mechanism(s) by Low Salinity Brines and Their Interaction with Chalk. *Energy & Fuels*, p. 6860-6868.
20. Hamouda, A. A., & Pranoto, A. (2016, March 21). Synergy Between Low Salinity Water Flooding and CO_2 for EOR in Chalk Reservoirs. Society of Petroleum Engineers.
21. Hamouda, A. A., & Rezaei Gomari, K. A. (2006, January 1). Influence of Temperature on Wettability Alteration of Carbonate Reservoirs. Society of Petroleum Engineers.
22. Hamouda, A.A. & Valderhaug, O.M., 2014a. Investigating Enhanced Oil Recovery from Sandstone by Low-Salinity Water and Fluid/Rock Interaction. *energy&fuels*, p.898-908.
23. Hirasaki, G.J., 1991. Wettability: Fundamentals and surface forces. SPE Formation Evaluation, June: 217-226.
24. Khilar, K. C., Valdya, R. N., and Fogler, H. S., 1990, Colloidally induced fines release in porous media: *Journal of Petroleum Science & Engineering*, vol. 4, no. 3, p. 213–221.
25. Lager, A., Webb, K. J., Black C. J. J., et al. 2008. Low Salinity Oil Recovery - An Experimental Investigation. *Petrophysics* 49 (1): 28- 35.

26. Ligthelm, D.J., Gronsveld, J., Hofman, J.P., Brussee, N.J., Marcelis, F. and van der Linde, H.A., 2009. Novel waterflooding strategy by manipulation of injection brine composition. Paper SPE 119835 presented at the 2009 SPE EUROPEC/EAGE Annual conference and exhibition, 8-11 June.
27. Mamonov, A. Mechanism of primary and secondary oil flooding for recovery from sandstones by low salinity water. MSc Thesis, University of Stavanger. 2014.
28. Mazzullo, S.J., Chilingarian, G.V. and Bissell, H.J., 1992. Carbonate rock classifications. In: G.V. Chilingarian, S.J. Mazzullo and H.H. Rieke (Editors), Carbonate reservoir characterization: a geologic - engineering analysis, part I. Developments in petroleum science 30. Elsevier Science Publishers B.V., pp. 59-108.
29. McGuire, P. L., Chatham, J. R., Paskvan, F. K., et al. 2005. Low Salinity Oil Recovery: An Exciting New EOR Opportunity for Alaska's North Slope. Paper SPE-93903-MS proceedings of the SPE Western Regional Meeting, Irvine, California, 30 March-1 April.
30. Milter, J. and Øxnevad, I.E.I., 1996. Spontaneous imbibition in two different chalk facies. Petroleum Geoscience, 2: 231-240.
31. Nasralla, R. A., & Nasr-El-Din, H. A. (2011, January 1). Coreflood Study of Low Salinity Water Injection in Sandstone Reservoirs. Society of Petroleum Engineers. doi:10.2118/149077-MS
32. Nasralla, R. A., & Nasr-El-Din, H. A. (2014, February 1). Double-Layer Expansion: Is It a Primary Mechanism of Improved Oil Recovery by Low-Salinity Waterflooding? Society of Petroleum Engineers. doi:10.2118/154334-PANnaemeka Ezekwe, 2011, *"Petroleum Reservoir Engineering Practice"*, Boston, USA, Pearson Education, Inc., ISBN: 0137152833.
33. Petrovich, R.; Hamouda, A. A. Dolomitization of Ekofisk Oil Field reservoir chalk by injected seawater. In Water-Rock Interaction; Arehart, G., Hulston, J., Eds.; Balkema: Rotterdam, The Netherlands, 1998; ISBN 9054109424.
34. Pourmohammadi, S. Waterflood Efficiency and Single-Phase Flow Properties of Carbonate Porous Media. PhD Thesis, University of Bergen. 2009.
35. Puntervold, T. Waterflooding of carbonate reservoirs - EOR by wettability alteration. PhD Thesis, University of Stavanger. 2008.

36. Ramez A. Nasralla and Hisham A. Nasr-El-Din, 2014, "*Double-Layer Expansion: Is It a Primary Mechanism of Improved Oil Recovery by Low-Salinity Waterflooding?",* Paper SPE 154334, Oil Recovery Symposium, Tulsa, April 2012.
37. RezaeiDoust, A. Low Salinity Water-flooding in Sandstone Reservoirs – A chemical wettability alteration mechanism. PhD Thesis, University of Stavanger. 2011.
38. Sajjad, M. F., Smart Water EOR Effects in Preserved Sandstone Reservoir Cores, Comparison between Sea Water and Low Salinity Brines at 136°C. MSc Thesis, University of Stavanger. 2015.
39. Seccombe, J., Lager, A., Jerauld, G., et al. 2010. Demonstration of Low-Salinity EOR at Interwell Scale, Endicott Field, Alaska. Paper SPE-129692-MS proceedings of the SPE Improved Oil Recovery Symposium, Tulsa, Oklahoma, USA, 24-28 April.
40. Sposito, G., 1989. The chemistry of soils. Oxford University Press, New York, XII, 277 s. pp.
41. Suijkerbuijk, B., Hofman, J., Ligthelm, D. J., et al. 2012. Fundamental Investigations into Wettability and Low Salinity Flooding by Parameter Isolation. Paper SPE-154204-MS proceedings of the SPE Improved Oil Recovery Symposium, Tulsa, Oklahoma, USA, 14-18 April.
42. Tang, G.-Q. And Morrow, N.R., 1999. Influence of brine composition and fines migration on crude oil/rock interactions and oil recovery. Journal of Petroleum Science and Engineering, 24: 99-111.
43. Todd, A. C. (n.d.). *The Resrvoir Engineering Module*. Institute of Petroleum Engineering. Heriot Watt University.
44. Torrijos, I. D., Puntervold, T., Strand, S., Austad, T., Abdullah, H. I., & Olsen, K. (2016). Experimental Study of the Response Time of the Low-Salinity Enhanced Oil Recovery Effect during Secondary and Tertiary Low-Salinity Waterflooding. *Energy & Fuels Energy Fuels*. doi: 10.1021/acs.energyfuels.6b00641
45. Tortike, W.S. and Farouq Ali, S.M.: "Saturated-Steam-Property Functional Correlations for Fully Implicit Thermal Reservoir Simulation," *SPERE* (Nov. 1989) 471-74; *Trans.*, AIME, 287.
46. Verwey, E. J. and Overbeek, T. G., 1948, *Theory of the Stability of Lyophobic Colloids*: Elsvier, New York, 218 p.
47. Vledder, P., Gonzalez, I. E., Carrera Fonseca, J., et al. 2010. Low Salinity Water Flooding: Proof of Wettability Alteration On a Field Wide Scale. Paper SPE-129564-MS proceedings of the SPE Improved Oil Recovery Symposium, Tulsa, Oklahoma, USA, 24-28 April.

48. Webb, K. J., Black, C. J. J. and Al-Ajeel, H. 2003. Low Salinity Oil Recovery - Log-Inject-Log. Paper SPE-81460-MS proceedings of the Middle East Oil Show, Bahrain, 9-12 June.
49. Wikipedia, Relative permeability from: http://en.wikipedia.org/wiki/Relative_permeability
50. Yildiz, H. O., and Morrow, N. R. 1996. Effect of brine composition on recovery of Moutray crude oil by waterflooding. *J. Pet Sci & Eng* 14 (3): 159-168.
51. Zhang, P., Tweheyo, M.T. and Austad, T. (2006) 'Wettability alteration and improved oil recovery in chalk: The effect of calcium in the presence of Sulfate', *Energy & Fuels*, 20(5), pp. 2056–2062.

APPENDIX

A.1. Ion Concentrations relative to SSW for Experiments

Table 14: Relative effluent concentrations during SSW/SO4 flooding in SG-1

Conc. Of Ion relative to SSW									
PV Injected	**Samples**	**Ca+2**	**Mg+2**	**Na+**	**K+**	**Cl-**	**HCO3-**	**SO4-2**	**pH**
0.69	**#1**	1.725	1.018016	1.111901	1.14751	1.085263	1.321429	0.944624	7.09
0.88	**#2**	1.494355	0.980157	1.11644	1.084291	1.081537	1.071429	1.011828	7.18
1.43	**#3**	1.298387	1.023238	1.089781	1.030651	1.069074	1.035714	1.081452	7.23
1.66	**#4**	1.177419	1.02611	1.125212	1.04023	1.085937	1	1.119355	7.28
1.89	**#5**	1.141129	1.061097	1.115825	1.193487	1.085916	1.035714	1.085215	7.31
2.12	**#6**	1.149194	1.131593	1.092204	1.103448	1.091621	0.892857	1.10457	7.32
2.35	**#7**	1.079839	1.039426	1.126481	1.049808	1.085263	1.035714	1.081452	7.36
2.58	**#8**	1.064516	1.024543	1.124942	1.049808	1.079832	0.964286	1.08414	7.34
2.81	**#9**	1.174194	1.16658	1.083125	1.049808	1.083074	0.892857	1.091667	7.31
3.04	**#10**	1.099194	1.086684	1.089434	1.022989	1.068989	0.928571	1.078226	7.43
3.27	**#11**	1.055645	1.034726	1.105361	1.155172	1.066463	0.928571	1.075	7.45
3.50	**#12**	1.13871	1.115144	1.116517	1.044061	1.096211	0.821429	1.119355	7.38
3.73	**#13**	1.133065	1.173107	1.116017	1.256705	1.080653	0.857143	1.022312	7.41
3.96	**#14**	1.072581	1.043603	1.102245	1.157088	1.071242	0.964286	1.084409	7.52
4.62	**#15**	1.091935	1.086684	1.051695	1.141762	0.995747	0.964286	0.927957	7.24
5.28	**#16**	1.105645	1.070757	1.10286	1.103448	1.085242	0.928571	1.094355	7.25
5.94	**#17**	1.131452	1.134204	1.10263	1.04023	1.056042	1	0.984409	7.21
6.60	**#18**	1.023387	1.010183	1.129212	1.065134	1.085284	0.964286	1.088978	7.34
7.26	**#19**	1.100806	1.065274	1.108054	1.024904	1.082105	0.892857	1.09328	7.28
7.98	**#20**	1.032258	1.030548	1.118864	1.028736	1.080589	0.964286	1.100806	7.29
8.21	**#21**	1.082258	1.063969	1.118556	1.06705	1.086337	0.892857	1.119086	7.6
8.44	**#22**	1.075	1.083812	1.067237	1.220307	1.006505	0.964286	0	7.68
8.67	**#23**	1.082258	1.087728	1.082164	1.017241	1.062842	1.035714	1.062634	7.47
8.90	**#24**	1.028226	1.015405	1.083241	1.111111	1.045074	0.928571	1.102419	7.51
9.13	**#25**	0.645968	0.578329	0.709427	0.601533	0.635916	1.357143	0.93414	7.45
9.36	**#26**	0.095161	0.052219	0.232667	0.153257	0.138695	2.214286	0.508871	7.81
9.59	**#27**	0.076923	0.022472	0.093598	0.038314	0.016968	5.857143	0.263978	8.14
9.82	**#28**	0.076923	0.022472	0.078133	0.017241	0.003579	6.321429	0.164516	8.13
10.05	**#29**	0.076923	0.022472	0.086904	0	0.001432	6.5	0.143817	8.13
10.28	**#30**	0.076923	0.022472	0.072016	0.017241	0.001558	6.714286	0.147043	8.16
10.51	**#31**	0.076923	0.022472	0.088674	0.01341	0.001495	6.857143	0.131452	8.19
10.74	**#32**	0.076923	0.022472	0.072131	0	0.0012	8.857143	0.144086	8.15
10.97	**#33**	0.076923	0.022472	0.068207	0.019157	0.001832	7.571429	0.14086	8.2

11.20	**#34**	0.076923	0.022472	0.068323	0	0.000716	6.5	0.122849	8.09
11.43	**#35**	0.076923	0.022472	0.064014	0	0.000653	6.75	0.119624	8.05
11.66	**#36**	0.076923	0.022472	0.067477	0	0.0008	6.642857	0.119086	8.05
11.89	**#37**	0.076923	0.022472	0.061514	0.01341	0.001747	6.535714	0.136559	8.24
12.55	**#38**	0.076923	0.022472	0.076979	0.036398	0.003053	5.178571	0.096505	8.3
13.21	**#39**	0.076923	0.022472	0.102138	0	0.008316	6.214286	0.138172	8.35
13.87	**#40**	0.076923	0.022472	0.084134	0.086207	0.005621	8.107143	0.122581	8.5
14.53	**#41**	0.076923	0.022472	0.062283	0	0.000611	9.535714	0.116935	8.72
15.19	**#42**	0.076923	0.022472	0.072401	0	0.001368	8.214286	0.129032	9.27
15.85	**#43**	0.076923	0.022472	0.075594	0	0.000632	8.785714	0.104301	9.43

Table 15: Relative effluent concentrations during SSW/Mg at 70°C flooding in SG-2.

Conc. Of Ions relative to SSW									
PV Injected	**Samples**	**Ca+2**	**Mg+2**	**Na+**	**K+**	**Cl-**	**HCO3-**	**SO4-2**	**pH**
1.64	**#1**	1.7675	1.053167	1.054598	1.08	1.062009	1.225806	0.856873	6.9
2.04	**#2**	1.571667	0.921749	0.971416	0.945455	0.982487	1.129032	0.884906	7.06
2.09	**#3**	1.4025	0.958962	0.945119	0.96	0.935825	1.032258	0.851752	7.1
2.32	**#4**	1.200833	0.907696	1.009679	0.976364	0.987991	1.096774	0.974933	7.13
2.55	**#5**	1.164167	0.920187	1.050415	0.983636	1.010213	1.096774	0.99434	7.15
2.78	**#6**	1.228333	0.95688	1.084205	1.018182	1.041513	1.032258	1.049596	7.15
3.01	**#7**	1.17	0.949854	1.073402	0.994545	1.032579	1.032258	1.016981	7.2
3.24	**#8**	1.329167	1.192652	1.052888	1.014545	1.038617	1	0.925606	7.23
3.47	**#9**	1.163333	1.033389	1.032811	1.001818	1.038309	0.967742	1.02345	7.25
3.7	**#10**	1.144167	0.95714	1.058344	1.005455	1.02956	0.967742	1.058491	7.24
3.93	**#11**	1.145	0.982123	1.087296	1.043636	1.055601	0.935484	1.040701	7.19
4.62	**#12**	1.225833	1.119787	1.020809	1.047273	1.043156	1.096774	1.013208	7.24
5.31	**#13**	1.0675	0.959222	1.074275	0.998182	1.035618	0.967742	1.029111	7.22
6	**#14**	1.2325	1.144769	1.00957	1.163636	1.038863	1.193548	1.006739	7.28
6.69	**#15**	1.140833	1.084395	0.979709	0.978182	0.994255	1.419355	0.957143	7.24
7.38	**#16**	1.118333	1.02376	1.033175	0.994545	1.03147	0.967742	1.02345	7.33
8.07	**#17**	1.176667	1.092462	1.018444	1.009091	1.036029	0.935484	1.032884	7.26
8.3	**#18**	1.419167	1.009968	1.074457	1.058182	1.044675	0.774194	1.355256	7.34
8.53	**#19**	2.549167	2.869599	2.048055	2.209091	2.215617	0.483871	1.969272	7.34
8.76	**#20**	1.67	2.421737	1.950361	2.110909	2.06563	0.483871	1.516981	7.41
8.99	**#21**	1.059167	0.974056	1.06951	1.005455	1.035721	0.935484	1.077898	7.39
9.22	**#22**	0.4975	0.391132	0.527899	0.48	0.459389	1.419355	0.768733	7.42
9.45	**#23**	0.035833	0.023942	0.20761	0.198182	0.122077	2.612903	0.254447	7.45
9.68	**#24**	0.005833	0.002863	0.151925	0.08	0.066809	3.419355	0.116712	7.5

9.91	**#25**	0.169167	0.063757	0.084782	0.070909	0.045389	6.129032	0.054178	7.57
10.14	**#26**	0.0775	0.029927	0.049866	0.023636	0.019018	5.806452	0.021024	7.61
10.37	**#27**	0.095	0.03357	0.06005	0.02	0.025775	6.774194	0.019137	7.69
10.6	**#28**	0.0425	0.013272	0.04812	0.007273	0.016964	6.290323	0.010512	7.74
10.83	**#29**	0.000833	0.00026	0.091766	0.012727	0.016759	5.290323	0.01159	7.79
11.06	**#30**	0.001667	0.00026	0.08591	0.010909	0.01604	5.322581	0.009704	7.85
11.29	**#31**	0.2025	0.125433	0.116062	0.030909	0.088087	4.290323	0.02938	7.78
11.52	**#32**	0.0025	0.000781	0.096931	0.034545	0.019162	5.290323	0.00566	7.74
11.75	**#33**	0.011667	0.002602	0.068161	0.054545	0.02101	7.290323	0.003504	7.77
11.98	**#34**	0.001667	0.00052	0.079981	0.132727	0.023393	6.322581	0.004043	7.68
12.67	**#35**	0.005833	0.001041	0.068779	0.04	0.023762	7.290323	0.001348	7.71
13.36	**#36**	0.004167	0.001041	0.060268	0.003636	0.017663	7.612903	0.000809	7.84
14.05	**#37**	0.038333	0.017175	0.057285	0.005455	0.018648	14.29032	0.018868	7.86
14.74	**#38**	0.073333	0.035392	0.057176	0.143636	0.025015	13.12903	0.037197	7.87
15.43	**#39**	0.000833	0.00026	0.065214	0.003636	0.017211	6.096774	0.004313	7.94
16.12	**#40**	0.001667	0.00052	0.087656	0.007273	0.033251	9.290323	0.015903	7.93

Table 16: Relative effluent concentrations during SSW/LSW 1:50 flooding in SG-3

Conc. Of Ions (mole/l)									
PV Injected	**Samples**	**Ca+2**	**Mg+2**	**Na+**	**K+**	**Cl-**	**HCO3-**	**SO4-2**	**pH**
1.54	**#1**	1.553846	0.994286	0.94025	0.944	0.916778	1.153846	0.733636	7.09
1.8	**#2**	1.441538	1.112857	1.016679	1.062	0.994906	0.130769	0.737045	7.11
2.06	**#3**	1.343077	1.028286	1.012821	1.014	0.961315	1.323077	0.896818	7.14
2.32	**#4**	1.218462	0.958571	1.116679	1.04	0.94803	2.784615	0.931591	7.19
2.58	**#5**	1.239231	1.067714	0.985643	1.038	0.936461	1.153846	0.946136	7.21
2.84	**#6**	1.332308	0.947429	1.004429	1.022	0.925082	1.538462	0.919545	7.31
3.1	**#7**	1.070769	1.004286	1.002321	1.024	0.922666	1.184615	0.962045	7.37
3.36	**#8**	1.097692	1.067429	0.986893	1.026	0.925006	1.261538	0.987955	7.61
3.62	**#9**	1.279231	1.115429	0.970929	1.054	0.918477	0.692308	1.063864	7.53
3.88	**#10**	0.987692	1.000571	1.013679	1.106	0.92678	1	0.969545	7.34
4.14	**#11**	0.993077	1.007429	1.017393	1.05	0.923421	1.069231	0.958636	7.26
4.8	**#12**	2.034615	2.247429	1.865321	2.11	1.799758	1.553846	1.810682	6.96
5.46	**#13**	1.186923	1.233429	1.062893	1.16	1.008588	1.061538	1.059773	7.11
6.12	**#14**	1.078462	1.165429	1.003821	1.056	0.947275	1.107692	0.986591	7.15
6.78	**#15**	0.978462	1.056	1.036607	1.066	0.949502	1.169231	0.992273	7.17
7.44	**#16**	2.402308	2.746857	2.208714	2.586	2.141238	0.823077	2.248864	7.11
7.7	**#17**	1.116923	1.210571	1.016929	1.128	0.9686	1.076923	1.023636	7.32
7.96	**#18**	1.307692	1.050857	1.045607	1.086	0.964806	1	1.001364	7.41

8.22	**#19**	1.020769	1.052571	1.047179	1.098	0.956786	0.961538	1.000455	7.69
8.48	**#20**	1	1.042	1.039143	1.08	0.938726	1	0.996591	7.45
8.74	**#21**	0.737692	0.686	0.708964	0.754	0.617344	1.715385	0.893409	7.47
9	**#22**	0.242308	0.189429	0.388929	0.358	0.251991	1.607692	0.485909	7.56
9.26	**#23**	0.197692	0.079714	0.183393	0.146	0.111304	1.892308	0.261591	7.63
9.52	**#24**	0.006923	0.014286	0.214357	0.094	0.062861	1.307692	0.078409	7.96
9.78	**#25**	0.005385	0.002571	0.204964	0.166	0.099566	2.292308	0.180909	7.88
10.04	**#26**	0.000769	0.000571	0.123107	0.022	0.032346	0.907692	0.035682	7.98
10.3	**#27**	0.003077	0.000571	0.086893	0.054	0.029628	1.030769	0.023864	7.97
10.56	**#28**	0.001538	0.000286	0.08225	0.014	0.023457	1.069231	0.018409	8.05
10.82	**#29**	0.003077	0.000286	0.069893	0.014	0.0224	1.1	0.014545	7.93
11.08	**#30**	0.002308	0.001143	0.165321	0.126	0.053538	1.430769	0.011818	7.93
11.34	**#31**	0.003077	0.001429	0.101179	0.016	0.019721	0.984615	0.023636	7.97
11.6	**#32**	0	0.000571	0.077786	0.008	0.020079	1.076923	0.024091	7.96
12.26	**#33**	0.001538	0.000286	0.096286	0.012	0.020042	0.961538	0.031591	7.92
12.92	**#34**	0.000769	0.000286	0.089679	0.02	0.018909	1.092308	0.014091	7.98
13.58	**#35**	0.002308	0.000286	0.065286	0.012	0.018758	1.123077	0.012045	8.07
14.24	**#36**	0.000769	0	0.084857	0.02	0.021589	1.076923	0.015455	8.35
14.9	**#37**	0.005385	0.000571	0.068679	0.02	0.019494	1.407692	0.012955	7.99

Table 17: Relative effluent concentrations during SSW/SO4 1:50 flooding in SG-4.

Conc. Of Ions relative to SSW									
PV Injected	**Samples**	**Ca+2**	**Mg+2**	**Na+**	**K+**	**Cl-**	**HCO3-**	**SO4-2**	**pH**
1.4	**#1**	1.8093	0.889697	0.919474	1.09	1.030166	1.2375	0.703158	6.89
1.565	**#2**	1.775976	0.924545	0.818208	1.48	1.04278	1.2875	0.938947	6.94
1.73	**#3**	1.813175	0.996667	0.771613	1.3575	1.056888	1.1625	0.985789	6.98
1.95	**#4**	1.773048	1.004848	0.699546	1.04	1.044315	1.2	0.992632	7.01
2.17	**#5**	1.788117	1.014545	0.675938	1.0625	1.000913	1.2875	0.924211	7.07
2.39	**#6**	1.767882	1.011515	0.651708	1.03	1.040581	1.3375	1.054211	7.1
2.61	**#7**	1.770809	1.02303	0.649223	1.21	1.042282	1.2125	1.071579	7.14
2.83	**#8**	1.767365	1.019697	0.630585	1.03	1.039461	1.175	1.055789	7.24
3.05	**#9**	1.751091	1.012121	0.611326	1.035	1.019253	1.075	1.024737	7.17
3.27	**#10**	1.739036	1.003333	0.605735	1.105	1.012863	1.125	1.041053	7.29
3.49	**#11**	1.750316	1.012424	0.605735	0.98	1.017552	1.05	1.026316	7.38
3.71	**#12**	1.772445	1.023333	0.610084	1.055	1.042531	0.9875	1.036842	7.17
4.498	**#13**	1.752555	1.014545	0.597658	1.175	1.019876	0.9875	1.046842	7.25
5.286	**#14**	1.762026	1.027273	0.593309	1.01	1.02527	1.05	1.007895	7.31
6.074	**#15**	1.76306	1.022727	0.593931	0.995	1.023817	1.1625	1.008421	7.34

6.862	**#16**	1.729908	1.002121	0.57902	0.985	0.969087	0.9375	0.9	7.34
7.65	**#17**	1.842279	1.075152	0.620645	1.0575	1.035187	0.8375	0.96	7.25
7.88	**#18**	1.876378	1.098788	0.627479	1.135	1.086141	0.7875	0.996316	7.33
8.11	**#19**	1.895838	1.114848	0.63307	1.1825	1.106017	0.8375	1.105789	7.4
8.34	**#20**	1.940873	1.142121	0.647981	1.1175	1.130041	0.9	1.141579	7.36
8.57	**#21**	1.910304	1.095758	0.682151	1.5175	1.075519	0.6625	1.018947	7.39
8.8	**#22**	1.796383	1.042121	0.608841	1.085	1.034564	0.6	1.136842	7.4
9.03	**#23**	0.925746	0.46697	0.285783	0.6175	0.493278	0.925	0.893158	7.44
9.26	**#24**	0.347876	0.145455	0.098781	0.225	0.174855	1.425	0.445789	7.51
9.49	**#25**	0.126406	0.056061	0.051565	0.1675	0.064481	1.6875	0.184211	7.52
9.72	**#26**	0.055281	0.02303	0.025472	0.035	0.027884	1.7875	0.1	7.61
9.95	**#27**	0.10729	0.001818	0.002485	0.015	0.012656	3.6875	0.109474	7.65
10.18	**#28**	0.023766	0.005758	0.010562	0.0325	0.007178	2.225	0.064211	7.7
10.41	**#29**	0.013519	0.004242	0.00994	0.05	0.004772	2.95	0.096842	7.81
10.64	**#30**	0.011452	0.002727	0.006834	0.0125	0.00249	2.8375	0.091053	7.88
10.87	**#31**	0.012055	0.003636	0.005591	0.0075	0.002158	2.575	0.035789	7.9
11.1	**#32**	0.013327	0.002727	0.004815	0.0275	0.003875	3.566667	0.06973	8.05
11.33	**#33**	0.006577	0.001818	0.004815	0.005	0.00075	3.4	0.085946	8.21
11.56	**#34**	0.00649	0.001515	0.004815	0.0075	0.000958	3.883333	0.062162	8.13
12.35	**#35**	0.007096	0.001212	0.003611	0.0075	0.000792	3.683333	0.062162	8.12
13.14	**#36**	0.007875	0.000909	0.003009	0.005	0.000583	3.866667	0.063784	8.18
13.93	**#37**	0.00675	0.000909	0.002407	0.005	0.000417	3.9	0.067027	8.58
14.72	**#38**	0.009952	0.001212	0.005417	0.0325	0.001833	3.866667	0.060541	8.95
15.51	**#39**	0.008654	0.000606	0.003009	0.0375	0.001917	3.883333	0.063243	9.21

Table 18: Relative effluent concentrations during SSW/LSW 1:10 (crude) flooding in SG-5

Conc. Of Ions relative to SSW									
PV Injected	**Samples**	**Ca+2**	**Mg+2**	**Na+**	**K+**	**Cl-**	**HCO3-**	**SO4-2**	**pH**
1.48	**#1**	1.170009	0.621212	0.011074	1.195	1.190289	1.03	1.115263	8.58
1.64	**#2**	1.047768	0.953636	0.031617	1.275	1.186983	0.83	1.000526	7.98
1.858	**#3**	1.160963	1.235152	0.043109	1.4575	1.346074	0.56	1.268421	7.11
2.076	**#4**	0.893781	0.995758	0.031842	1.035	1.025496	0.74	1.034737	7.19
2.294	**#5**	2.787887	3.441515	0.104867	3.39	3.182851	0.32	3.292105	7.2
2.512	**#6**	0.904349	1.035758	0.030719	1.0525	1.036446	0.61	1.072105	7.21
2.73	**#7**	0.97945	1.135455	0.033736	1.19	1.075041	0.67	1.044737	7.27
2.948	**#8**	1.003455	1.157273	0.035533	1.39	1.147314	0.69	1.163158	7.27
3.166	**#9**	0.889128	1.02303	0.030109	1.005	1.030248	0.69	1.065789	7.31
3.384	**#10**	1.036026	1.211515	0.035244	1.215	1.191488	0.74	1.203158	7.33
3.602	**#11**	0.899783	1.021515	0.030398	1.28	1.02876	0.84	1.054211	7.38

3.82	**#12**	1.121608	1.193333	0.037235	2.2675	1.267727	1.05	1.214737	7.41
4.47	**#13**	1.061596	0.93697	0.028086	6.32	1.112107	1.43	1.081053	7.43
5.12	**#14**	0.969709	1.124545	0.034089	1.075	1.110785	0.58	1.130526	7.32
5.77	**#15**	0.879431	1.005758	0.031264	0.985	1.00624	0.67	1.052105	7.3
6.42	**#16**	0.906088	1.025758	0.031489	2.0725	1.040579	0.63	1.074737	7.29
7.07	**#17**	1.018414	1.133939	0.033896	1.955	1.168802	0.69	1.210526	7.31
7.72	**#18**	0.904871	1.033333	0.031232	1.045	1.032562	0.6	1.072632	7.36
7.938	**#19**	1.099865	1.17697	0.03579	3.0675	1.217438	1.03	1.230526	7.51
8.156	**#20**	0.891694	1.016364	0.02982	1.05	1.030909	0.86	1.068947	7.52
8.374	**#21**	0.875821	0.955455	0.029306	1.39	0.993719	0.84	1.056842	7.55
8.592	**#22**	0.628643	0.495152	0.015086	3.4425	0.633347	1.42	0.911579	7.56
8.81	**#23**	0.802474	0.141212	0.005168	2.5675	0.271736	1.94	0.523158	7.79
9.028	**#24**	0.342443	0.098788	0.005168	1.1775	0.139587	1.8	0.265263	7.97
9.246	**#25**	3.160263	1.375758	0.04436	2.3125	1.364421	0.97	1.435789	7.69
9.464	**#26**	0.433127	0.135152	0.006067	0.4875	0.184835	1.53	0.256842	7.76
9.682	**#27**	0.256629	0.053636	0.004044	0.2625	0.106405	1.49	0.115789	7.8
9.9	**#28**	0.227754	0.049697	0.003948	0.0925	0.097314	1.79	0.135263	7.84
10.118	**#29**	0.235176	0.051212	0.004269	0.2125	0.101074	1.5	0.108947	7.89
10.336	**#30**	0.22961	0.048788	0.003884	0.065	0.098347	1.63	0.103684	7.84
10.554	**#31**	0.228798	0.05	0.003948	0.135	0.098554	1.88	0.138947	7.87
10.772	**#32**	0.225551	0.04697	0.00382	0.1075	0.097107	1.81	0.144737	7.84
10.99	**#33**	0.223116	0.048182	0.003563	0.1	0.096074	1.91	0.139474	7.84
11.208	**#34**	0.224971	0.048485	0.003435	0.08	0.096901	1.87	0.130526	7.92
11.426	**#35**	0.224391	0.048788	0.003435	0.1225	0.096901	1.83	0.123684	7.87
12.076	**#36**	0.231117	0.051212	0.00321	0.125	0.098388	1.87	0.142105	8.01
12.726	**#37**	0.234364	0.055455	0.003114	0.0925	0.100372	1.6	0.09	8.07
13.376	**#38**	0.248164	0.051515	0.003049	0.2125	0.103182	1.81	0.144737	8.2
14.026	**#39**	0.231349	0.055455	0.00276	0.2125	0.100537	1.98	0.14	8.28
14.676	**#40**	0.218361	0.053333	0.002472	0.095	0.095992	1.95	0.136316	8.33

Table 19: Relative effluent concentrations during SSW/LSW 1:50 (crude) flooding in SG-6

Conc. Of Ions relative to SSW									
PV Injected	**Samples**	**Ca+2**	**Mg+2**	**Na+**	**K+**	**Cl-**	**HCO3-**	**SO4-2**	**pH**
1.27	**#1**	2.30125	1.651333	1.419917	29.036	1.589875	2.175	1.022778	7.03
1.468	**#2**	1.94625	1.172	1.08	4.938	1.229167	1.8375	0.920556	7.13
1.666	**#3**	1.4875	1.065333	0.952667	2.918	1.146417	1.1	1.018333	7.19
1.864	**#4**	1.4225	1.152	0.910792	1	1.040833	1.175	0.952222	7.24
2.062	**#5**	1.33625	1.186333	0.929083	0.858	1.076	1.4	1.011111	7.27
2.26	**#6**	1.32	1.204667	0.986042	0.88	1.111083	1.2375	0.917222	7.33

2.458	**#7**	1.34	1.230333	0.9415	0.86	1.063917	1.975	0.977222	7.36
2.656	**#8**	1.39875	1.34	1.020708	0.954	1.164083	1.525	1.097222	7.39
2.854	**#9**	1.2525	1.206333	0.928167	0.89	1.063708	1.325	0.999444	7.39
3.052	**#10**	1.3775	1.300667	0.997375	0.972	1.110958	1.6375	1.040556	7.4
3.25	**#11**	1.53	1.395667	0.996542	1.806	1.191	1.375	1.123889	7.38
3.448	**#12**	1.52125	1.343667	0.984	1.036	1.115	1.2	1.056667	7.41
3.646	**#13**	1.50625	1.270667	1.078292	1.04	1.203	1	1.032222	7.27
4.276	**#14**	1.48625	1.344667	1.033625	1.126	1.162417	1.15	1.093889	7.19
4.906	**#15**	0.85375	0.948	1.021375	0.938	1.097792	1.3875	1.077778	7.27
5.536	**#16**	1.05375	1.133333	1.08175	0.922	1.097208	1.7375	1.085556	7.16
6.166	**#17**	1.19625	1.215667	1.01725	0.938	1.097458	1.15	1.078889	7.2
6.796	**#18**	1.00625	1.109333	1.137458	1.03	1.138333	1.5625	1.132778	7.29
6.994	**#19**	1.13875	1.163333	1.067083	1.374	1.119833	1.275	1.101111	7.42
7.192	**#20**	0.96	0.976	1.02575	0.988	1.075958	1.475	1.082222	7.38
7.39	**#21**	0.99125	1.08	1.078	0.922	1.248667	1.1375	1.132778	7.36
7.588	**#22**	0.98625	0.869333	1.022458	1.03	1.043792	1.7125	1.071111	7.49
7.786	**#23**	0.38875	0.374667	0.542625	0.45	0.446875	1.6375	1.016667	7.51
7.984	**#24**	0.0475	0.036667	0.1565	0.12	0.066458	2.125	0.443889	7.55
8.182	**#25**	0.01875	0.013333	0.125583	0.106	0.027958	2.6875	0.216667	7.57
8.38	**#26**	0.01875	0.008667	0.130625	0.04	0.028458	2.7625	0.243333	7.59
8.578	**#27**	0.01875	0.016333	0.297542	0.572	0.1395	3.675	0.231111	7.66
8.776	**#28**	0.03	0.015667	0.126292	0.182	0.036083	3.4625	0.189444	7.72
8.974	**#29**	0.02875	0.008	0.099625	0.04	0.02775	3.2875	0.143333	7.89
9.172	**#30**	0.015	0.004333	0.121417	0.058	0.024667	3.2875	0.155	7.91
9.37	**#31**	0.0175	0.021	0.150542	0.06	0.028583	4.4375	0.146111	8.09
9.568	**#32**	0.0625	0.036	0.281	0.402	0.168	3.1125	0.301667	8
9.766	**#33**	0.02875	0.012667	0.227208	0.058	0.039917	5.6	0.172778	8.12
9.964	**#34**	0.025	0.008667	0.161833	0.088	0.031875	4.7125	0.093889	8
10.162	**#35**	0.015	0.004667	0.11075	0.144	0.062708	3.4875	0.089444	8.2
10.792	**#36**	0.01	0.003333	0.098292	0.03	0.027792	3.3625	0.067778	8.26
11.422	**#37**	0.00875	0.003667	0.174458	0.056	0.066833	4.35	0.143333	8.52
12.052	**#38**	0.01	0.004667	0.12775	0.076	0.027792	4.85	0.106667	8.62
12.682	**#39**	0.0175	0.006333	0.094	0.064	0.050625	3.075	0.066111	8.66
13.312	**#40**	0.03375	0.014333	0.362875	0.102	0.380458	4.05	0.061667	8.79
13.942	**#41**	0.02	0.011667	0.204958	0.066	0.026958	6.8875	0.1	8.64

Table 20: Relative effluent concentrations during SSW/Mg+Na flooding in SG-7

Conc. Of Ions relative to SSW									
PV Injected	**Samples**	**Ca+2**	**Mg+2**	**Na+**	**K+**	**Cl-**	**HCO3-**	**SO4-2**	**pH**
1.14	**#1**	1.241053	0.887879	0.999005	1.08	0.986612	1.25	0.788333	6.9
1.34	**#2**	0.922105	0.704545	0.786667	0.8275	0.818531	1.2	0.731667	6.97
1.54	**#3**	1.165263	0.901212	1.003532	1.055	1.034776	1.1	0.994444	7.19
1.74	**#4**	1.163158	0.951515	0.995025	0.995	0.98502	1.175	0.975	7.16
1.94	**#5**	1.235789	1.065455	1.08194	1.065	1.07102	1.225	1.094444	7.25
2.14	**#6**	1.222105	1.077576	1.085274	1.07	1.068367	1.1	1.090556	7.27
2.34	**#7**	1.197895	1.090606	1.08592	1.0625	1.06751	1	1.107222	7.31
2.54	**#8**	1.151579	1.073333	1.067512	1.06	1.050163	0.975	1.084444	7.39
2.74	**#9**	1.143158	1.080909	1.070448	1.0575	1.053429	1.025	1.091667	7.41
2.94	**#10**	1.065263	0.990909	1.044428	1.085	1.081388	1.125	1.112222	7.46
3.14	**#11**	1.123158	1.055758	1.042189	1.115	1.029714	1.075	1.073333	7.49
3.34	**#12**	1.025263	0.966667	1.009701	1.1825	1.047837	0.95	1.092222	7.51
3.54	**#13**	1.135789	1.081818	1.069303	1.06	1.05898	1.2	1.098889	7.39
3.74	**#14**	1.005263	0.936061	0.988756	0.9925	1.020367	1.225	1.065556	7.25
3.94	**#15**	1.297895	1.534545	1.178159	1.205	1.210735	1.2	1.184444	7.22
4.62	**#16**	1.195789	1.260606	1.132985	1.1225	1.125469	1.1	1.162222	6.93
5.3	**#17**	1.086316	1.081212	1.096915	1.16	1.129388	0.95	1.168333	7.01
5.98	**#18**	1.132632	1.113636	1.124129	1.1975	1.164286	0.95	1.235	7.15
6.66	**#19**	1.134737	1.131212	1.098806	1.1075	1.087061	1.025	1.136667	7.18
7.34	**#20**	1.06	1.059394	1.094129	1.1375	1.126612	1.075	1.169444	7.15
7.54	**#21**	1.288421	1.194545	1.175821	1.175	1.155796	0.875	1.208889	7.2
7.74	**#22**	1.18	1.180303	1.148209	1.145	1.135429	0.975	1.190556	7.23
7.94	**#23**	1.16	1.169394	1.141045	1.2275	1.128694	0.975	1.181667	7.26
8.14	**#24**	1.197895	1.162424	1.142537	0	1.130122	0.875	1.168333	7.28
8.34	**#25**	0.996842	0.88303	1.260796	1.055	1.240612	0.825	1.072778	7.38
8.54	**#26**	0.616842	0.565455	0.605124	0.5725	0.578735	1.775	0.797222	7.42
8.74	**#27**	0.349474	0.274242	0.323881	0.295	0.305878	2.175	0.506667	7.48
8.94	**#28**	0.210526	0.126061	0.166567	0.11	0.158327	2.5	0.281111	7.52
9.14	**#29**	0.18	0.08	0.120945	0.065	0.118	3.175	0.182222	7.54
9.34	**#30**	0.145263	0.048485	0.090249	0.1575	0.094612	3.15	0.113333	7.57
9.54	**#31**	0.144211	0.077273	0.112886	0	0.113388	4.25	0.106111	7.61
9.74	**#32**	0.154737	0.04697	0.09199	0.08	0.097306	3.45	0.070556	7.63
9.94	**#33**	0.16	0.043939	0.10597	0	0.107796	3.65	0.059444	7.64
10.14	**#34**	0.150526	0.038182	0.09801	0	0.105265	4.15	0.058333	7.67
10.34	**#35**	0.158947	0.03697	0.085771	0.12	0.093347	3.75	0.043889	7.7
10.54	**#36**	0.129474	0.032121	0.084826	0.0225	0.08698	3.775	0.035556	7.72
10.74	**#37**	0.135789	0.032424	0.081343	0.0525	0.087469	4.125	0.041111	7.69

10.94	**#38**	0.134737	0.032727	0.110398	0.06	0.108041	4.075	0.039444	7.77
11.14	**#39**	0.107368	0.031515	0.080597	0.045	0.086776	4.075	0.036111	7.77
11.34	**#40**	0.1	0.031818	0.08005	0.0525	0.084816	4.175	0.035556	7.82
12.02	**#41**	0.105263	0.03697	0.088308	0.03	0.089878	3.75	0.035556	7.74
12.7	**#42**	0.086316	0.035758	0.079602	0.035	0.086735	3.625	0.033889	7.9
13.38	**#43**	0.075789	0.035758	0.090995	0	0.093061	3.9	0.043889	7.95
14.06	**#44**	0.088421	0.042727	0.093682	0	0.096816	3.65	0.034444	8.02
14.74	**#45**	0.062105	0.03303	0.074826	0.0425	0.080449	3.9	0.031111	8.11
15.42	**#46**	0.064211	0.037576	0.077363	0.03	0.080531	3.725	0.027778	8.16

Table 21: Relative effluent concentrations during SSW/Mg at 90°C flooding in SG-8

Conc. Relative to SSW									
PV Injected	**Samples**	**Ca+2**	**Mg+2**	**Na+**	**K+**	**Cl-**	**HCO3-**	**SO4-2**	**pH**
1.11	**#1**	1.165556	0.666061	0.911256	0.992857	1.001667	1.027778	0.628	6.47
1.315	**#2**	1.32	0.805455	0.956329	1.121429	0.989	1	0.748	6.67
1.52	**#3**	1.184444	0.800606	0.936329	0.942857	1.017125	0.805556	0.920571	6.78
1.725	**#4**	1.122222	0.838485	0.958309	0.954762	1.0415	0.833333	0.989143	6.8
1.93	**#5**	1.225556	0.989394	1.022705	0.97619	1.049792	0.861111	1.018857	6.83
2.135	**#6**	1.12	0.945152	1.006087	1.028571	1.100792	0.805556	1.107429	6.87
2.34	**#7**	1.088889	0.927576	1.02686	1.485714	1.109792	0.916667	1.113143	6.91
2.545	**#8**	1.061111	0.904545	0.964396	1.371429	1.032125	0.916667	1.026286	6.94
2.75	**#9**	0.992222	0.892727	0.938744	0.930952	1.016958	0.916667	1.030857	6.96
2.955	**#10**	1.048889	0.954545	0.99744	1.038095	1.0785	0.972222	1.097714	7
3.16	**#11**	1.045556	0.953636	0.993333	1.021429	1.075625	0.888889	1.092	7.03
3.365	**#12**	1.152222	1.087576	1.05372	1.016667	1.070125	0.916667	1.089143	7.05
3.57	**#13**	1.152222	1.099091	1.05744	1.019048	1.087792	0.888889	1.121714	6.97
3.775	**#14**	0.995556	0.943636	0.974879	0.964286	1.049458	0.888889	1.079429	7
3.98	**#15**	0.982222	0.938485	0.970242	0.961905	1.050875	0.916667	1.078857	6.98
4.63	**#16**	1.087778	1.055455	1.021498	0.980952	1.046292	0.833333	1.065143	6.93
5.28	**#17**	1.042222	1.017273	1.041594	1.05	1.125417	0.805556	1.138857	6.88
5.93	**#18**	1.047778	1.019091	1.045217	1.107143	1.119583	0.777778	1.152	7
6.58	**#19**	1.103333	1.079394	1.042899	1.009524	1.076375	0.861111	1.103429	7.22
7.23	**#20**	1.055556	1.051515	1.0143	0.990476	1.054458	0.916667	1.087429	7.23
7.88	**#21**	1.077778	1.070909	1.034106	1.014286	1.0525	0.861111	1.081714	7.32
8.085	**#22**	0.97	0.952424	0.972415	0.983333	1.057042	0.861111	1.097714	7.31
8.285	**#23**	1.061111	1.031818	1.05058	1.038095	1.139542	0.861111	1.206286	7.36
8.485	**#24**	1.047778	1.016667	1.029227	1.107143	1.123042	0.777778	1.173143	7.21
8.685	**#25**	1.141111	1.120909	1.074638	1.238095	1.11	0.972222	1.157143	7.28

8.885	**#26**	0.827778	0.802727	0.834444	0.859524	0.907208	1.111111	1.113143	7.26
9.085	**#27**	0.525556	0.48	0.491836	0.497619	0.487667	1.777778	0.790286	7.45
9.285	**#28**	0.276667	0.216364	0.221932	0.27619	0.233458	2.222222	0.484571	7.51
9.485	**#29**	0.192222	0.125758	0.10715	0.130952	0.116083	2.972222	0.311429	7.55
9.685	**#30**	0.203333	0.088788	0.054251	0.090476	0.0605	3.916667	0.208571	7.6
9.885	**#31**	0.14	0.073333	0.039179	0.152381	0.051292	4.611111	0.138857	7.68
10.085	**#32**	0.132222	0.050909	0.012657	0.038095	0.024667	4.25	0.108	7.71
10.285	**#33**	0.122222	0.045455	0.01971	0.042857	0.025583	4.833333	0.088571	7.77
10.485	**#34**	0.137778	0.044848	0.008164	0.05	0.020292	4.888889	0.090286	7.81
10.685	**#35**	0.127778	0.039697	0.006425	0.016667	0.017958	4.472222	0.064571	7.83
10.885	**#36**	0.127778	0.037273	0.004348	0.019048	0.016833	4.388889	0.042857	7.86
11.085	**#37**	0.127778	0.03697	0.006377	0.078571	0.020625	4.388889	0.049143	7.81
11.285	**#38**	0.13	0.037273	0.003188	0.02381	0.01725	4.555556	0.050286	7.81
11.485	**#39**	0.127778	0.037576	0.00744	0.059524	0.01975	4.722222	0.038857	7.75
11.685	**#40**	0.125556	0.037576	0.003865	0.019048	0.017458	4.861111	0.042286	7.72
12.335	**#41**	0.223333	0.116061	0.099469	0.12381	0.12525	4.5	0.131429	7.63
12.985	**#42**	0.128889	0.062424	0.036377	0.409524	0.052292	5.027778	0.054857	7.64
13.635	**#43**	0.113333	0.053939	0.016473	0.054762	0.032583	5.111111	0.051429	7.74
14.285	**#44**	0.087778	0.04303	0.012271	0.038095	0.02525	5.055556	0.038286	7.82
14.935	**#45**	0.081111	0.040303	0.005894	0.064286	0.02025	5.527778	0.034857	7.84

A.2. AN and BN Measurements

The procedure to measure AN and BN is described below:

1. Using standard buffer solution with pH 4,7 and 10 pH electrode is calibrated.
2. Standardize the titrant with 50 ml of standard solution.
3. Make a sample of 1ml spiking solution and 50 ml of blank solution, using titrant. Spiking solution is added to improve the accuracy for oil having low AN.
4. Make a new sample of 1ml spiking solution and 50 ml of blank solution, and add 1 ml of oil to the mixture. Titrant is used to measure the acid/base content of new sample.
5. The amount of oil added is represented by the difference in the total acid/base content between the blank and the sample containing oil.